BLIMP: Bidirectional Lightweight Inflatable Mobile Pathway

NASA X-Hab

South Dakota State University

Jerome J Lohr College of Engineering



Authors:

Tyler Iverson

Anthony Perales

Addison Walz

Will Zavesky

Wyatt Reece

Faculty Advisor:

Dr. Todd Letcher

Graduate Advisor:

Nick Sieler

Project Sponsors:

Ryan Brown

Doug Litteken

Thomas Jones

Table of Contents

Acronyms and Abbreviations 3
1.0 Introduction 5
2.0 Preliminary Research 7
3.0 Supported Documentation 13
4.0 Early Trade Studies and Design Iterations 20
5.0 Conceptual Design 27
6.0 Concept of Operations and System Operations 40
7.0 Simulation and Optimization 48
8.0 Prototype Design 57
9.0 Inflatable Prototyping 68
10.0 Prototype Results 79
11.0 Future Work/Community Outreach 83
12.0 Conclusion 85
13.0 References 86

Acronyms and Abbreviations

AO: Atomic Oxygen; highly reactive single oxygen atoms found in planetary atmospheres that cause material erosion. [1].

ASME: American Society of Mechanical Engineers. [2],

ASTM: American Society for Testing and Materials; an international standards organization that establishes strict materials testing metrics. [3].

BLIMP: Bidirectional Lightweight Inflatable Mobile Pathway.

CCHP: Constant Conductance Heat Pipe; a thermal management loop system used to regulate internal vehicle or module temperatures [4].

CDPR: Cable-Driven Parallel Robots; robotic mechanisms that use compliance and cable tension as main articulation elements [5].

CDR: Critical Design Review [2].

CF/CFRP: Carbon Fiber / Carbon Fiber Reinforced Polymer; high-strength composite framing alternatives used to minimize system mass [6].

CNC: Computer Numerical Control; automated machine and manufacturing processes [7].

DoF: Degree of Freedom; translation and rotation coordinate measurements of a geometric body in space [8].

DWG: Drawing; a binary vector file format used to define precision CAD profiles for automated laser manufacturing systems [7].

ECLSS: Environmental Control and Life Support System; a suite of hardware that regulates pressure containment, oxygen concentration, and climate limits to support safe human habitability [9].

EDS: Electrodynamical Dust Shielding; active electrostatic fields utilized to protect windows, sensors, and external equipment from regolith accumulation [10].

EVA: Extravehicular Activity; activities performed by space-suited astronauts outside their spacecraft or pressurized surface assets [11].

FEA: Finite Element Analysis; a computerized numerical method used to predict how a structural component or solid model reacts to real-world physical forces, loads, and thermal stresses [12].

FOS: Factor(s) of Safety (Safety Factors); multiplying factors applied to limit loads or stresses for analytical assessment or test verification of structural adequacy [13].

LiDAR: Light Detection and Ranging; an optical remote sensing and profiling technique that uses pulsed laser light to measure ranges, map topography, and analyze atmospheric properties [14].

MMOD: Micrometeoroid and Orbital Debris; high-velocity hypervelocity space environment particulates that present catastrophic puncture risks to structural envelopes [15].

MTS: Materials Test Systems; specialized mechanical simulation and testing equipment utilized to evaluate the physical, structural, and fatigue properties of aerospace materials [16].

NASA: National Aeronautics and Space Administration [2].

NDS: NASA Docking System; standardized direct electric docking hardware mechanisms supporting spacecraft and habitat element integration [17].

PDR: Preliminary Design Review [2].

PLA: Polylactic Acid; a common biodegradable thermoplastic polymer used in additive manufacturing and 3D printing configurations for structural prototyping [18].

PTFE: Polytetrafluoroethylene [19].

RANS: Reynolds-Averaged Navier-Stokes; a class of time-averaged mathematical equations and computational fluid dynamics (CFD) simulation modeling techniques used to predict turbulent fluid flows [20].

RGB: Red, Green, Blue; a multi-spectral composite imagery and visualization technique used to enhance feature discrimination in satellite and meteorological data products [21].

SDR: System Definition Review [2].

SDSU: South Dakota State University.

SOA: State of the Art; the current baseline tier of validated technical maturity across aerospace concepts [22].

TPU: Thermoplastic Polyurethane; an elastic, heat-sealable polymer compound used as a dynamic pressure liner [23].

TRL: Technology Readiness Level; a standardized metric system consisting of nine levels used to assess and communicate the technical maturity of a particular technology or concept [24].

1.0 Introduction

1.1 Project Problem and Goal

As humanity gets closer to establishing colonies on the lunar and Martian surface, the shift from short-term to deep-space exploration emphasizes a growing need for long-term infrastructure. Existing mission architectures identified in the National Aeronautics and Space Administration (NASA) Technology Roadmap underline the necessity for habitation systems to sustain crew health during space exploration [25].

A significant hurdle to these goals is the transfer between pressurized assets. Relying on Extravehicular Activity (EVA) for routine transfer introduces three main risks:

- Regolith Contamination: Lunar regolith is characterized as an abrasive, glass-like dust. According to NASA/TM-2005-213610, the damage caused by this dust can be sorted into nine categories: Vision obscuration, false instrument readings, contamination, traction reduction, clogging of mechanisms, abrasion, thermal control related issues, seal failures, and inhalation and irritation [26]. An articulating tunnel allows for isolated transfer, thereby reducing the impact of contaminants on internal environments.
- Radiation Exposure: Radiation exposure is a key issue concerning the health of astronauts. Astronauts see an elevated risk of developing cancer, experiencing a decline of the central nervous system, and other degenerative conditions when exposed to space radiation [25]. A pressurized tunnel provides a “shirtsleeve” transfer, maintaining atmospheric shielding while reducing the exposure period.
- Safety and Efficiency: The complex mechanical docking between assets on uneven terrain demands a system that can adapt to misalignments without compromising the integrity of the assets. By minimizing exposure to the environment, the crew transfer tunnel reduces the physical stress on the astronauts.

The South Dakota State University X-Hab team has dedicated much of their time to building a lightweight, articulating crew transfer tunnel to fill these gaps. By adhering to standards provided by NASA, this project focuses on providing a reliable and safe bridge for clean and efficient transportation between lunar as well as Martian assets.

1.2 Design Overview

The proposed design is referred to as BLIMP, or the Bidirectional Lightweight Inflatable Mobile Pathway. BLIMP is designed to connect pressurized surface assets, including rovers, landers, and habitats, to support protected crew and cargo transfer. The system is stored in a condensed configuration referred to as standby mode, allowing it to remain compact when not in use. Once deployed, aligned, and connected, the system transitions into transfer mode, where it provides a pressurized pathway between surface elements.

BLIMP uses a combination of inflatable bellows and winch motors to achieve cable-driven articulation. As the bellows inflate, the winches maintain the assembly in tension, increasing system stability and providing controlled rigidity during extension and alignment. This allows the tunnel to actively position itself between compatible interfaces while maintaining a lightweight and compact architecture.

The tunnel uses an outer softgoods shell to protect the system from the harsh lunar surface environment, including dust, thermal variation, and surface debris. Cameras mounted at each end of the system provide visual feedback for hazard avoidance, operator awareness, and autonomous articulation. These vision systems support alignment with compatible interfaces and allow the system to operate in both autonomous and teleoperated modes.

Once in transfer mode, BLIMP allows astronauts to move between rovers, landers, and habitats without requiring EVA operations or spacesuits. This reduces crew workload, limits dust intrusion into habitable volumes, and improves operational efficiency for lunar surface missions. The system is also scalable in both length and diameter. The baseline design described in this document is best suited for spanning gaps of approximately 4 to 5 ft; however, tunnel length can be increased through repetitive manufacturing and the addition of modular sections. Similarly, the tunnel diameter can be reduced for cargo-only transfer applications, saving mass and volume when a full crew-sized transfer tunnel is not required.

2.0 Preliminary Research

Before beginning BLIMP development, the team established a baseline understanding of current technologies to determine which actuation methods were best suited to the project requirements. Existing active tunnel concepts commonly rely on large electric linear actuators, which can create significant mass and volume penalties for a lightweight surface transfer system. To address this limitation, the team investigated softgoods and inflatable actuation methods as a lower-mass approach for providing both positioning capability and structural support. Cable-driven robotic systems were also evaluated because of their potential to provide precise motion control and fine alignment during berthing operations.

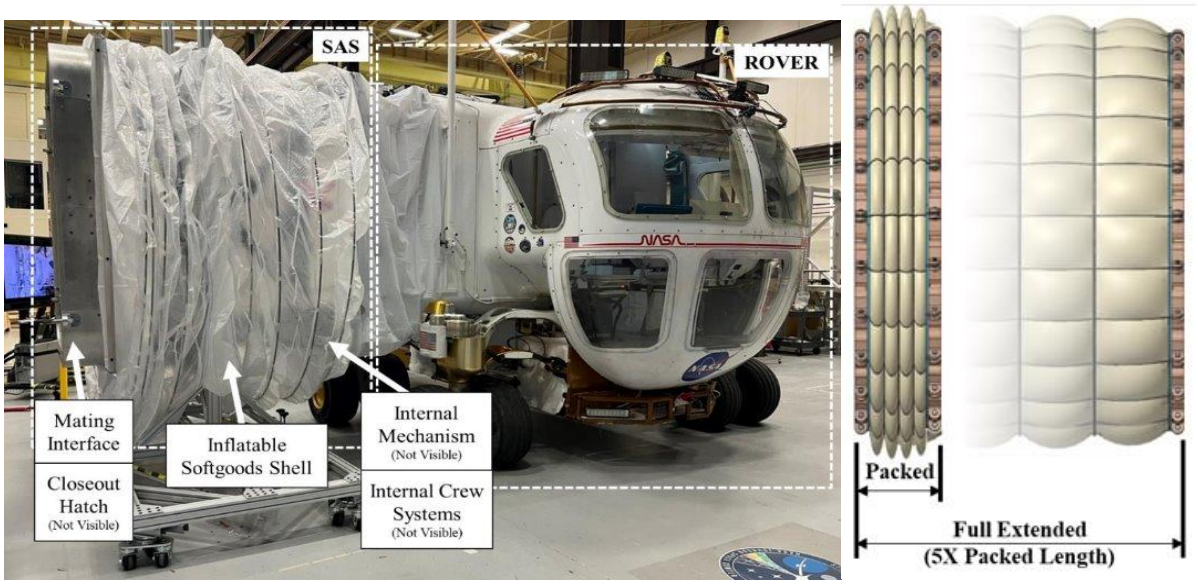

Figure 1: State-of-the-Art [27]

2.1 Existing Actuation Architectures

Preliminary research focused on identifying an actuation methodology which balanced 6-Degree-of-freedom (DOF) docking precision with the complex mass constraints of the M2M X-Hab 2026 solicitation [28]. The team categorized existing technologies into three families to find the optimal State-of-the-Art (SOA) for a deployable tunnel.

2.1.1 Rigid-Body Stewart Platforms

Current state-of-the-art docking, such as the NASA Docking System (NDS), uses Stewart Platform technology. Studies in this area highlight the undeniable efficiency in minimizing impact energy while maintaining accuracy during docking maneuvers [29]. Nonetheless, it must be noted that the “control-to-mass” overhead of this technology is pronounced. To achieve 6-DOF alignment, six independent high-torque linear actuators, and complex sensors are needed. In an articulating tunnel with maximum possible extension, the mass of the required infrastructure was identified as a key bottleneck for its implementation.

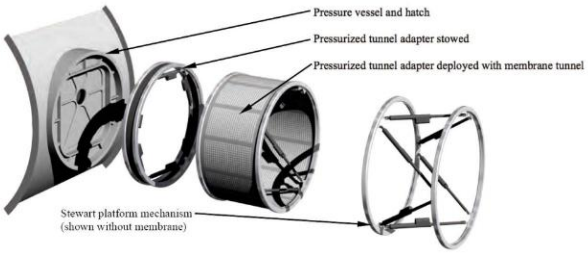

Figure or Table containing sensitive information, or possible unauthorized copyright information has been removed.

Figure 2: Stewart Platform [28][29]

2.1.2 Mechanical Telescoping and Prismatic Systems

Transfer solutions on Earth, such as the airport jetway typically rely on nested telescoping sections driven by prismatic actuators. These systems offer rigidity in simple 1-DOF extension; however, these systems are not suited for the lunar environment. Research shows sliding surfaces create potential pinch points which are highly vulnerable to the abrasive regolith [26]. The friction reduction and seizing risks associated with a telescoping mechanism necessitates extensive sealing or dust mitigation techniques, increasing system complexity, thereby increasing system mass.

2.1.3 Soft Robotics and Cable-Driven Parallel Architectures

To address the mass limitations of rigid systems, the team conducted a review of Soft Robotics and Cable-Driven Parallel Robots (CDPR). These fields offer a conceptual shift by utilizing compliance and tension as the main articulation elements rather than rigid structure members.

Figure or Table containing sensitive information, or possible unauthorized copyright information has been removed.

Figure 3: Cable Drive Parallel Robot [30]

2.1.4 Soft Robotic Principles and Pneumatic Air Beams.

Research into soft robotic systems identified the use of pneumatic “muscles” or flexible pressure vessels as a safe alternative to linear actuators. While mostly seen in the healthcare industry, where rigid actuation is considered hazardous during human-robotic interaction, the inherent compliance of soft robotics makes them an ideal alternative to human-related space infrastructure [31].

Figure or Table containing sensitive information, or possible unauthorized copyright information has been removed.

Figure 4: Military Air Beams [32]

A key terrestrial example of this technology is found in the military Air-Inflated Fabric Structures. These "air beams" are used as a replacement for rigid-frame tents because they offer:

- Low Volume: Air-beam tents can collapse into a small volume for transport.
- Simple Deployment: They eliminate the need for complex assembly of heavy, high-volume frames.
- Resilience: Unlike rigid structures, which are heavy, and nearly impossible to repair on site if bending or fracturing occurs, air-inflated structures are naturally compliant and easily repairable [33].

Alongside the research into soft body actuation, the team evaluated Cable-Driven Parallel Robots (CDPR) for high-span articulation. Research into CDPRs identifies them as a superior alternative for large-scale workspaces where high payload-to-weight ratio is required. A fundamental characteristic of CDPRs is their 'unilateral property,' where cables are only able to exert tension. However, one drawback in the implementation of CDPRs is their required infrastructure. A CDPR can be defined as the number of cables against the DOFs as seen in the following theory [5]:

$$m = n + 1$$

Equation for a fully constrained system

Where:

m = Number of cables

n = Degrees of freedom

The major limitation in this regard is that the CDPR requires significant external support to maintain tension if the system is expected to operate independently.

2.2 Review of Inflatable Softgoods [34]

Historically, inflatable technology has been used extensively in space applications because of its inherent compliance in human contact applications, and because of its capability to be deployed effectively in a vacuum environment, using less mass and volume compared to rigid structures.

2.2.1 A History of Inflatable Structures

The following is a summary of inflatables and their space applications.

March 15th, 1952, Dr. Wernher von Braun is published in Collier's "Man Will Conquer Space Soon" with his contribution "Crossing the Last Frontier". This toroidal concept was to be a livable satellite traveling 20 times the speed of sound at 1,075 miles above Earth with its own gravity. This concept predates NASA by roughly 6 years [35]

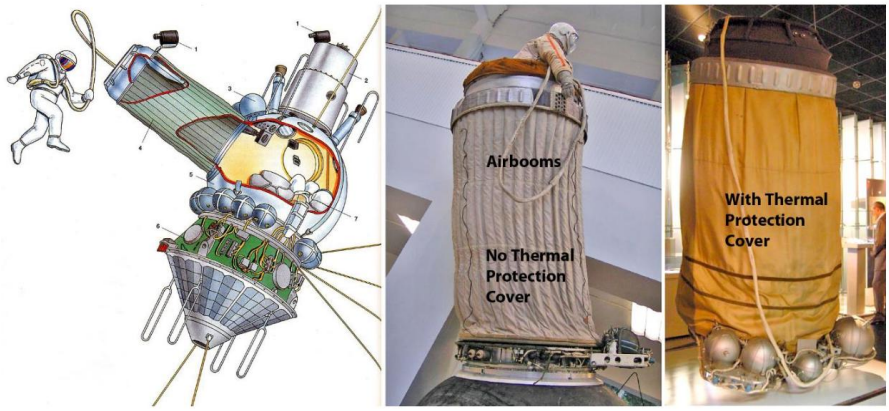

Figure 5: Volga Inflatable Airlock [36]

Figure 5: *Volga Inflatable Airlock*. In 1965 the USSR developed an inflatable airlock which had an inner length of 8.2 ft, a width of 3.9 ft, with a resulting inner volume of 88.3 ft^3, and pressurized to 5.8 psia. The Volga inflatable airlock served as the platform for the first ever EVA, which was designed out of necessity as the Voskhod capsule could not be depressurized. This design was sized for a single crew member and was jettisoned after its single use.

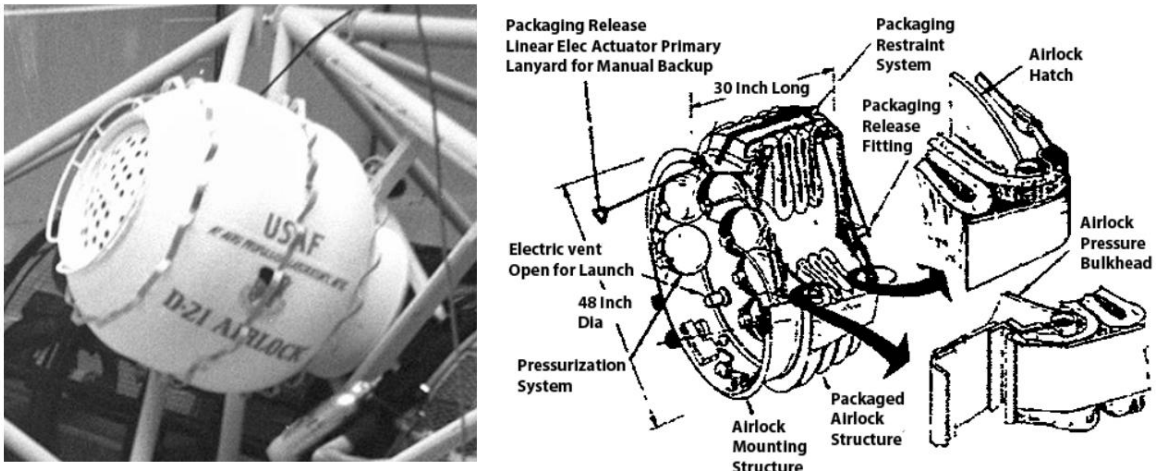

Figure 6: D-21 Goodyear Inflatable Airlock [36]

Figure 6: *D-21 Goodyear Inflatable Airlock*. Following the success of the Volga airlock, the 1960s saw major industrial interest, specifically from Goodyear Aerospace. In this time, Goodyear developed full-scale inflatable infrastructure, most notably the D-21 Goodyear inflatable airlock which was designed for the Skylab mission with a single crew member [36].

During the 1960s, alongside the development of inflatable softgoods, NASA slowly pivoted away from "experimental" softgoods and toward rigid structures. NASA ultimately chose a rigid airlock over the Goodyear airlock for the final mission. This pivot to rigid structures effectively "paused" the development of habitable inflatable infrastructure for nearly two decades, and although the D-21 Airlock never flew, this project paved the way for later projects.

Long after Apollo, NASA returned to inflatables with the TransHab Project. The goal of the TransHab project was to design a multi-use living space for a human mission to Mars.



Figure 7: (a) TransHab Module [34] (b) SDU II Inflated Shell updated with Index Stitches (c) TransHab SDU Hydrostatic Test [37]

Some key outcomes of the TransHab Project were as follows:

- A full-scale test article was fabricated and fully deployed in a vacuum at NASA JSC in 1998.
- **Figure 7 (c)**: *TransHab SDU Hydrostatic Test.* A development unit was hydrostatically pressurized to 60 psig without failure, proving that inflatables could be as, or more stable than rigid systems.
- The project pioneered a multi-layered shield consisting of open-cell foam, and Nextel capable of providing superior protection against micrometeoroids and orbital debris (MMOD)

After the conclusion of TransHab in 1999, NASA shifted its focus into characterizing performance of inflatables in space.



Figure 8: (A-B) Creep Burst Test (C) Damage Tolerance Testing [34]

Figure 8 (C): *Damage Tolerance Testing.* This figure shows the leak before burst testing (damage tolerance testing) initially completed in 2012. The goal of this testing was to show if the article would leak rather

than burst catastrophically. This test showed that the material indeed has inherent leak-before-burst capabilities.

Figure 8 (A-B): *Creep Burst Test.* The creep burst test had the goal of quantifying the creep life knockdown which is a reduction in structural lifespan. At this point, NASA already had data on individual webbing straps, now the goal was to understand how a complete assembly affected performance. This test showed that a full assembly does in fact negatively impact resistance to creep with the article failing after 49 minutes.

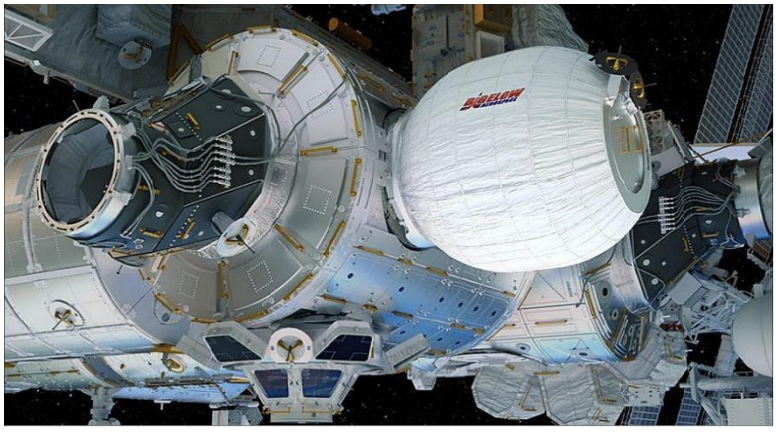

Figure 9: Bigelow-Expandable-Activity-Module (BEAM) [38]

Figure 9: *Bigelow-Expandable-Activity-Module*. In 2016 Bigelow sent up the inflatable activity module which was derived from patents created as a result of the TransHab project. This project was to serve as a demonstration for human-rated inflatable structures in space. BEAM is still on the International Space Station ten years after integration (2026).

2.3 Environmental Hazards

2.3.1 Thermal Extremes

During peak lunar night and day conditions, surface temperatures can range from approximately -173 °C to 127 °C [39]. These extreme thermal fluctuations require surface assets to withstand significant thermal cycling throughout operation. Additionally, crewed areas must be properly insulated to maintain habitable internal conditions, while temperature-sensitive equipment must also be adequately protected to ensure it remains within operational limits.

2.3.2 Abrasive Environment

Protecting surface technologies from both lunar and Martian regolith is a critical design consideration for long-duration extraterrestrial operations. Regolith on both bodies consists of extremely fine, abrasive particles capable of penetrating seals and causing damage to exposed surfaces and electronic systems. Additionally, dust particles in both environments can become electrostatically charged, causing them to strongly adhere to anything that carries a charge. In addition to this, Mars experiences dust storms, causing increased wear on electronics as dust is thrown throughout the atmosphere [40].

2.3.3 Vacuum Effects

The lunar and Martian environment present significant challenges due to their atmospheres being near vacuums [41]. Due to there being essentially no atmosphere, there is virtually no convective heat transfer, only radiative heat transfer. This greatly complicates thermal management, requiring unique solutions to reject sufficient heat from vital system components. Furthermore, the large pressure differential between pressurized systems and the surrounding near-vacuum environment increases stress on pressure-retaining structures and seals, requiring careful design to ensure adequate material strength, structural integrity, and leak resistance.

2.3.4 Radiative environment

The Moon and Mars have a negligible atmosphere and also lack global magnetic fields [42]. As a result, much higher levels of space radiation reach the lunar and Martian surfaces compared to Earth. This presents many challenges as humanity makes strides to put humans back on the lunar and Martian surfaces. The radiation found on the lunar and Martian surfaces can cause both short and long-term health conditions, including acute radiation sickness and cancer. Additionally, radiation can cause single event effects, causing minor data errors that can lead to later system malfunctions [43]. Another consideration for engineers when designing space technology is the change in material properties. For example, metals tend to reduce in plasticity and ductility, while increasing in hardness [44]. This means that engineers have to ensure that all space systems that support human life are adequately shielded from the radiation on the lunar and Martian surfaces.

3.0 Supported Documentation

To aid in the support of the design of the solution system, supporting documentation was used to outline key requirements of both the conceptual and prototype system as well as the breakdown of the project. Each subsection of both the conceptual and prototype design have the listed key requirements that pertain to them as well as other imposed requirements related to various subsystems.

3.1 Project Breakdown with Requirements Overview

The project breakdown flow chart can be seen below in **Figure 10**. The overall project was split into two main categories, prototype and conceptual. These sub-categories have the same subsystems so requirements can be directly compared to the two as well as identical subsections within each subsystem. Not listed are con-ops and system operations due to being related to all subsystems for both prototype and conceptual.

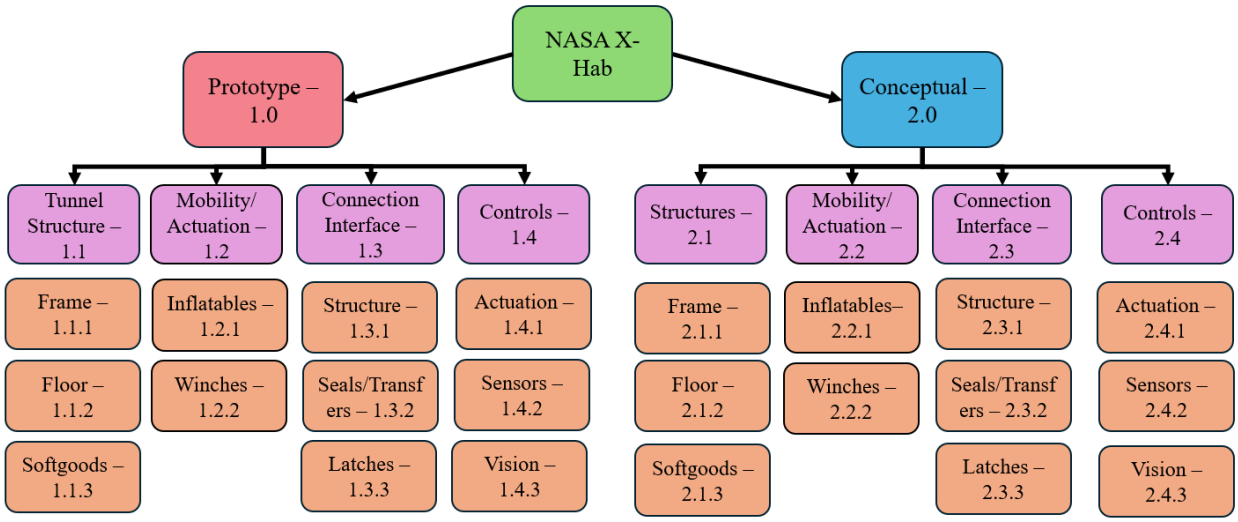

Figure 10. Project Breakdown Structure

In the following sections, the key requirements for both the prototype and conceptual system will be elaborated on and how these requirements flow down into the subsections. Additional inferred requirements are not listed in sections 3.2/3.3 but will be elaborated on during the specific design sections.

3.2 Conceptual Requirements Breakdown

The conceptual system requirements were developed to define the key functions needed for a pressurized transfer tunnel operating in lunar and Martian environments. The system must be capable of operating on both the Moon and Mars while providing accurate articulation for docking alignment, as described in Requirements 1 and 2. Because the purpose of the tunnel is to allow crew and cargo transfer without EVA suits, requirement 3 addresses the need for a pressurized and climate-controlled internal environment. Structural efficiency is also critical for space applications, so Requirement 4 focuses on minimizing system mass while maintaining the required factor of safety. Requirement five emphasizes scalability, ensuring that the design can either support multiple interface types or be easily manufactured in different configurations. To improve operational reliability, Requirements 6 and 8 address the need to maintain position during power loss and continue functioning under single-point failure conditions. Since dust intrusion is a major concern for lunar and Martian surface systems, Requirement 7 was included to protect the internal transfer environment and mechanical components. Finally, Requirement 9 ensures that the system aligns with NASA visual and audio safety standards to support safe operation around crew members.

L1-C01	System shall be operable on the Moon and Mars
L1-C02	System shall articulate to align with an accuracy of one inch for three directional dimensions and 2.5° for three angular measurements
L1-C03	System shall be pressurized and climate controlled to prevent the need for EVA suits
L1-C04	System shall be mass optimized to be as lightweight as possible maintaining desired FOS
L1-C05	System shall use a scalable design, either one-size-fits-all or easily manufacturable
L1-C06	System shall maintain its position during loss of power
L1-C07	System shall prevent dust intrusion during use
L1-C08	System shall maintain functionality under single-point failure
L1-C09	System shall align with NASA standards for visual and audio safety

A new mass requirement was derived from the lander payload capacities. Based on these values, the total system mass was limited to 500 kg, with an additional 25% mass margin implemented to support design growth and account for uncertainty during development. For most lander options, the system would not be delivered as a standalone payload. Instead, it would be launched already attached to a larger piece of surface infrastructure and stored in a condensed configuration along the side of that structure. The exception is the Astrobotic Griffin lander, which has a smaller payload capacity and would require the system to be delivered as a dedicated standalone mission. Therefore, the 500 kg mass requirement provides a practical upper limit that supports compatibility with multiple lunar delivery platforms while still allowing margin for structural, actuation, pressurization, and control subsystems.

Lander	Capacity (kg)
Blue Origin MK2 [45]	20,000
Blue Origin MK1 [45]	3,000
Intuitive Machine Nova [46]	2,500
Astrobotic Griffin [47]	625
SpaceX Starship [47]	15,000

The conceptual software requirements were developed to define the control, monitoring, communication, and safety functions needed for operation of the system. The primary software function is autonomous alignment, which is addressed in Requirement 1 using an alignment program capable of controlling the system during docking operations. To maintain operational flexibility, Requirement 2 includes a tele operable mode that allows a human operator to take control when manual intervention is needed. Requirements 3 and 4 focus on software communication and perception capabilities, including the ability to manage multiple video feeds, support AprilTag image recognition, and handle internal and external system communications. To improve reliability, Requirement 5 requires routine system checks, while Requirement 6 ensures that emergency stop functionality is included for safe operation. Requirement seven addresses data storage by requiring monitoring data to be saved until it is ready to be communicated. Requirement eight focuses on providing an easy-to-interpret user interface for human control and system monitoring. Finally, Requirements 9 through 11 ensure that the software can process sensor inputs related to the internal environment, external environment, interface cleanliness, and successful pressurization.

CSW-01	Software shall contain alignment programs to autonomously control alignment
CSW-02	Software shall include tele operable setting in case of human need to control
CSW-03	Software shall handle multiple video feeds for human viewing and image recognition of AprilTags
CSW-04	Software shall handle communications internal and external to the system
CSW-05	Software shall perform routine checks of the system to reinforce system usability
CSW-06	Software shall handle emergency stop functionality
CSW-07	Software shall store monitoring data until it needs to be communicated
CSW-08	Software shall provide an easy to interpret user interface for human control and monitoring
CSW-09	Software shall handle sensor inputs that monitor system's internal environment
CSW-10	Software shall handle sensor inputs that monitor system's external environment
CSW-11	Software shall handle sensor inputs for validating clean connection interface and pressurization success

The conceptual hardware requirements were developed to define the physical components needed to support system control, alignment, safety, and environmental regulation. Requirement one addresses the need for onboard computing hardware, including a CPU and GPU, to process control commands, sensor data, video feeds, and autonomous alignment functions. Requirement two focuses on vision hardware, such as cameras and LiDAR, to support navigation, interface detection, and alignment with external structures. Requirement three identifies the need for motors and actuators to physically articulate the system during alignment and docking operations. Requirements 4 and 5 addresses, operator, and crew safety by requiring alarms for audio indications and lights for visual clarity during system use. Requirements 6 and 7 ensure that the hardware includes sensors for monitoring both internal and external environments, as well as validating the condition of the connection interface. Finally, Requirement 8 addresses the need for thermal and pressurization components to regulate the internal environment and maintain conditions suitable for pressurized crew or cargo transfer.

CHW-01	System shall have a CPU and GPU for handling main functions
CHW-02	System shall have cameras/LiDAR for vision needs
CHW-03	System shall have motors/actuators for movement
CHW-04	System shall have alarms for noise indications
CHW-05	System shall have lights for visual clarity
CHW-06	System shall have sensors for monitoring internal and external environment
CHW-07	System shall have sensors for validating connection interface
CHW-08	System shall have thermal/pressurization components for regulating internal environment

3.3 Prototype Requirements Breakdown

The prototype was developed to validate the core functionality of the conceptual system, with the primary focus on the articulation method and control approach identified in Requirements 1 and 2. Because the system is intended to operate near personnel, safe operation was also a major consideration. Requirement three addresses the inclusion of safety features to reduce the risk of accidents during testing and operation. Requirement four focuses on developing an effective user interface that allows the operator to control and monitor the system. Another key function to validate was the connection interface method, which is addressed in Requirement 5 through the simulated latching mechanism. Finally, because the system uses inflatable components, Requirement 6 was added later in the project to ensure that the inflatables are properly inspected, safe to use, and capable of withstanding the intended operating pressure.

L1-PR01	Prototype shall validate articulation method of conceptual design
L1-PR02	Prototype shall autonomously align to simulated interfaces
L1-PR03	Prototype shall include safety features to minimize risk during operation
L1-PR04	Prototype shall provide a user interface for easy control and monitoring
L1-PR05	Prototype shall simulate latching mechanism of the connection interface
L1-PR06	Prototype inflatable shall go through documented quality inspection to mitigate risks of leaks or bursts

Prototype software requirements were developed to define the key functions needed to operate, monitor, and control the physical prototype. Requirement one focuses on providing system data through a telemetry-based user interface so the operator can easily monitor prototype performance during testing. Requirement two addresses the use of telemetry feedback to actively adjust the actuation system and support controlled

movement. Requirement three requires the software to combine multiple camera feeds into an easily viewable format for the user, improving situational awareness during operation. Requirements 4 and 5 focus on human control by requiring the software to connect to a controller, read operator command inputs, and respond accordingly. Finally, Requirement 6 ensures that the software can manage communication between the connected microcontrollers, allowing the different electronic subsystems to work together as one integrated prototype.

PSW-01	Software shall provide all data to use through telemetry user interface
PSW-02	Software shall use telemetry to actively adjust actuation system
PSW-03	Software shall compile camera feeds for easily viewable methods to the user
PSW-04	Software shall connect to controller for human operation
PSW-05	Software shall read all command inputs and react accordingly
PSW-06	Software shall handle communication between microcontrollers

Prototype hardware requirements were developed to define the physical components needed to operate and validate the prototype system. Requirement one addresses the need for Raspberry Pi and Arduino hardware to support processing, control, and communication between prototype subsystems. Requirement two focuses on cameras for vision support, allowing the operator to view the system during operation and providing the foundation for future interface detection. Requirement three identifies the need for motors and actuators to physically move and articulate the prototype during alignment testing. Requirements 4 and 5 address operator awareness and safety by requiring alarms for audio indications and lights for visual clarity during operation. Because the prototype uses inflatable bellows, Requirement 6 was included to ensure relief valves can vent excess pressure above the defined safety threshold. Requirement seven requires pressure sensors to monitor the bellows during inflation and operation, while Requirement 8 identifies solenoids as the primary hardware used to open and close airflow paths throughout the pneumatic system.

PHW-01	System shall have RaspberryPi/Arduino for processing needs
PHW-02	System shall have cameras for vision needs
PHW-03	System shall have motors/actuators for movement
PHW-04	System shall have alarms for noise indications
PHW-05	System shall have lights for visual clarity
PHW-06	System shall use relief valves to vent excess pressure above safety threshold
PHW-07	System shall use pressure sensors for bellow monitoring
PHW-08	System shall use solenoids to open and close airflow

3.4 Requirements Flow Down

This project was divided into two primary design paths: the prototype system and the conceptual system. Each design path was further decomposed into major subsystems, including actuation, structure, connection interface, and controls. These subsystems were then broken down into lower-level subcomponents to support requirement flow down and traceability throughout the design process. The following table identifies each subsystem and subcomponent, and shows how the applicable requirements are allocated across the system architecture.

1.1 Tunnel Structure	1.1.1 Prototype Exoskeleton	L1-PR01
	1.1.2 Prototype Floor	L1-PR01
	1.1.3 Prototype Softgoods	L1-PR01
1.2 Mobility/Actuation	1.2.1 Inflatables	L1-PR01
		L1-PR02
		L1-PR06
		PSW-02
		PHW-03
	1.2.2 Winches	L1-PR01
		L1-PR02
		PSW-02
		PHW-03
1.3 Connection Interface	1.3.1 Structure	L1-PR05
	1.3.2 Seals/Transfer	L1-PR05
	1.3.3 Latching Mechanism	L1-PR05
1.4 Controls	1.4.1 Actuation	L1-PR01
		L1-PR02
		PSW-02
		PHW-03
	1.4.2 Sensors	L1-PR01
		L1-PR02
		L1-PR03
		PSW-02
		PSW-04
		PSW-05
		PSW-06
		PHW-01
		PHW-06
		PHW-07
		PHW-08
	1.4.3 Vision	L1-PR02
		L1-PR03
		L1-PR04
		PSW-01
		PSW-03
		PHW-02
		PHW-05
2.1 Tunnel Structure	2.1.1 Conceptual Exoskeleton	L1-C01
		L1-C04
		L1-C05
	2.1.2 Floor Assembly	L1-C02
		L1-C04
		L1-C05
	2.1.3 Outer Softgoods	L1-C01
		L1-C03
		L1-C04
		L1-C05

2.2 Mobility/Actuation	2.2.1 Inflatables	L1-C02
		L1-C05
		L1-C06
		L1-C08
		CHW-03
	2.2.2 Winch System	L1-C02
		L1-C06
		L1-C08
		CHW-03
2.3 Connection Interface	2.3.1 Structure	L1-C01
		L1-C03
		L1-C04
	2.3.2 Seals/Transfer	L1-C01
		L1-C03
		L1-C07
	2.3.3 Latching Mechanism	L1-C02
		L1-C03
		L1-C07
2.4 Controls	2.4.1 Actuation	L1-C02
		L1-C06
		L1-C08
		CSW-01
		CSW-02
		CHW-03
	2.4.2 Sensing Suite	L1-C01
		L1-C02
		L1-C03
		L1-C06
		L1-C07
		L1-C09
		CSW-04
		CSW-05
		CSW-07
		CSW-09
		CSW-10
		CSW-11
		CHW-01
		CHW-06
		CHW-07
		CHW-08
	2.4.3 Vision Capabilities	L1-C02
		L1-C09
		CSW-03
		CSW-08
		CHW-02
		CHW-05
		L1-PR06
		PSW-02
		PHW-03

3.5 Gantt Chart

This project schedule outlines the major design, review, testing, documentation, and final delivery milestones for the X-Hab tunnel project from late August 2025 through early June 2026. The early portion of the schedule focuses on project definition activities, including receiving the project, completing the state-of-the-art and standards reviews, and creating design matrices to support concept selection. The first semester then transitions into SDR preparation, initial testing, the Systems Definition Review, and the senior design conference. During the second semester, the team moves into preliminary inflatable testing, the Preliminary Design Review, and the Critical Design Review before shifting heavily toward paper development, NASA progress review preparation, and final project documentation. The final phase of the schedule is centered around completion of the final paper, class project deadline, Engineering Expo deliverables, disclosure materials, school delivery, NASA completion and evaluation, journal paperwork, and Johnson Space Center travel. Overall, the timeline shows the progression from research and concept development into testing, formal NASA reviews, final reporting, and project closeout.

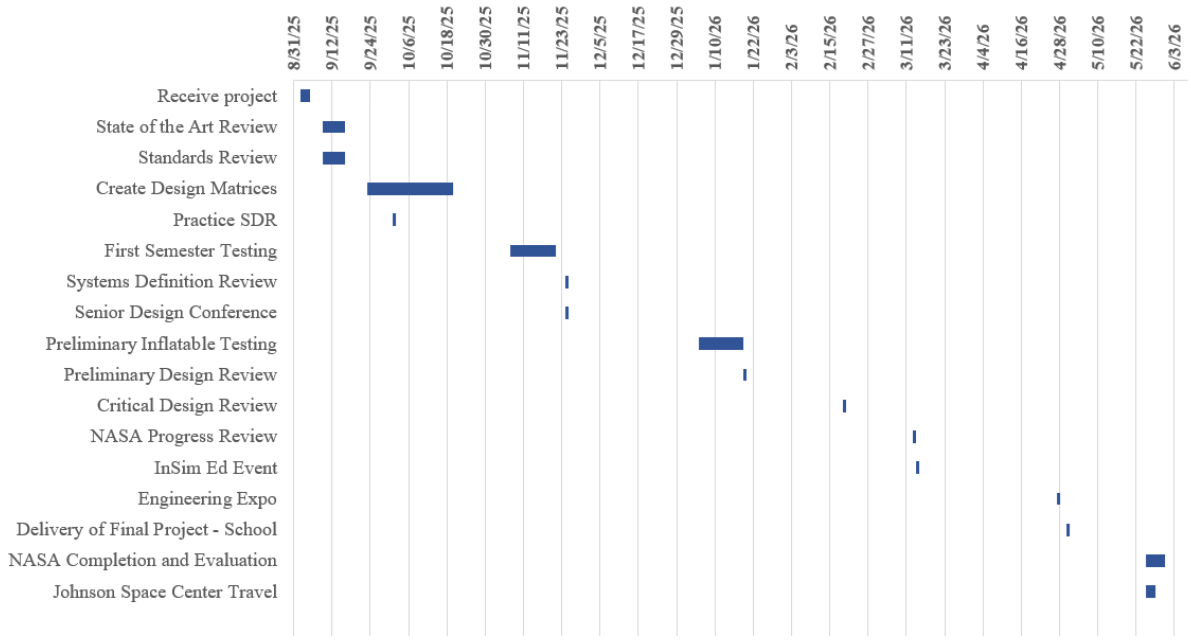

3.6 Risk Register

The project risk register was used as a living document to track and reduce the highest-priority risks throughout the design, fabrication, and review process. In total, 13 risks were identified, with the most significant risks focused on the project timeline and schedule, inflatable bellows fabrication, 3D printing fabrication, sealing and leakage, and structural reliability. The risks shown in the main register were selected because they had the highest priority levels and the greatest potential impact on project completion. Initial scoring was based on impact and probability, while the new score represents the reduced priority level after mitigation actions were applied. Early procurement was treated as one of the most important schedule controls because receiving materials sooner allowed the team to address fabrication issues, testing delays, and redesign needs without jeopardizing the overall timeline. Several fabrication-related mitigations have already been implemented, including the use of laser cutting to improve inflatable seam consistency, and quality checks to reduce heat-sealing and leakage issues. As the bellow manufacturing process was refined through the PDR then CDR, the team added additional inflatable-related risks. The risk matrix shows the before-and-after movement of the highest-priority risks, demonstrating how mitigation actions reduced several risks from high-priority regions into more acceptable ranges.

Risk ID Number	Risk Description	Impact Description	Impact Level	Probability	Priority Level	Mitigation or Control Strategy	New Score
1	Shipment/Order Delays	Different materials will need to be used or it doesn't get done	5	4	20	Order materials as soon as possible so if delays happen there is	8
2	Structural Failure	Tunnel could collapse and fail	5	2	10	Ensure adequate FOS and fabrication, and inspect structural	4
10	Inconsistent Fabric Cutting	Creates inconsistent seams along the inflatable resulting in higher pressure areas	4	3	12	Use laser in shop to consistently cut and seal edges	2
11	Failed heat sealing	Results in seams that are not sealed and will leak	5	3	15	Will need to quality check all seams during fabrication process	2
12	Failed 3D print	Increases material usage and extends fabrication time-line	3	3	9	Order excess material, have contingency plans in place in case extra	3

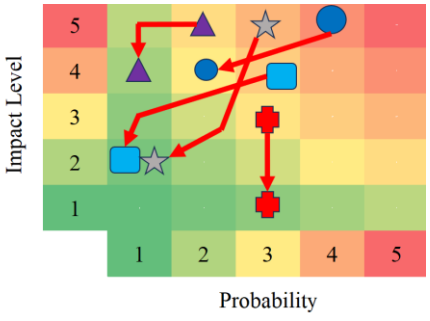

Figure 11. Partial Risk Register and Risk Mitigation Chart

4.0 Early Trade Studies and Design Iterations

Early conceptual iterations focused on a variety of technologies which aimed to fulfill key requirements of being lightweight, scalable, and maintaining six DoF. The use of electric and pneumatic actuators, driving systems, and electric motors contributed to early design trade studies between different concepts. After thoroughly completing design matrices (See section 4.2) focused on the main subsystems as well as refining requirements, two primary conceptual designs were presented in the preliminary design review.

4.1 Early Concepts

The primary focus of the early concept iteration was finding current technologies with DOF capabilities from the SOA and reusing these to meet the lightweight, articulating requirements. Previous concepts for pressurized tunnel transfer used large, heavy stewart platforms for electric actuation and precise alignment. Early concepts aimed to provide the same level of control while either increasing system usability or decreasing system mass. Some early concepts can be seen below in the following figures. These concepts used inflatables, winches, driving bases, and scissor lift mechanisms to perform actuation.

4.1.1 Early Concepts and Outcomes



Figure 12: AutoCAD-to-Blender, Linear Actuator Concept

Figure 12: *AutoCAD-to-Blender, Linear Actuator Concept*. This figure shows the initial concept for a linear actuator-based design utilizing six total linear actuators as well as a driving base, and a horizontal scissor lift to control axial extension. This design served as a baseline for this project.



Figure 13: Scissor Lift, Roller Concept

Figure 13: *Scissor Lift, Roller Concept*. A scissor lift concept which allowed control over each interface. One hoop represents a bulkhead on both ends, and the center to articulate independently. The entire system

was to be driven by a rack-and-pinion system and utilized rollers to allow for easy actuation. One drawback to this concept is the pinch points derived from a rolling mechanism, leading to potential softgoods strain.



Figure 14: Driving Base Concept

Figure 14: *Driving Base Concept*. A preliminary concept for a driving base scissor lift which achieved actuation in the z direction via a scissor lift coupled with a linear actuator.



Figure 15: Pulley Tunnel Concept

Figure 15: *Pulley Tunnel Concept*. This figure shows a tunnel articulated by a system of pulleys, driven by a driving base.

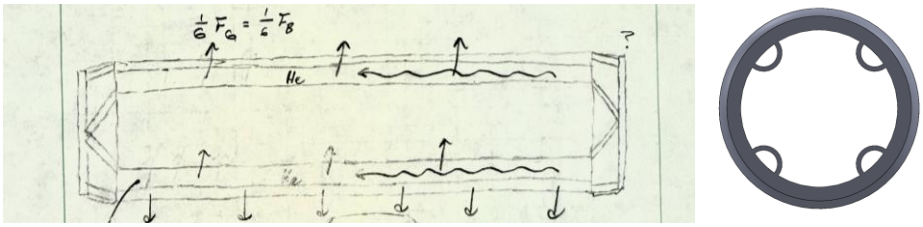

Figure 16: Gas/Fluid Actuation System

Figure 16: *Gas/Fluid Actuation System*. A design which utilized air beams to extend and served as a lightweight alternative to heavy, rigid actuators. Original concept utilized on board helium supply.

After evaluating the trade studies, the team selected inflatable actuators for the final design due to their low mass and volume.

4.2 Design Matrices

Focused areas for design optimization were identified by reviewing the project requirements and determining which subsystems had the greatest impact on system performance. Five primary design matrices were developed for the conceptual system: actuation method, actuator placement, pathway design, structural material selection, and vision system. Each matrix used a 1 to 5 scoring scale, where five represented the most favorable performance. Weighting factors were assigned by the team based on mission importance and the relative impact of each design consideration.

The actuation method matrix compared different approaches for producing motion and alignment. Although a single actuation method did not fully satisfy all design needs, the matrix helped identify the value of combining low-mass inflatable actuation with a more controllable mechanical system. As a result, inflatable actuation was retained for axial extension because of its low mass and scalability, while winches were added to address limitations in precision, controllability, and alignment.

Actuation Method		Design Components			
Design Considerations	Weightage (%)	Electric Linear Actuators	Inflatable Actuators	Rotary Actuators	Inflatable Tubes
TRL	5.00%	4	2	4	2
Dust Mitigation	5.00%	4	3	4	2
Precision and Accuracy	32.50%	5	1	5	2
Power Consumption	12.50%	3	4	1	3
System Mass	45.00%	1	4	2	4
Overall Rating	100%	57.00%	57.50%	61.00%	60.50%

Figure 17. Actuation Method Design Matrix

The actuator placement matrix evaluated how actuator location affected articulation, packaging, complexity, and system performance. This trade helped guide the decision to place the main actuation elements near the tunnel ends, allowing the connection interfaces to be controlled during alignment while maintaining a compact system layout. The pathway design matrix compared internal transfer surface options and supported selection of a lightweight pathway approach that could accommodate crew and cargo transfer while remaining compatible with the tunnel's condensed and extended configurations.

Actuation Design		Design Components					
Design Considerations	Weightage (%)	Stewart Platform	Actuator on ends	Actuators in middle	Driving Base	Scissor Lift	Winches/Pulleys
TRL	5.00%	4	4	3	5	3	4
Scalable	17.50%	2	3	2	4	4	4
Precision and Accuracy	22.50%	5	4	3	1	3	3
Power Consumption	10.00%	2	4	3	1	3	3
System Mass	32.50%	2	5	3	1	2	4
Complexity	7.50%	2	3	2	4	4	3
Dust Mitigation	5.00%	4	4	4	1	2	3
Overall Rating	100%	54.50%	77.00%	53.00%	33.00%	51.50%	66.50%

Figure 18. Actuation Design Matrix

The structural material matrix compared aluminum, titanium, steel, and carbon fiber reinforced polymers. Aluminum and CFRP were closely rated, but CFRP was selected because its lower density and lightweight nature better supported the project's mass-optimization goals.

Structural Exoskeleton Material		Design Components			
Design Considerations	Weightage (%)	Aluminum	Titanium	Steel	Carbon Fiber Reinforced Polymers
Thermal Cycling	10.00%	4	5	2	1
Ductility	5.00%	4	3	5	1
Strength	25.00%	2	4	4	4
Abrasion Resistance	10.00%	2	4	5	1
Density	40.00%	4	2	1	5
Repairability	10.00%	5	2	4	1
Overall Rating	100%	68.00%	61.00%	55.00%	67.00%

Figure 19. Structural Material Design Matrix

The vision system matrix compared LiDAR, standard RGB cameras, and stereo cameras based on technology readiness, mass, precision and accuracy, power consumption, capability, and range. This trade supported the use of a camera-based vision system because cameras provide a lower-mass and lower-power solution while still enabling autonomous alignment, operator viewing, and future hazard detection capabilities.

Vision System		Design Components		
Design Considerations	Weightage (%)	LiDAR	Standard RGB Camera	Stereo Camera
TRL Level	5.00%	5	5	5
Volume	10.00%	2	4	5
Precision and Accuracy	30.00%	4	2	3
Power Consumption	10.00%	2	4	3
Capabilities	35.00%	3	3	4
Range	10.00%	5	4	3
Overall Rating	100%	68.00%	62.00%	73.00%

Figure 20. Vision System Design Matrix

Overall, the design matrices were used as decision-support tools rather than the sole basis for final selection. The results helped guide the conceptual architecture toward a lightweight, scalable, and actively controlled tunnel system.

4.3 System Definition Review Iterations

From the early design iterations and the design matrices, two conceptual designs were formed. One used a driving base, scissor lift, and small electric stewart platform for alignment and the other used inflatable actuators to handle articulation. In addition to these two concepts, some early testing was completed as part of SDSU's class requirements. The testing primarily focused on the first design iteration where the driving/vision was tested as well as a 3D printed scissor lift.

4.3.1 SDR Final Concept

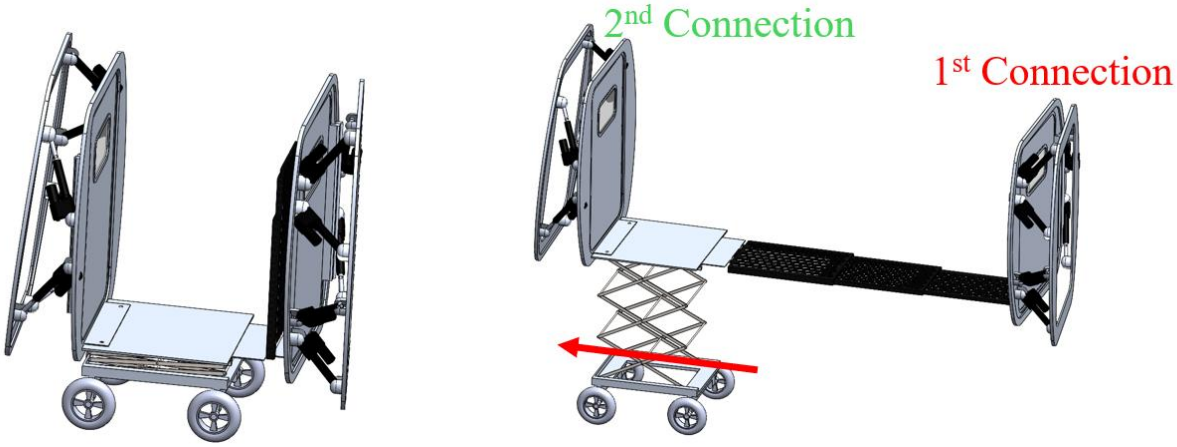

Figure 21: System Definition Review Design Iteration

Figure 21: *System Definition Review Design Iteration*. The first design as seen was designed to handle large misalignment between connection interfaces as well as offer advanced mobility around the Lunar base. The driving base was intended to be powered allowing the system to autonomously move around the base to various connection interfaces when requested. Additionally, for far travel the system could be towed by a different rover to the desired location. Once the base would be in position the scissor lift would rise until the height of the first connection interface was aligned, allowing the small electric stewart platform on the end to perform the final adjustments and initialize the first connection. After successfully verifying the first connection, the base would drive towards the second interface where the telescopic floor and softgoods outer layer would freely extend until the second interface was aligned. If the height of the interfaces were different than the scissor lift could adjust this as well.



Figure 22: SDSU Rover Performing Autonomous Alignment

Figure 22: *SDSU Rover Performing Autonomous Alignment*. To verify this concept early on, initial testing was completed on the manufacturing and design process on a working scissor lift as well as autonomous alignment to AprilTags. Using a past SDSU rover and its equipped camera, AprilTag detection software was implemented and used to perform autonomous alignment with the rover's four-wheel tank steering driving base. Since this rover had the same drivetrain configuration as the early concept, getting it to work with the rover early into the design process would have directly helped the efforts later in the project.

4.3.2 Scissor Lift Validation

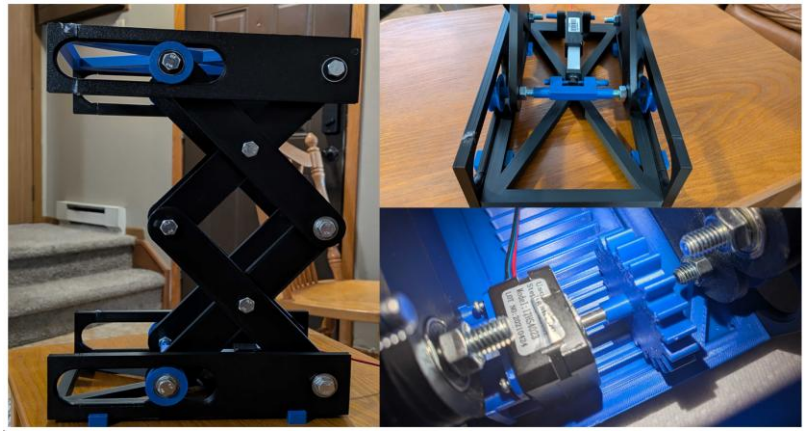

Figure 23: Early Design Validation - Motor Driven Scissor Lift

Figure 23: *Early Design Validation - Motor Driven Scissor Lift*. To validate the use of a scissor lift, a small-scale prototype was developed. The team designed the prototype to function with two interchangeable bases and equipped one base with a rack-and-pinion system, while the other was driven by a linear actuator. The linkages and the base were designed to be 3D printed out of PLA filament. Each half of the scissor lift utilizes four linkages to lift objects, as shown in Figure 23. At the end of one of the linkages on each side, a roller was placed on both the top and bottom of the scissor lift to enable sliding as the system raises and lowers.

The first base tested was the linear actuator setup, which used a 12V 3-inch actuator. The actuator was controlled by a motor controller attached to an Arduino Mega. A potentiometer was attached to provide the input for the actuator. The scissor lift was then raised and lowered to evaluate the actuator's ability to actuate the lift. The lift was overall smooth and showed promising functionality for the lift mechanism.

The second base actuation method that was tested is a rack and pinion gear system. The actuation of the system was provided by a stepper motor. The stepper motor was also controlled via the use of a motor controller attached to an Arduino Mega. Like the first system, the motor controller is powered by a 12V battery. The pinion gear rotated a fixed amount back and forth based on the hard-coded information to have a steady oscillation of the system. The stepper motor that was used did not provide sufficient torque to the system and could not actuate the system through its full range of motion. The stepper motor lacked sufficient torque to actuate the system through a full range of motion, confirming why industrial scissor lifts typically utilize linear actuators.

4.4 Preliminary Design Review Conceptual Design

Further concept iteration focused on the inflatable actuator design because of its lightweight construction, scalability across multiple tunnel lengths, and ability to collapse into a compact form factor during loading, unloading, and stowage. The inflatable actuators were arranged in a ring configuration to help the softgoods maintain a symmetrical circular shape under pressurization while preserving a clear transfer pathway through the center of the tunnel. Although the inflatable actuators provided extension capability, they did not independently provide retraction or the ability to correct pitch and yaw misalignment. To address this limitation, four winches were implemented on each end of the system to keep the tunnel in tension and provide controlled adjustment of the connection interfaces. These winches allow the system to retract and

make small angular corrections in pitch and yaw during alignment. Together, the inflatable actuators and winches provide control over three of the six required degrees of freedom. To account for the remaining degrees of freedom, the connection interface incorporates cone-shaped alignment features that slot into the receiving interface as the tunnel extends toward the desired connection point. These cones provide tolerance for small translational misalignments and help guide the interface into its final position, allowing the system to achieve the remaining three degrees of freedom needed for alignment and connection. The system also includes six external cameras to support visibility and alignment during operation. Each side of the tunnel has two cameras mounted along the top and one mounted along the bottom, providing coverage of the surrounding interface area. The middle ring includes external mounting points that can support additional hardware, such as antennas or solar panels, when the system is connected in extended-use mode. These mounting provisions allow the system to improve operational efficiency by supporting communication, power generation, or other mission-specific equipment. The floor structure is made from titanium and does not include cutouts, providing a continuous and durable walking surface through the tunnel.



Figure 24. Preliminary Design Review Concept Iteration

Key discussion points from the preliminary design review centered around the number of bellows and how many were necessary, developing a solution to accommodate roll misalignment, better defining the misalignment, and developing a plan for prototyping the bellows.

5.0 Conceptual Design

The conceptual system is intended for use on the lunar and Martian surfaces to provide a lightweight, scalable, and actively articulating pressurized transfer pathway. The system is designed to connect rovers, landers, habitats, and other pressurized surface infrastructure, allowing crew and cargo to transfer between assets without requiring EVA suits. The system remains condensed in standby mode when not in use and extends into transfer mode during alignment and connection operations.

The actuation approach uses inflatable actuators and winch assemblies together to provide controlled extension, retraction, and alignment. The inflatable actuators provide axial extension force, while the winches maintain tension and control the orientation of the connection interface. Operating internal pressure is intended to match the pressure of the connected surface assets, allowing the tunnel to serve as a compatible pressurized pathway between systems. Structurally, the internal system consists of aluminum, carbon fiber reinforced polymer, and titanium components selected to reduce mass while maintaining the required factor of safety. An outer softgoods shell surrounds the internal structure and provides pressure retention, dust protection, thermal protection, and environmental shielding from the harsh lunar or Martian surface environment.

The system is also designed with scalability in mind. The tunnel length can be increased through the addition of repeated structural and inflatable sections, while the diameter can be reduced for cargo-only transfer applications where a full crew-sized tunnel is not required. The system is intended to operate most effectively at prepared connection interfaces with universal standardized interface geometry, reducing alignment uncertainty and improving repeatable connection performance.

5.1 System Specifications and Overall Design

The primary specifications of the baseline conceptual design are summarized in Figure 25. The system has a compressed length of 36 in. and an extended length of 52.25 in., allowing it to remain compact during storage while providing usable reach during operation. The outer diameter is 105 in., and the inner diameter is 86.5 in., providing internal clearance for crew transfer. The floor width and cargo width are both 32 in., allowing the internal pathway to support both crew movement and cargo transfer. The estimated system mass is 393 kg (867 lb.), which represents the full structural and mechanical system mass without electronics or the applied mass margin. Figure 25 shows the conceptual tunnel with a 6 ft human included for scale.

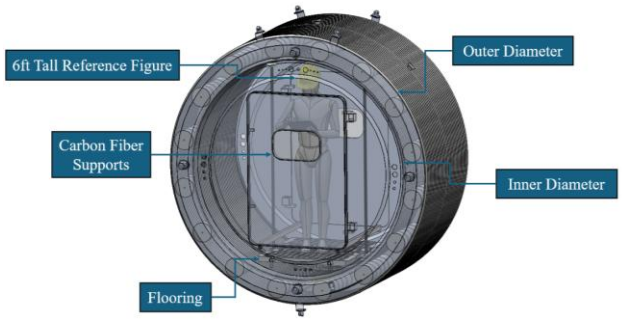

Figure 25.Transparent System with 6' Tall Man Inside

Compressed Length	36”
Stretched Length	52.25"
Outer Diameter	105"
Inner Diameter	86.5"
Floor Width	32"
Cargo Width	32"
System Mass	393 kg.

5.2 Actuation Subsystem

The actuation of the tunnel is completed by 16 inflatable actuators. These actuators used a Vectran outer layer for strength with a 1000D nylon inner bladder to hold air. These 16 bellows will inflate to a 6 psi difference to provide sufficient thrust and buckling resistance. Additionally, each side of the tunnel has four winches, eight in the total system, to perform adjustments during inflation. This will allow the system to accommodate misalignment in the pitch and yaw offsets. Lastly, to aid in the roll misalignment, an angular rack and pinion was implemented on the connection interface.

5.2.1 Conceptual Actuation Specifications

Each bellow can condense and extend over a range of 12 to 24 in. For the two-bellow prototype configuration, this allows the full system to extend and condense between 36 and 52.25 in, with the final range limited by the flooring assembly. The bellows provide a maximum axial force of 4,240 lb_f and a maximum buckling resistance of 94,400 lb_f. When compared to the total system mass of 393 kg, evaluated at a lever arm length of 26.13 in, the system can support itself when it is not connected on both ends. The lever arm was taken as half of the total extended system length, representing the distance from the fixed support point to the approximate center of mass of the unsupported tunnel section. The equations and supporting calculations for these values are discussed in Section 7.2 as part of the MATLAB analysis.

Direction of Misalignment	Max Offset	Limiting Factor
X-Axis (Direction of system extension)	3’ – 4.25’	The folding and telescopic floor can lay flat within this range. Bellows easily extend and contract at this length.
Y-Axis (Width of system)	1.86”	Connection interface cones max displacement while still functioning using the max displacement between upper and lower diameters
Z-Axis (Height of system)	1.86”	Same as Y-Axis
Pitch	10°	Winch motor functionality and max moment on inner components
Yaw	10°	Winch motor functionality and max moment on inner components
Roll	10°	Combine infrastructure level requirements (ground <3°), system roll capabilities (15°), and connection interface cone misalignment (2.3°)

Using these three methods of articulation, the systems max misalignment accommodation can be seen in the above table.

5.2.2 Bellow Design

The conceptual inflatable bellow should take all which is learned in this paper and make appropriate adjustments which maximize force output, minimize buckle, and column instability.



Figure 26: Conceptual Bellow

Figure 26: *Conceptual Bellow.* The Bellow which is employed for space applications should optimize the manufacturing process in such a way that each bellow is nearly identical to ensure proper balance and accuracy.

The bellow is treated as a softgoods stack with its own bladder, and restraint layer to take on the stress accumulated from internal pressure.

- Bladder: The bladder should be made of 1000D urethane coated nylon which remains flexible at low temperatures. This is crucial for the design because the main articulation method is the inflatable actuator, and as highlighted in previous sections, must be capable of withstanding harsh temperature swings.
- The conceptual bladder should utilize 1000D Nylon:
    - Lower Denier PU Nylons exhibit greater flexibility, however these materials are more prone to burst, as well as display a poor response to abrasion. The system is expected to cycle underneath a restraint layer creating a need for a balance between flexibility and durability [48].
    - Higher Denier PU Nylons such as 1680D are strong but incredibly stiff and heavy, ballooning to a fabric weight of 360GSM, making a medium classic plain-weave the best choice [48].
- Restraint Layer: As described in **section 5.3.2**, Vectran is the primary choice for a dynamic restraint layer as it is not inherently brittle and does not share the same self-abrasive nature as alternatives [47] [49]. Furthermore, even though the Bellows are not designed to remain inflated for extended periods of time, creep still plays a crucial role in material selection for the bellows as a safety factor is dependent on these scenarios [50]. This means that because Vectran displays “effectively zero” creep, it is the ideal choice to decrease the likelihood of failure.
    - Balanced Plain Weave: A balanced plain weave was chosen using Vectran UM (Ultra-Modulus) because it provides the high-modulus structural stiffness required to minimize fabric elongation, proving to be the most robust design capable of delivering equal support against axial forces and hoop stresses [49].

A conceptual bellow manufacturing process was also prepared using concepts learned as a result of the X-Hab Project. The original plan for SDSU’s X-Hab was to manufacture a bellow to the maximum capabilities then, present it to NASA. The goal was to design a process which would yield a NASA-grade prototype at student cost.

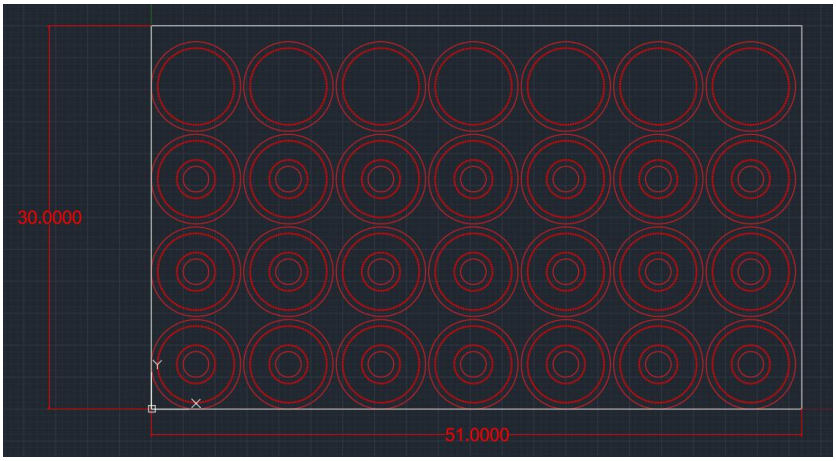

Figure 27: Conceptual Vectran Laser Cut

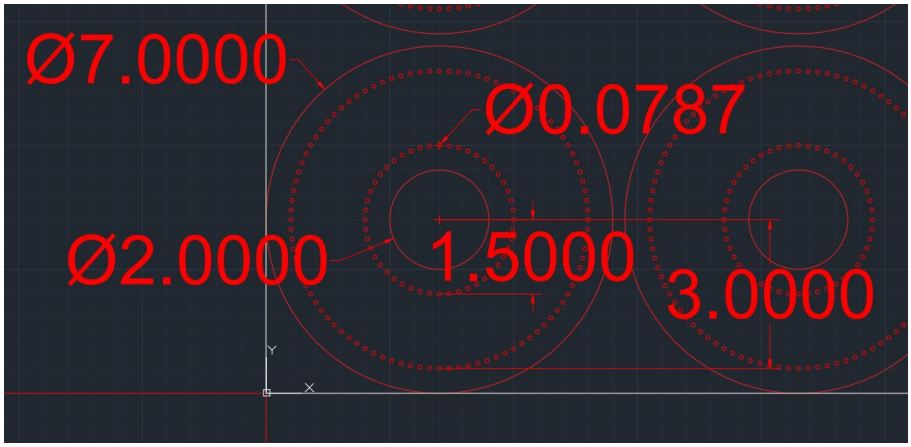

Figure 28: Internal Ring Cut

The manufacturing strategy for the bellows utilizes high-performance materials as well as CNC-guided assembly to ensure reliable structure.

Material Specs:

- Restraint Layer: 1500D Vectran (2x2 Twill).
- Pressure Liner (Bladder): TPU-Coated 70D Nylon.
- Structural Thread: 1000D Bonded Vectran thread was chosen to ensure seams which match the mechanical properties of the parent material.

Manufacturing Workflow:

1. Using an Epilog Fusion Pro 48, the Vectran and TPU layers are cut to precise geometry. A high-power pass was chosen for the outer profiles; the goal was to cauterize the edges or reduce fraying. A low power pass to pre-drill 2.0 mm holes for assembly.
2. Due to the difficulty working with Vectran derived from its mechanical properties, traditional sewing methods were rejected. Instead, a manual lockstitch method was chosen to allow for more control of the heavy threads.

3. A custom TPU-Coated Nylon drawing would be made in which the bladder is 5% larger than the restraint layer to ensure that the internal pressure loads entirely on the restraint layer, shielding the TPU seams from mechanical stresses.

This manufacturing process was to be evaluated but due to time, availability of materials, and budget constraints, this process was never tested.

5.2.3 Winch Assembly Design

During axial extension of the inflatable bellows, the tunnel assembly must remain in tension to maintain stability and control alignment. To accomplish this, the system uses eight winch assemblies, with four winches mounted on each connection interface face. These winches provide active control of the connection interface and are used primarily to adjust pitch and yaw during alignment. The winches must be capable of resisting the thrust force generated by the pressurized bellows. For sizing purposes, the total bellows thrust force was divided across the four winches on the active face. This force was then converted into the required winch torque using a four in diameter operational spool. In addition to resisting the bellows thrust force, the winches were sized to retract the full 12 in actuation stroke in approximately 15 seconds. With a four in diameter spool, this requires a spool speed of approximately 3.82 rpm. Based on this analysis, each winch must provide a minimum torque of 220 lb_f-ft, corresponding to an ideal required motor power of approximately 119 W per winch. Because the required motors are expected to be relatively large, the winch assemblies are stored within the connection interface cones to reduce interference with the tunnel interior and external softgoods. A gear set is then used to redirect the motor shaft rotation by 90°, allowing the motor output to align with the cable spool while maintaining a compact packaging configuration.

5.3 Structural Subsystem

The conceptual structural system consists of an internal exo-ring, two end interfaces, flooring, vertical carbon fiber supports, and outer softgoods layers. Although the term exo-ring is used, this structure is located inside the pressurized tunnel volume but outside the primary walking path. Together, these components provide the primary support structure for the tunnel during operation. The exo-ring and vertical supports are designed to use T700 carbon fiber reinforced polymer (CFRP) to achieve a high strength-to-weight ratio while minimizing overall system mass. This mass optimization is especially important for lunar delivery, where the structure must remain lightweight while still maintaining the required factor of safety.



Figure 29. Conceptual Internal System Structure

The structural load path is shared between the internal CFRP structure and the outer softgoods layers. The exo-ring carries loads from the inflatable bellows, winch assemblies, pneumatic components, and floor structure, while the softgoods layers contribute to pressure retention, environmental protection, dust resistance, and overall tunnel containment. Although CFRP materials can be sensitive to temperature fluctuations and material property changes in extreme environments, the internal structural components are located within the pressurized volume. As a result, they are expected to remain within a temperature-controlled environment during operation, reducing thermal exposure concerns compared to externally mounted structural components.

5.3.1 Interior Structure

The interior structure consists of exo-ring support, a passive folding floor assembly, and two vertical support members. The primary purpose of this structure is to provide rigidity to the tunnel interior while also creating a stable walking surface for crew transfer. The floor assembly is constructed from a similar CFRP material and is designed to passively fold and telescope as the tunnel transitions between standby and transfer configurations. In standby mode, the floor folds upward along the centerline to reduce stored volume. As the tunnel extends, the floor deploys into a usable walking surface and accommodates changes in tunnel length during alignment and articulation.

The two vertical supports provide additional strength to the internal ring structure while also serving as mounting and storage locations. These supports house removable cargo beams used to help roll cargo through the tunnel during transfer operations. They also provide attachment points for internal lighting and camera systems. The exo-ring provides the main mounting structure for the bellows and pneumatic components, including pressure sensors, solenoids, and relief valves. In addition, the exo-ring supports the winch assemblies used to control system actuation and alignment.

5.3.2 Softgoods Shell

As highlighted in section 2.4, the harsh lunar and Martian environments require shielding which can mitigate the impact of environmental factors on cargo, infrastructure, and most importantly humans. To protect astronauts as they traverse the tunnel, a complex 11-layer laminate was used. See the following:

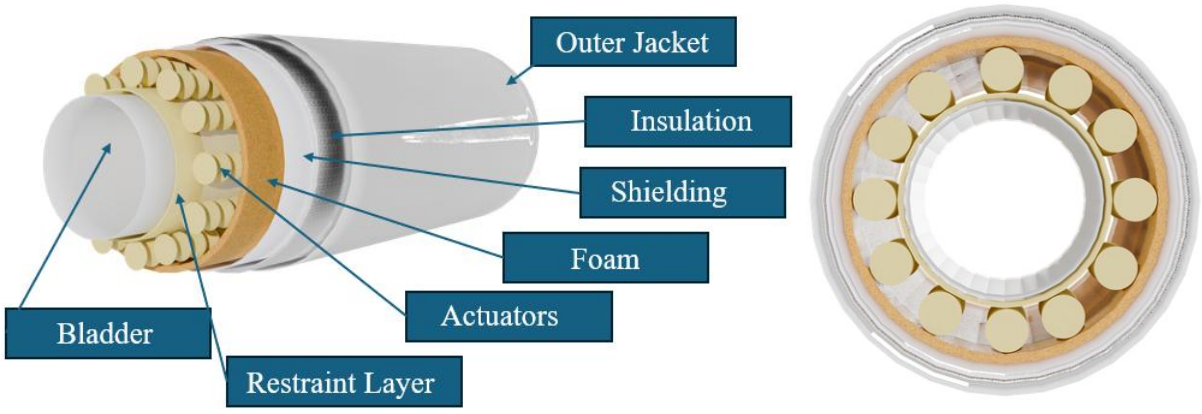

Figure 30: Softgoods Isometric & Front View

Table 1: Softgoods Selection [51], [49], [52], [53], [54], [55]

Layer	Material	Areal Density (kg/m^2)	Mean Diameter (m)	Area (m^2)	Mass (kg)
Bladder	Double PU-Nylon	0.225	2.20	4.23	0.95
Slip Layer	PTFE Film	0.112	2.20	4.23	0.47
Restraint Layer	Biaxial Vectran	1.680	2.20	4.23	7.11
Slip Layer	PTFE Film	0.112	2.20	4.24	0.47
Inflatable Actuators		N/A	2.42	4.65	N/A
Slip Layer	PTFE Film	0.112	2.63	5.07	0.57
Foam	Solimide	5.000	2.65	5.09	0.32
Shielding	Nextel-312	0.899	2.66	5.12	4.60
Insulation	Aluminized Mylar	0.450	2.66	5.12	2.31
Outer Jacket	Betacloth	0.227	2.66	5.13	1.17

Table 1: *Softgoods Selection*. BLIMP's conceptual softgoods stack and each layer and the respective conceptual mass, leading to a total softgoods mass of 35.9 kg (79.15 lb.).

A detailed breakdown is as follows:

1. Bladder: The bladder houses the internal pressure of the tunnel, for the articulating crew transfer tunnel design, this layer needs to be flexible under low temperatures.

- Double Polyurethane coated Nylon layering was chosen for the bladder. For redundancy, the bladder should have two layers, this way the system will not fail under a single point.

2. Restraint Layer: The restraint layer houses all the mechanical stresses (hoop and axial load) which come from the internal pressure.

- For BLIMP, 1500D Biaxial Vectran is chosen. Vectran is known as a "zero creep" material, and while research shows that this is not actually the case [56]the effective creep seen in Vectran is significantly lower than alternatives such as Kevlar-49. The biaxial arrangement of the weave allows for the Vectran fibers to align with the primary stress paths seen in a pressurized cylinder. Furthermore, because the tunnel is designed to articulate in 6-DOF, the restraint layer is expected to bend and crease in cycles without weakening, and while alternatives show tremendous strength, they are often brittle and suffer from self-abrasion when creased, making Vectran a NASA standard for dynamic structures [49].

3. Nested Actuators: This is the dedicated bellow section. BLIMP utilizes a nested actuator design in which the bellows are nested inside of the softgoods stack to increase deployment efficiency.
4. Foam: An open-cell foam is integral in the softgoods stack as this layer dissipates any energy from broken-up hypervelocity micrometeoroids. The foam layer must be open-celled as it cannot trap air, whereas something like Styrofoam (which is closed-cell) would expand in a vacuum.
    - Solimide is chosen for this layer because not only is it open cell, but it also has NASA heritage, seen in the TransHab project, and flown on Orion[51] [57].
5. Shielding: The goal of this layer is to shatter incoming micrometeoroids into less lethal fragments whose energy can be dissipated by the foam layer.
    - The selected material for BLIMP is Nextel 312. This material is very capable when it comes to shocking projectiles, but, since the material is also ceramic, it maintains critical mechanical properties at temperatures up to 1200°C, making it the ideal choice over alternatives like Kevlar 29 which begins to degrade at 160°C[54] [58].

6. Insulation: This layer serves as the primary defense against radiant heat transfer.
    - Aluminized Mylar is chosen for the softgoods stack as the aluminum coating reflects up to 97% radiant heat. While Kapton might seem like the better option because of its high-heat capabilities, it is heavier and more prone to tearing which are two main concerns for BLIMP [59].
7. Outer Jacket: This layer is the only layer which is directly exposed to the environment.
    - Beta Cloth (PTFE-impregnated Fiberglass) is selected due to its' resistance to AO erosion. Furthermore, Beta Cloth is made from woven silica glass fibers which will not burn [60].
8. To facilitate geometric shifting and mitigate material-material friction during articulation, thin Polytetrafluorethylene (PTFE/Teflon) Film slip layers are strategically placed in the softgoods stack. As BLIMP undergoes 6 Dof articulation, the high-tenacity structural layers slide past each other, these layers must do this smoothly.
    - To facilitate this smooth articulation PTFE Film is introduced which is chosen due to its low coefficient of friction (≈ 0.04) [61].

5.4 Connection Interface

The conceptual connection interface uses two identical 6061 aluminum end plates that act as the external sealing and hatch structures during operation. Aluminum 6061 was selected for its strength, machinability, availability, and mass efficiency. The end plates function as pressure-containing bulkheads while also transferring operational loads from the tunnel into the connected infrastructure. These loads include internal pressure loads, seal compression loads, winch loads, bellows thrust, and crew or cargo transfer forces.

The interface geometry includes angled cone features that provide passive, coarse alignment during final approach. These features allow the tunnel to slot into the receiving interface during actuation and help guide the system into its final seated position. The cone geometry allows approximately 1.86 in. of lateral tolerance on any side. Small angular misalignments can also be tolerated, although most pitch, yaw, and roll error is intended to be corrected by the actuation system before final seating. The interface is designed around a universal standardized geometry to support connection with rovers, landers, habitats, and other pressurized surface assets.

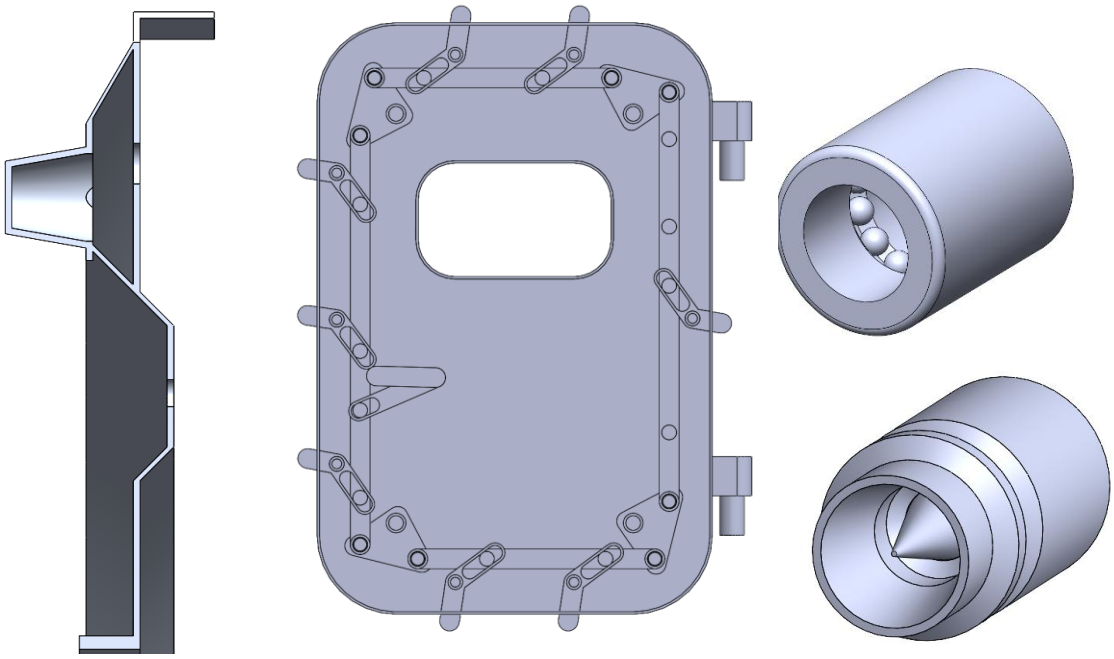

Figure 31: Connection Interface Cross Section; Hatch Locking Mechanism; Fluid Transfer Ports

Sealing is achieved using three large O-ring-style seals located around the connection interface. Seal sensors are positioned between the seal locations to verify contact and support leak detection before transfer operations begin. The system also includes pressure sensors on both sides of the interface to verify pressure equalization before opening the hatch. Once the interface is seated and latched, the system checks latch engagement, seal contact, port connection status, and pressure conditions before entering transfer mode. If a leak or pressure drop is detected, the hatch closes, the door locks, and the tunnel isolates itself from the internal crew environment.

The latching system uses four linear actuator-driven latch points. As each actuator extends, a wedge-style geometry pulls the interface inward and compresses it against the seals. This creates a tighter mechanical connection while improving seal compression around the interface. The connection sequence can be treated as two distinct operations: first, the latch actuators capture and pull the tunnel into the receiving interface; second, the door actuators release after sealing and pressure equalization are confirmed. The hatch opens inward and is designed so that it does not block the transfer route when open. A manual override is included in case the powered latch system fails.

The interface also includes automatically connected utility ports for breathable air, inflatable air, thermal control, data, and power. The breathable air-ports support internal cabin air exchange, while the inflatable air-ports are used for the softgoods and bellows systems. Thermal ports are intended to support a CCHP-style thermal control loop, and the data and power ports provide general connectivity between the tunnel and the connected infrastructure. These ports are protected with covers or sealed features during standby mode to reduce dust intrusion and are arranged by function to improve crew understanding and reduce training complexity.

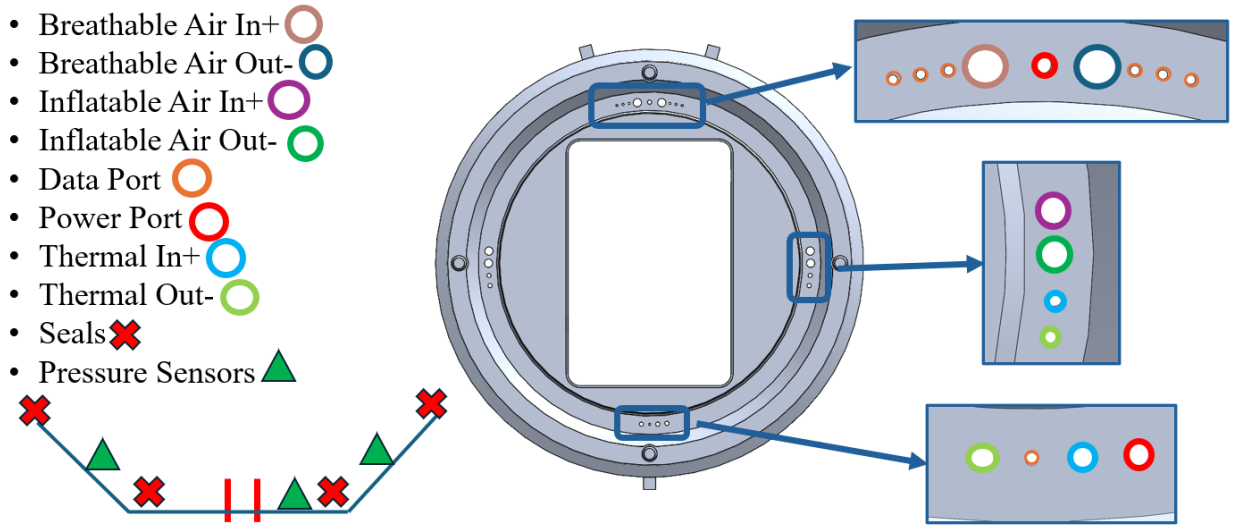

Figure 32: Connection Interface Pressure Sensors, Seals, and Transfer Ports Layout

Additional sensors and inspection features are included to support safe connection. Load sensors detect when contact is made during docking, latch sensors verify engagement, and port sensors confirm successful utility connection. Cameras are used to inspect the interface before sealing. A 10 in. by 20 in. passive viewing window allows crew to see through the interface without relying on electronics, and electrostatic dust shielding is used to protect the window from regolith accumulation. Together, the angled guide geometry, redundant seals, latch actuators, sensors, utility ports, and passive viewing features allow the connection interface to support repeatable, pressurized transfer between compatible lunar or Martian surface assets.

5.5 Dust Mitigation

Due to the abrasive and adhesive nature of lunar regolith, dust mitigation is a critical design consideration for the tunnel system. The proposed design uses a layered mitigation approach consisting of electrodynamic dust shielding, protective coatings, sealed interfaces, and physical isolation of sensitive mechanisms. Electrodynamic dust shields will be applied to exposed solid surfaces where visibility and sensing are required, including the bulkhead windows and external camera covers. These shields will use transparent indium tin oxide to maintain optical clarity while helping prevent regolith accumulation on critical viewing surfaces. EDS was selected because of its high technology readiness and demonstrated relevance to lunar dust mitigation.

Additional dust protection is provided through surface coatings and sealing features. The outer softgoods shell will use a lotus-style coating to reduce dust adhesion and limit buildup on exposed fabric surfaces. At the hatches and connection interfaces, O-ring gaskets will be used to help maintain pressure containment while preventing dust intrusion into the internal transfer volume. The system also benefits from the placement of actuation components inside the pressurized tunnel volume, allowing the outer softgoods layer to function as a protective dust sock around the moving mechanisms. Multiple O-ring seals are incorporated to provide redundant dust and pressure protection, so that if one sealing layer is compromised, secondary barriers can continue to protect the tunnel interior and connection interface.

5.6 System Scalability

To address the need for scalability, the system was designed so that additional bellows, internal structural rings, and floor assemblies can be incorporated with minimal changes to the overall architecture. Each added section increases the condensed length by approximately 11.5 in. and the extended length by approximately 49.25 in., while increasing total mass by approximately 93 kg. This effectively doubles the tunnel's length capability while only increasing the system mass by about 25%. Additional sections could also be implemented beyond a four-section configuration, provided that structural integrity, pressurization performance, and articulation loads are revalidated.

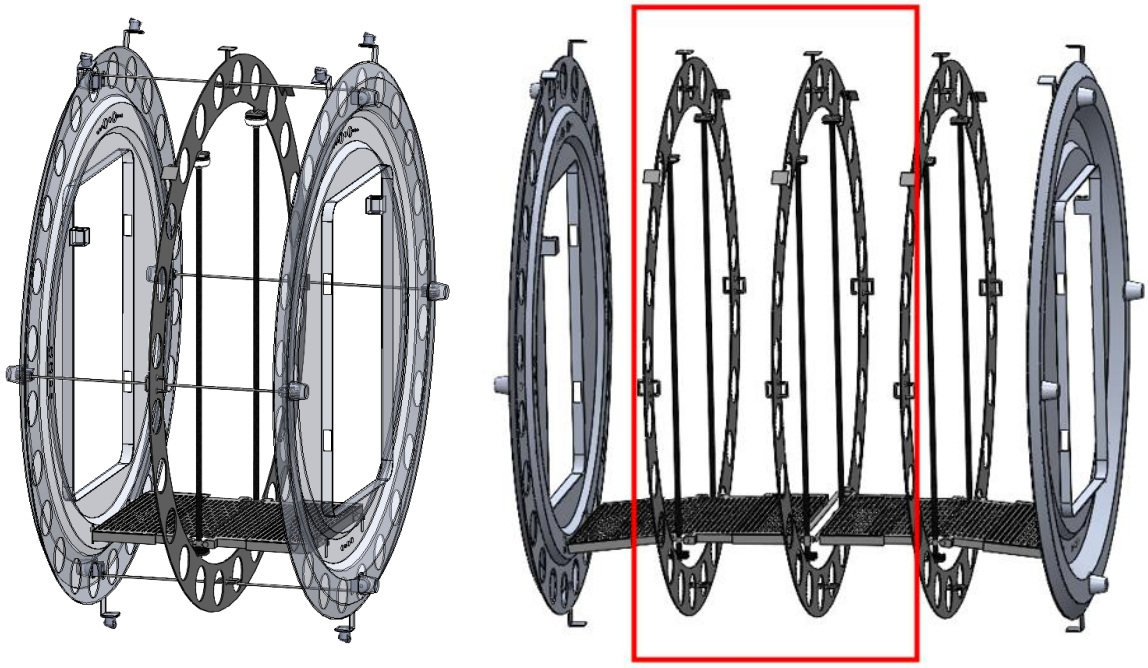

Figure 33: Two Section Assembly; Scaled Four Section Assembly

Increasing the number of sections also improves the system's articulation capability. In the two-section configuration, the winch system primarily controls the pitch and yaw of the connection interface. However, when additional structural rings are connected in series, the winches can provide distributed control along the tunnel length. This allows the system to form a controlled, snake-like curvature, improving side-to-side positioning capability and enabling greater alignment flexibility between pressurized surface elements.

Figure or Table containing sensitive information, or possible unauthorized copyright information has been removed.

Figure 34: Flexible Robot Arm [62]

Figure 34: *Flexible Robot Arm*. For diameter scalability, the system architecture can be adapted by reducing the structural ring and bellows diameters to match the intended transfer application. This approach was demonstrated through the subscale prototype, which was built at approximately 45% of the conceptual system diameter. A reduced-diameter configuration could be used in applications where pressurized transfer is beneficial, but crew ingress and egress are not required.

In a cargo transfer scenario, the tunnel diameter could be reduced to the minimum size required for cargo movement, the hatch interface could be redesigned for the smaller transfer path, and the rigid floor assembly could be replaced with a roller conveyance system. This would allow cargo to move smoothly between pressurized elements without requiring a tunnel sized for human passage or larger crew loads. As a result, a cargo-focused variant could reduce system mass, power demand, and structural loading in mission scenarios where a full human-sized tunnel is unnecessary.

5.7 Conceptual Vision and Controls

The conceptual vision system is designed to support autonomous alignment, hazard detection, leak identification, and transfer monitoring. The tunnel is equipped with seven total cameras, with three exterior cameras located on each end of the system and one camera located inside the tunnel. All cameras include pan-and-tilt capability, allowing the system to inspect a wider field of view and giving the operator additional flexibility during teleoperated control.

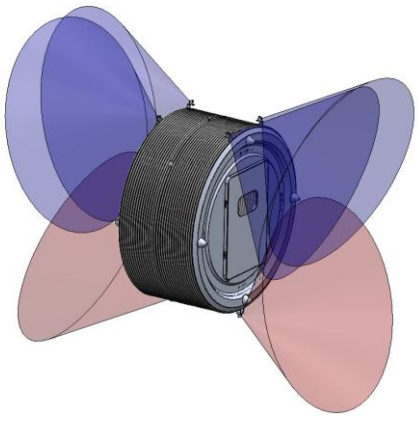

Figure 35: Conceptual Vision System

Figure 35: *Conceptual Vision System*. The three exterior cameras on each end work together to support autonomous alignment with the connection interface. The outer camera layout includes one lower camera and two upper cameras. The two upper cameras are positioned approximately 45° off the vertical plane, creating a 90° separation between them. This arrangement provides redundant vision coverage between the two upper cameras, while the upper and lower cameras provide partial field-of-view overlap at longer distances. Although the system could still function with only one operational exterior camera on each side, alignment response would be slower and may require human intervention through teleoperation.

Autonomous alignment is performed using image recognition of geometric hatch features rather than relying only on artificial markers. Image recognition would run locally on the tunnel's onboard computer, with footage and processed data transferred through a wired connection at the interface. Once connected to surface infrastructure, this data could then be routed through the connected asset's higher-powered communication system. The exterior cameras also support hazard detection near the tunnel ends, with the lower camera handling the majority of hazard monitoring due to its view of the interface area, ground region, and surrounding obstacles.

The vision system includes dual RGB and thermal camera capability. Thermal imaging is used to support leak detection by identifying gas escaping from the system when the gas temperature differs from the surrounding environment. If a leak is detected, the system would pneumatically isolate the affected area and alert the crew. This leak response would be used alongside pressure monitoring and other onboard sensors to reduce the risk of continued gas loss or inflatable over-pressurization.

The internal camera is used to monitor transfer operations inside the tunnel. It can verify that the floor is deployed, the transfer path is clear, lighting is functional, and no objects are obstructing crew or cargo movement. Interior and exterior lights are included to support camera visibility during low-light or shadowed operations, which is especially important for lunar south pole environments.

To reduce optical degradation from lunar regolith, the cameras are equipped with EDS. The recognition software would be trained before flight using simulation, Earth-based testing, and relevant environmental conditions, with at least one day of thermal-vacuum testing planned to evaluate performance in a more representative environment. The operator can manually control the cameras and override autonomous functions when needed. If the alignment target is lost during autonomous operation, the system pauses actuation. If the target is required before teleoperation begins, the system can resume autonomous alignment.

6.0 Concept of Operations and System Operations

The operation of the BLIMP system on the Lunar and Martian surface depends on how it will be intended to be used. The bidirectional design increases usability through rover relocation, allowing the tunnel system to be used in many different operational modes all around the base. The main three modes defined later are the primary-use mode, extended-use mode, and standby mode. Additionally, in preparation for various mission scenarios or emergency different contingency plans would be in place. Lastly, the limitations of the system as well as the assumptions pertaining to the existing infrastructure level of the base are listed and required before system may be used continuously.



Figure 36: Rover-to-Rover Connection

6.1 Operational Modes

The primary-use mode defines a bidirectional surface to surface pressurized transfer system that enables docking between crewed assets such as habitats, landers, and pressurized rovers without requiring predefined orientation.

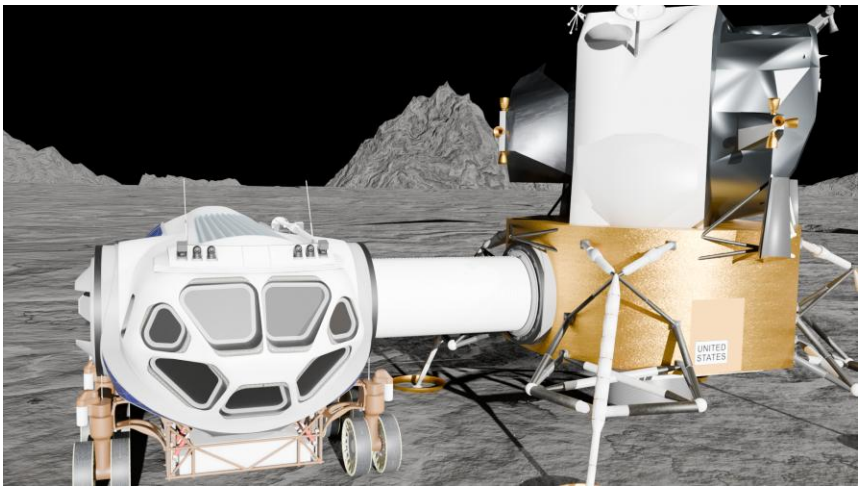

Figure 37: Lander-to-Rover Connection

This allows flexible integration across mission architecture. A rover initiates a docking request, and the tunnel verifies system readiness, safety interlocks, and interface availability. After verification, the tunnel transitions into an active sensing mode and activates externally mounted vision systems to detect an

AprilTag fiducial marker. The system then designates the correct forward interface, resolves bidirectional symmetry, and assigns actuation authority for the docking sequence. Once the rover reaches a nominal staging position and transmits a ready-to-dock state, both the rover and tunnel independently verify a fully static condition through continuous pose monitoring over a five-second interval. This static verification eliminates residual motion prior to deployment. The tunnel then initiates axial extension using environment-specific pressurization. In lunar vacuum conditions, axial extension is driven by passive gas expansion from stored low-pressure sources. In Martian atmospheric conditions, axial extension is driven by a controlled electrically powered compressor system using stored or filtered ambient gas. Inflatable ring actuators generate controlled axial translation toward the rover docking interface while maintaining structural compliance. Throughout this process, continuous vision-based pose estimation enables closed-loop fine alignment through four symmetrically mounted winches. These winches dynamically modulate cable tension to correct lateral translation, pitch, and yaw, while roll is passively constrained by system geometry and interface design. Secondary localized inflatable actuators then provide low-force, high-compliance insertion assisted by passive alignment guides to ensure proper interface seating. Internal position and load sensors confirm engagement and trigger the primary mechanical latching mechanism to achieve structural capture and pressure sealing. Once latched, the external softgoods shell is pressurized to operational levels to increase structural stiffness and provide protection against micrometeoroids, dust intrusion, and thermal variation. The system then conducts a full integrity check and Environmental Control and Life Support System verification to ensure human-rated conditions before enabling crew access through manual hatch operation for personnel or cargo transfer. Undocking operations can be initiated from either interface through administrative authorization. This supports either leaving the tunnel attached to a fixed asset or retracting it with the rover for relocation. Before undocking, both hatches must be closed and locked, and internal sensors must verify complete clearance of crew and cargo. The system then performs environment-dependent deflation procedures. For lunar operations, gas is passively vented and captured for reuse. For Mars operations, gas is either vented or actively reclaimed through the compressor system, depending on the mission resource strategy. After deflation, the mechanical latch disengages, internal actuators are vented, and the winch system actively retracts and collapses the structure in a controlled manner while expelling residual gas. The tunnel is secured into a compact stowed configuration against the designated interface, where it remains mechanically locked and ready for subsequent deployment cycles.

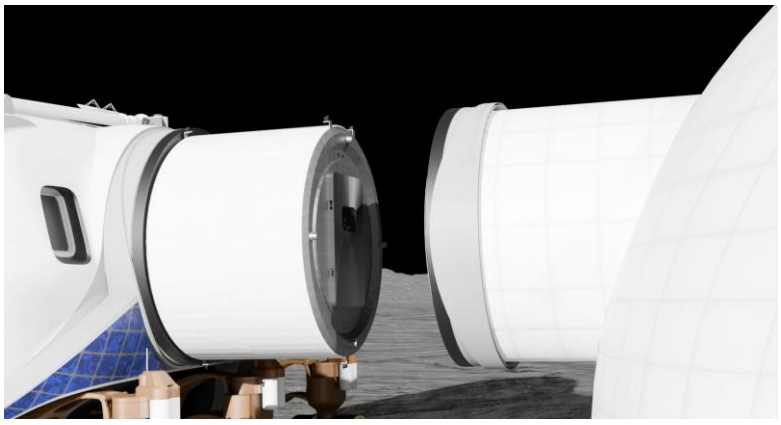

Figure 38: Rover-to-Habitat Connection

The extended-use mode defines an extended use and standby configuration in which the tunnel system transitions from a transient docking mechanism into a long duration pressurized structural connection between two crewed elements such as habitats, landers, or rovers, enabling continuous crew and cargo transfer while also serving as a multifunctional infrastructure component.

Upon successful latching, sealing, and certification for sustained operation, the system enters Extended Use Mode through administrative authorization. It then reconfigures its structural load path by fully depressurizing and isolating the inflatable actuators previously used for axial deployment. This transfers load-bearing responsibility to the pressurized softgoods shell and internal structural elements to minimize cyclic fatigue, reduce long-term material strain, and preserve actuator lifespan for future redeployment operations, while maintaining continuous mechanical attachment at both interfaces with stable load transfer through interface hardware and internal pressurization. In this configuration, the tunnel exterior functions as an infrastructure backbone with standardized mounting interfaces that allow robotic servicing systems to install, reposition, or remove auxiliary systems such as supplemental solar arrays, radiation or micrometeoroid shielding, and communications hardware including relay antennas or small satellite deployment mechanisms. This expands habitat capabilities without requiring additional primary structures. Internally, the tunnel operates as a fully integrated extension of the connected pressurized volumes, with hatches optionally remaining open and unlocked for unrestricted crew movement under administrative control. This suppresses nuisance latch alarms while maintaining continuous health monitoring through embedded sensors that track pressure stability, seal integrity, and structural performance consistent with Environmental Control and Life Support System requirements. Throughout extended operation, seal performance is actively monitored using pressure transducers and leak rate calculations across the tunnel and interface regions. The system enforces defined allowable thresholds and generates crew-visible alerts and maintenance logs in response to elevated leak rates or abnormal trends. Additional integrity monitoring through latch position sensing, preload indicators, and differential pressure signatures enables detection of anomalies such as partial disengagement, structural deformation, or seal degradation. These anomalies trigger appropriately prioritized alarms to ensure crew awareness without excessive false positives. In contingency scenarios, the system supports emergency disconnect from either interface under controlled authorization and safety constraints. After emergency disconnect, the tunnel is classified as an uncertified or potentially contaminated pressure system requiring transport to a controlled pressurized environment for inspection, dust mitigation, reconfiguration, and recertification before being returned to operational service.

This ensures that pressure integrity, mechanical functionality, and sensor performance are fully validated to maintain crew safety and system reliability.

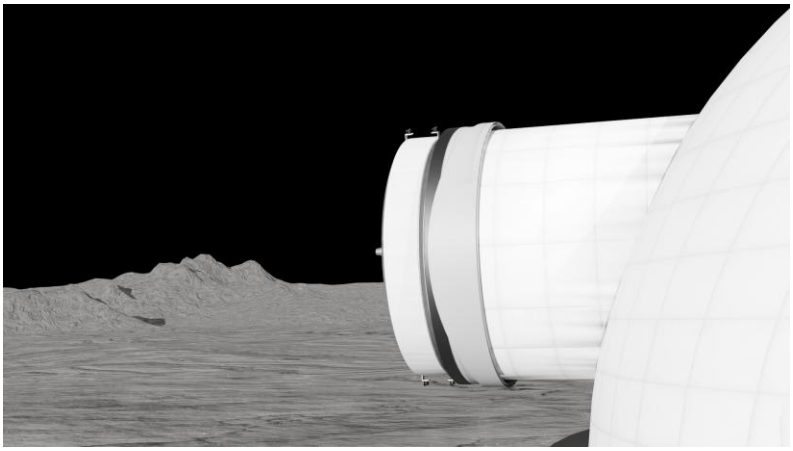

Figure 39: Standby Mode Configurations

Lastly, Standby Mode defines a standby configuration in which the tunnel system remains attached to a single pressurized asset but is not actively deployed for transfer operations. The system maintains a safe, dormant, and structurally secure state while preserving readiness for future use. In this mode, the tunnel is fully collapsed against the host interface and mechanically locked into a compact stowed configuration. All winch systems are fully retracted and inhibited from actuation. Inflatable structures are maintained at a minimal residual pressure sufficient to preserve geometric integrity and prevent creasing, material fatigue, or long-term damage, while remaining structurally secured to the host asset but unavailable for crew ingress or egress. In this mode, the system operates in a reduced power state with most active subsystems dormant. Critical functions such as thermal management and structural health monitoring remain active at low duty cycles to ensure continued system integrity. Embedded temperature sensors and controlled heating elements maintain softgoods, composite structures, and sealing interfaces above minimum allowable temperatures to mitigate risks of material embrittlement, thermal contraction, and dimensional instability in extreme lunar or Martian environments. All hatches remain closed, mechanically locked, and system-inhibited to prevent inadvertent access or depressurization. The attached interface on the host asset is treated as unavailable for external operations. Transition out of standby requires explicit administrative authorization, system readiness checks, and reactivation of dormant subsystems prior to any deployment or docking sequence.

6.2 Special Operation Scenarios

Contingency plans have been put in place in the event of an unforeseen emergency of system interruption. Various scenarios defined are sudden power loss, sudden communication loss, repairability of the system, loading and unloading from lander, end of lifecycle, and rapid ejection of system from connection.

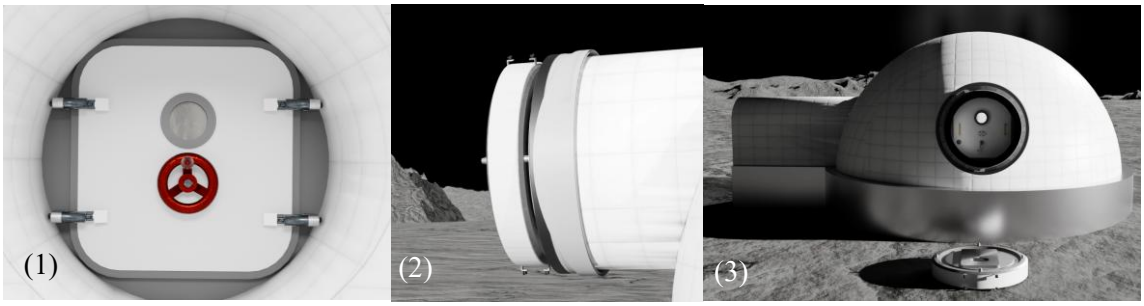

Figure 40: (1-3) Rapid Detachment Operation

6.2.1 Sudden Power Loss

In the event of sudden loss of electrical power, the tunnel system defaults to a fail-safe, non-actuating configuration that prioritizes crew safety, pressure integrity, and structural stability, with responses dependent on the current operational state. If power is lost during Standby Mode, all mechanical latches and seals remain engaged. Inflatable supply and exhaust lines automatically close through normally closed valves to prevent unintended pressure changes. Winches remain retracted and inhibited, resulting in a fully static configuration that stays structurally secured to the host asset. Manual disconnect procedures remain available if required, after which the system is considered non-operational until inspected and recertified. If power is lost during Extended Use Mode, latches and seals remain engaged and inflatable lines close to isolate internal pressure. However, no active pressure regulation or make-up gas is available, so the system relies on seal integrity and may experience gradual leakage. Both hatches automatically close and lock to prevent unsafe use. Any necessary crew passage must occur under EVA conditions via manual override, and the system remains in this inhibited state until power is restored. If power is lost during active deployment or docking, all solenoid valves immediately close to lock inflatable actuators at their current pressure. This halts motion in place and prevents uncontrolled extension or collapse. Winches stop and mechanically hold position, leaving the system paused in a stable intermediate configuration. Upon power restoration, the system performs a controlled recovery sequence rather than immediately resuming operation. It executes diagnostics on pressure systems, sensors, latches, interfaces, and valve states. The system then returns to the appropriate mode by restoring thermal control in standby, repressurizing, and validating ECLSS in extended use, or performing a controlled collapse and homing sequence if interrupted during docking. All operations require operator authorization before resumption.

6.2.2 Sudden Loss of Communication

In the case of loss of communication, the system shall remain in its current state if it is not actively actuating. Personnel in the base will be notified of communication changes and can initiate system diagnostics and reboot. If the error is internal, the system will attempt to correct the issue but may require external help from users. In the case of active actuation, the system will wait 15 seconds and try to reestablish connection. If unsuccessful, the system will un-actuate and return to Standby Mode, where it will condense and lock to the original connection point.

6.2.3 System Repair

System repair strategy supports both in situ repair and off-site maintenance depending on fault severity, location, and system risk. All repair activities are conducted under conservative safety assumptions due to the potential for inadvertent depressurization. Personnel are required to operate in EVA suits unless the system is fully isolated and certified safe for internal access. Tunnel hatches must remain closed and sealed

during any operation that could impact adjacent pressurized volumes. Minor internal repairs, such as localized leaks, small fabric damage, or non-critical stress fractures, are performed with the tunnel fully extended and connected at both ends. Inflatable isolation seals are used to localize the affected region and prevent pressure loss. Crew members then apply compatible repair materials such as Vectran-based patches and use only low-risk approved tooling to avoid damage to adjacent inflatable structures. This is followed by controlled repressurization and verification of leak rate and structural integrity before returning the system to service. Minor external repairs involving damage to the outer softgoods shell or protective layers are conducted while the tunnel remains deployed and structurally supported. These repairs are performed using either EVA crew or robotic systems with environment-compatible patching methods. Repairs are validated through visual inspection and system monitoring prior to resuming operations. For large-scale damage, including structural failures, significant degradation, or interface hardware faults that cannot be safely addressed in place, the tunnel is disconnected and transported to a pressurized maintenance facility. There, it undergoes detailed inspection, repair, and refurbishment using specialized equipment. Upon completion, the system is revalidated through full system checks, including pressure integrity, sensor functionality, latch performance, and leak rate verification, before being redeployed via pressurized rover transport to its next operational location.

6.2.4 System Initialization

System initialization transitions the tunnel from a stowed, dormant, relocated, or repaired state into a certified operational configuration prior to any crewed use or docking. This process verifies structural integrity, pressure containment, sensor functionality, actuation readiness, and control system health while preventing unintended motion or depressurization. Initialization begins only after required preconditions are met, including secure attachment or controlled environment placement, contamination removal, verified power and command interfaces, and administrative authorization, with no unresolved faults present. The system powers up into a non-actuating safe state and performs self-checks on processors, communications, sensors, and control paths. This is followed by validation of pressure, seal, latch, and thermal sensors against expected conditions. The system then performs a controlled low-pressure integrity test of the softgoods shell with leak rate monitoring and automatic abort if limits are exceeded. Actuation systems are then verified in low-force, limited-motion modes. The thermal system is activated to bring materials within operational temperature ranges. Upon successful completion, the system transitions to either Standby Mode or an operational ready state. Initialization is complete only after all verification data are logged and the system is certified for use.

6.2.5 Rapid Ejection Mode

Rapid Ejection Mode is used when immediate hatch access is required for crew egress, EVA, or emergency scenarios. This mode enables the tunnel to quickly depressurize and disengage without executing a full retraction sequence. Mechanical latches release, and the structure separates or folds clear of the hatch interface to eliminate obstructions. This ensures the hatch area is fully accessible for manual or automated operation. Afterward, the system transitions into a safe, non-interfering state to allow for inspection, recovery, or subsequent operations.

6.2.6 Lander Loading and Unloading

Lander loading and unloading operations define how the tunnel system is transported and integrated during mission deployment. For large-scale lander missions, the tunnel is delivered pre-integrated with a habitat or pressurized rover and structurally attached so that launch and landing loads are reacted through the

primary structure. Restraints and isolation protect sensitive components during transport and landing. For standalone delivery, the system is stowed within a protective transport container that restrains and isolates it from vibration and mechanical loads. All configurations are designed to support reusability, efficient surface integration, and rapid readiness for deployment following landing.

6.2.7 End of Lifecycle

End-of-lifecycle operations define the process for safely retiring or repurposing the tunnel system after mission completion. The system is fully depressurized, electrically powered down, and mechanically locked to preserve structural integrity. Interfaces are disengaged to enable reuse, relocation, or repurposing without impacting other surface assets. Hardware may be retained for extended testing, including thermal cycling, dust exposure, and durability evaluation. Components support iterative upgrades and continued technology maturation for future pressurized transfer systems.

6.3 Transfer Operations

BLIMP is critical to human and cargo transfer operations. Human transfer occurs as expected, when the tunnel is connected on both ends and internal conditions are safe for human use without the need of spacesuits then astronauts can use it to transfer from one piece of infrastructure to another. Cargo transfer is more complicated though due to the bottom of the door not being level with the floor.

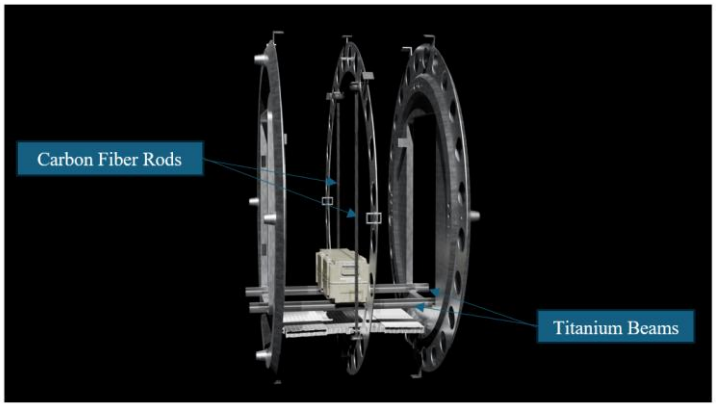

Figure 41: Cargo Transfer

Figure 41: *Cargo Transfer.* Two titanium beams are attached to the carbon fiber vertical support rods. Upon entry to the system, the astronaut will need to take the titanium beams off the vertical supports and place them on the notches located on the end interfaces. This placement will allow all cargo to use rails to get through the tunnel if it can be raised and lowered manually to the doorway height. Also, by resting these beams on the notches all forces will be directly transfer through end plates into the connection interface effectively offloading these forces from bearing down on the softgoods and bellows.

6.4 System Limitations and Assumptions

Lunar Infrastructure (LI) level is a key constraint governing the functionality of the system on the lunar surface [63]. Rather than providing core infrastructure capabilities, the system is designed to operate within an environment where specific infrastructure conditions are already established. These include level ground at connection interfaces, reliable power availability, consistent in-situ resource utilization (ISRU) support, and standardized, universal connection interfaces. Additional requirements are summarized in Table 2.

Given these dependencies, the system is most appropriately implemented at Lunar Infrastructure levels 4–6, when sufficient surface preparation, power distribution, and operational support systems are in place. In the context of the Artemis campaign, this corresponds to the mid-phase missions (Artemis V–VII), depending on whether early deployment is pursued or delayed until more mature infrastructure is established.

Table 2: Lunar Infrastructure Levels Needed for Total System Success[64]

Provide power storage on lunar surface crewed exploration sites	LI-1
Demonstrate capability for autonomous compaction of pathways	LI-4
Demonstrate capability for maintenance of pathways	LI-4
Provide pressurized crew surface mobility	LI-6
Demonstrate operation of oxygen production ISRU	LI-7
Docking/berthing of spacecraft elements	LI-8

7.0 Simulation and Optimization

An important part of the engineering process is validating that the design is structurally sound as well as using simulations and scripts to optimize components to save mass and volume. All structural components had FEA completed as well as the conceptual bellows. Additionally, the onboard storage tank was optimized with a MATLAB script. Lastly, even though the atmosphere on Mars is minimal and nonexistent on the Moon, the drag force on the Martian surface was observed to validate tunnel stability.

7.1 FEA

While designing both the conceptual and prototype designs, completing finite elements analysis to verify that all components are strong enough to perform their function while minimizing mass was critical to creating a functional lightweight solution. FEA was completed on all of the conceptual structure components as well as the conceptual and prototype bellows to predict how they would behave. For the prototype, FEA was used to validate the FOS of the bellows and when they would fail as well as the important structural pieces and making sure they could handle all loads. All critical FOS can be seen in the table below.

Table 3: FEA FOS for Critical Components

Components	FOS
Conceptual Internal Structure	7.03
Conceptual Connection Interface	1.60
Conceptual Vectran Bellow @5 psi	>>4.0
Prototype TPU Nylon Bellow @5 psi	4.0
Prototype Mock Hatch	4.24

7.1.1 Conceptual Structure

A structural analysis was performed on the bulkhead to evaluate its ability to withstand expected loading during operation. The analysis used fixed boundary conditions around the alignment guides to represent the constrained connection points of the system. Thrust loads were applied at the inflatable mounting locations, with the total load distributed as 1,000 N at each inflatable location. Additional loading was applied at the cargo beam holders, with each holder receiving an additional 1,000 N load. The winch mounting holes were also evaluated using a 4,000 N load at each location, along with a 400 N·m torque applied about the center axis to represent actuation loading from the winch system. The resulting factor of safety plot showed a minimum factor of safety of 1.604, indicating that the bulkhead remains above the required safety threshold under the applied loading conditions. Figure 42 shows the bulkhead mesh and corresponding factor of safety results.

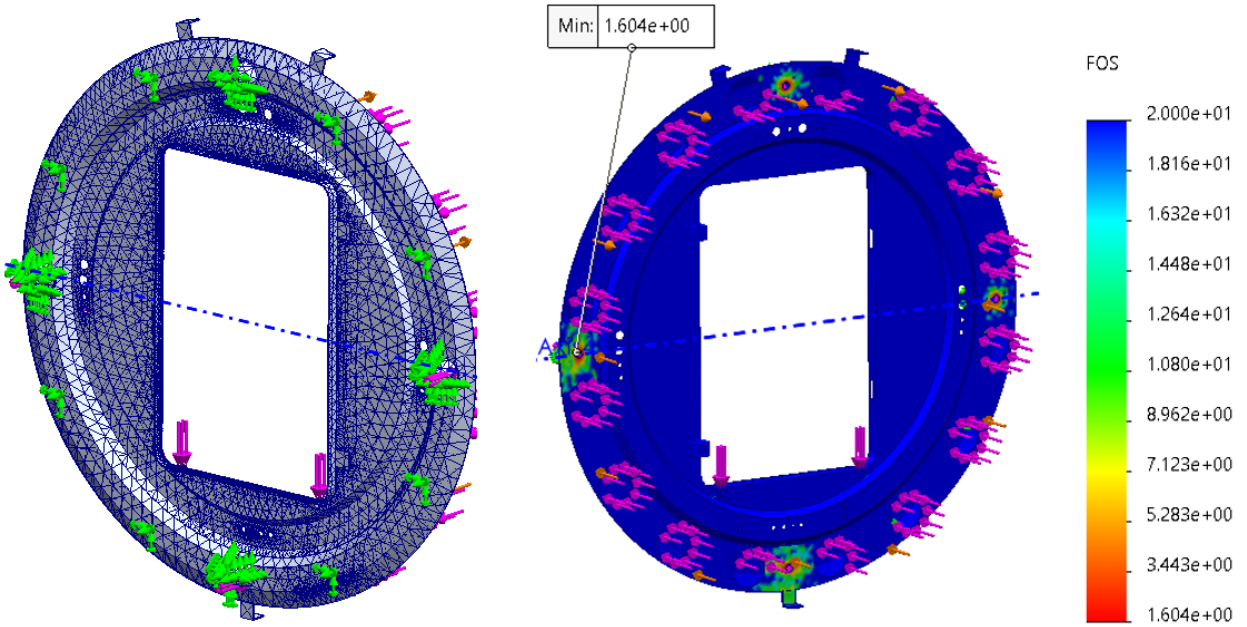

Figure 42: Bulkhead FEA

Figure 42: *Bulkhead FEA*. A structural analysis was also performed on the internal ring and floor support assembly to evaluate deformation and strength under representative operational loading. The structure was modeled using T700 composite material properties, with fixed constraints applied around the softgoods connection points and floor ends. Loads included a suited crewmember load of approximately 400 lb. applied to the floor, 1,000 N applied at each inflatable connection, and 4,000 N applied at each winch connection. The displacement results showed a maximum deflection of 32.5 mm under the applied suited crewmember load. The factor of safety analysis produced a minimum factor of safety of approximately 7.03, indicating that the structure remains well above the required strength margin for the applied loading conditions. Figure 43 shows the displacement results and expanded factor of safety view for the analyzed structure.

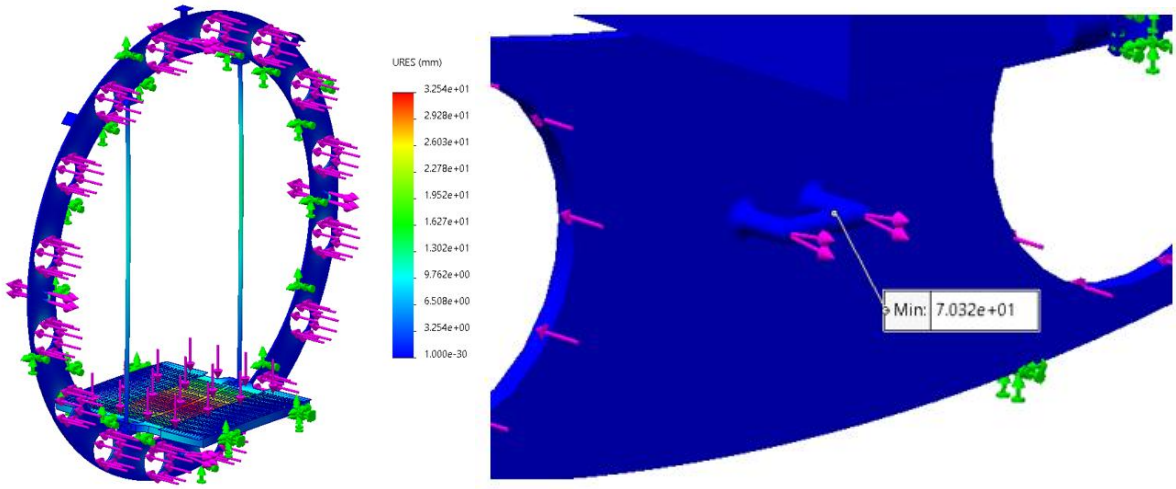

Figure 43: Conceptual Internal Structure

7.1.2 Conceptual and Prototype Bellows

SolidWorks simulation is used with custom material libraries to computationally analyze bellow performance under various pressures. This is especially important for conceptual design as obtaining aerospace-grade textile fabrics are out of scope of the SDSU X-Hab project.

The setup for simulation is consistent throughout the section:

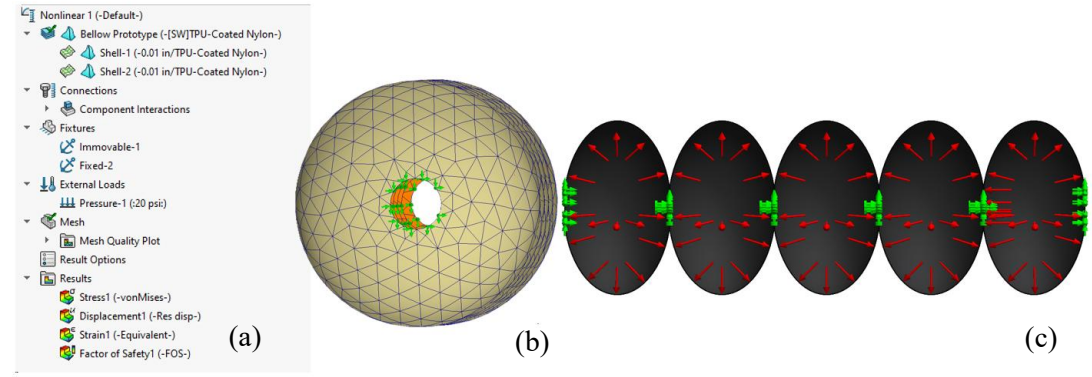

Figure 44: (a) Constraints (b) Shell Element (c) Forces

Figure 44: *(a) Constraints (b) Shell Element (c) Forces.* The Simulated Bellow assumes a shell thickness identical to material thickness at 0.01 inches. The team also fixes the outer and inner air-flow diameters to ensure simulation convergence. Pressure is added to each inner surface including the surrounding-modeled heat-profiles.

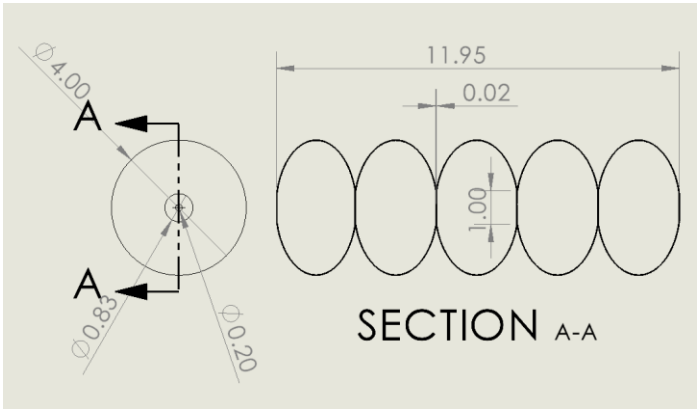

Figure 45: SolidWorks Bellow Dimensions

Figure 45: *SolidWorks Bellow Dimensions*. This figure shows the dimensions used to create the bellow for simulating. NOTE: From measurements, the team found that the thickness of the 70D TPU-Coated Nylon was in the 0.008 – 0.012 in range (0.2032 - 0.3048 mm). For this simulation, 0.01 in thickness was chosen.

Table 4: TPU-Coated Nylon Material Properties [65]

Property	Value	Units
Elastic Modulus	827.37	N/mm^2
Poisson's Ratio	0.3	N/A
Shear Modulus	318.21	N/mm^2
Mass Density	1,051.84	kg/m^3
Tensile Strength	89.63	N/mm^2
Yield Strength	62.05	N/mm^2

Table 4: *TPU-Coated Nylon Material Properties*. The values for custom material properties which come from the manufacturing page.

To complete the simulation as well as the custom properties table, the following assumptions were made:

- Homogeneity – The material is assumed to be a single uniform substance.
- Isotropic – The material will act the same in any direction.
- Tensile strength is calculated based on assumed thickness.

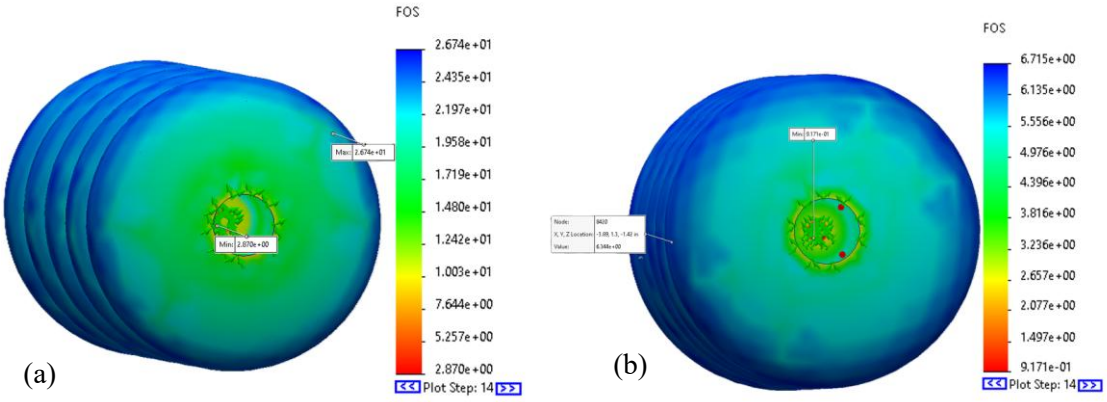

Figure 46: TPU Coated Nylon, FOS Plot (a) 5 psi (b) 20 psi

Figure 46: *TPU Coated Nylon, FOS Plot (a) 5 psi (b) 20 psi*. This figure shows the simulated bellow under 5 psi **(a)**, and 20 psi **(b)**, and their respective FOS plots. For this, and all subsequent simulations, the bellows will be simulated under working pressure, however, for the prototype, since the team can validate the FOS using a real specimen as seen in (**Section 9.2**) a 20-psi simulation is also completed. It can be noted that the prototype has a sub-optimal FOS on the inner air passageways, and a large safety factor near its seams. This is consistent with the physical burst test (See **section 9.2.2**).

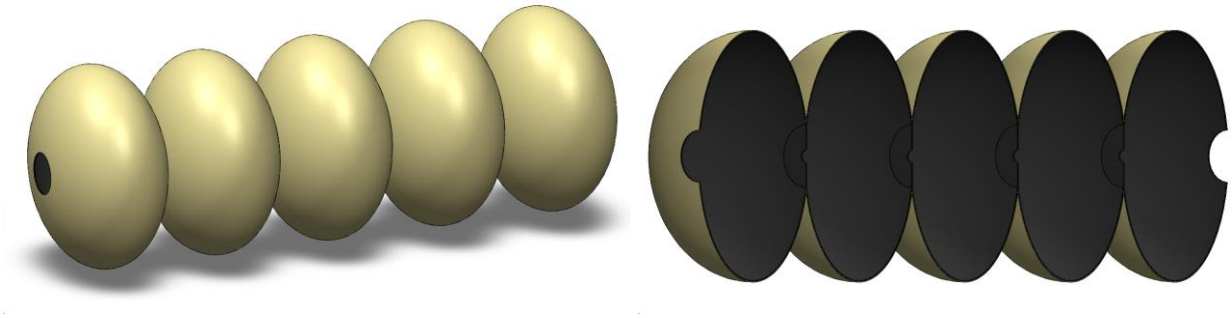

Figure 47: Vectran Shell

Figure 47: *Vectran Shell*. This figure shows a conceptual bellow design of a Vectran shell encasing the previous TPU-Coated Nylon Prototype (See **Figure 45**) with a thickness of 0.015 in (0.38 mm) having a total bellow thickness of 0.025 in (.635 mm).

Table 5: Vectran Properties [49]

Property	Value	Units
Elastic Modulus in X	103,000	N/mm^2
Elastic Modulus in Y	103,000	N/mm^2
Elastic Modulus in Z	1,000	N/mm^2
Poisson's Ratio (XY)	0.35	N/A
Shear Modulus (XY)	2,500	N/mm^2
Mass Density	1,400	kg/m^3
Tensile Strength (X, Y)	3,000	N/mm^2
Yield Strength	3,000	N/mm^2

Table 5: *Vectran Properties*. This table shows the properties for the selected UM Balanced Plain Weave Vectran. This material is assumed Orthotropic.

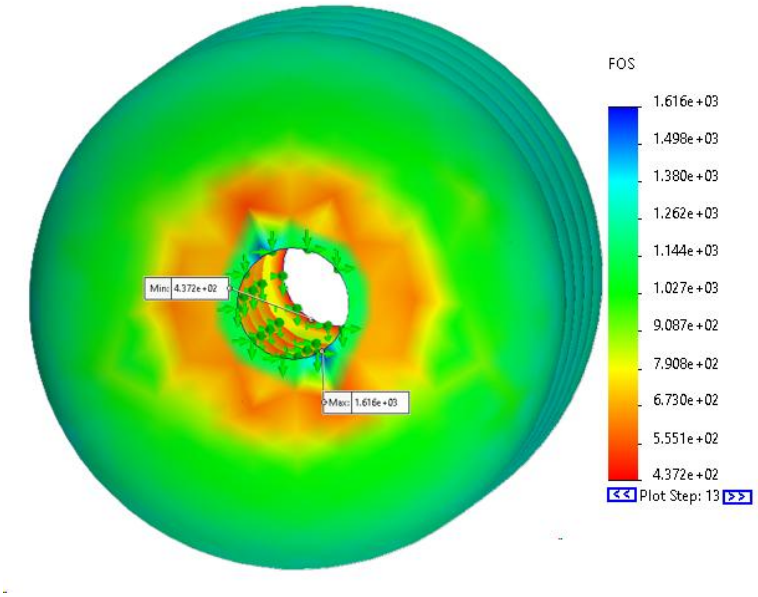

Figure 48: Vectran Bellow - FOS Plot (High Quality Mesh)

Figure 48: *Vectran Bellow - FOS Plot (High Quality Mesh)*. This figure shows the Vectran shell under 5 psi working pressure.

For further validation, each simulation was rerun under three different mesh qualities:

- Coarse
- Fine
- Very Fine

Each simulation presented in this paper converged to the values seen in each figure.

7.1.3 Prototype Mock Hatches

The prototype mock hatch was simulated to define that 5052-H32 aluminum was sufficient to support the loading caused by the tunnel pressing against the mock hatch interface. The initial selected alloy of aluminum for this was 6061, however significant cost savings were possible using alternative alloys.

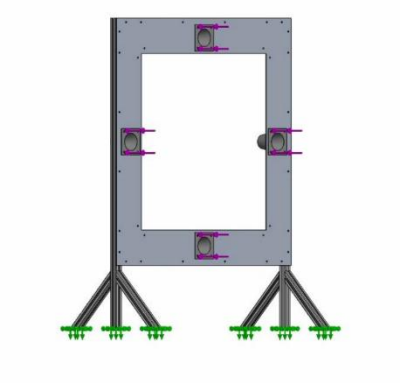

Figure 49: Mock Hatch Fixtures

Fixtures were placed at the bottom of the vertical posts as well as the bottom of the 45-degree angled aluminum. This represents the bottom of the hatch being fixed to the ground. It should be noted that additional measures to fix the bottom of the mock hatch may be put in place to prevent tipping. These include, but are not limited to, weighing down the base to keep the base upright. The loadings for the tunnel were placed on the funnel cones of the mock hatch aluminum sheet. This was deemed to be the most realistic loading as the mock hatch will be coming in contact with these cones as it is extended and slotted into place. A 250lb load was applied and evenly distributed across all of the faces of the cone that were closest to the extending bulkhead of the tunnel **(figure. 50).** The force of 250lb was chosen as it is approximately 35% of the total force generated axially by the six in outer diameter of all eight of the bellows while at 3 psi. Under normal conditions, the winches would be holding back the force of the bellows, not allowing them to reach a force of this magnitude.

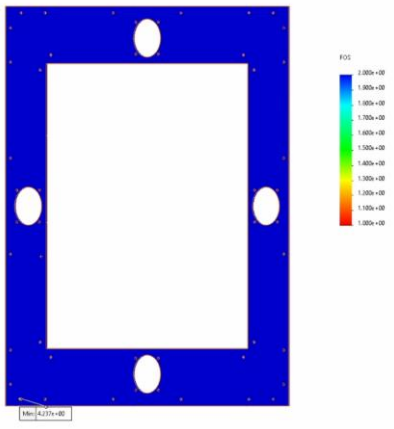

Figure 50. Mock Hatch Plate FEA

The minimum FOS present within the system using 5052-H32 aluminum is 4.237, which shows a sufficient factor of safety for this scenario. This was the alloy that was eventually chosen, saving overall costs by enabling purchases from a greater variety of vendors with cheaper overall costs.

7.2 MATLAB

To optimize the onboard storage tank specifications and estimate expected bellows performance, MATLAB scripts were developed for parametric analysis. The storage tank script modeled a cylindrical pressure vessel

using Ti-6Al-4V material properties. A range of potential tank geometries was evaluated, with radii from 1.18 to 5.91 in. and lengths from 1.97 to 19.69 in. Operating pressures from 100 to 200 psi were also considered. Each design variable was divided into 50 values, allowing the script to evaluate a wide range of possible tank configurations.

A factor of safety of four was applied due to the critical nature of the pressurization system. Using the required gas mass and operating conditions, the script calculated the tank dimensions needed to minimize both container volume and mass while still satisfying the gas storage requirement. The resulting optimized design produced a tank mass of approximately 1.32 lbm at an operating pressure of 198 psi. The selected tank geometry used a diameter of 5.64 in. and a length of 19.69 in., providing an internal volume of 0.285 ft^3. This satisfies the required gas volume of 0.282 ft^3 for the bellows system.

Additionally, MATLAB was used to perform calculations on the forces the bellows would produce and be able to withstand. Important forces were the axial thrust force, buckling force, and the vertical displacement. The thrust force was calculated using equation one. This just took the change in pressure compared to the outer environment and multiplied it by the effective area of all bellows combined.

$$Thrust = P \times A \tag{1}$$

Where:

P = Bellow Pressure

A = Effective Bellow Cross Sectional Area

Next was the buckle force along the axis of the bellows. Euler buckling equation was used for this as shown in equation two. Important assumptions were as follows…

$$P_{cr} = \frac{\pi^2 \times E \times I}{K \times L^2} \tag{2}$$

Where:

E = Young's Modulus

I = Area moment of inertia

K = Effective Length Factor

L = Unsupported Length

Lastly, the vertical displacement as the end of the system while extending was calculated using equation three.

$$\delta = \frac{F \times L^3}{3 \times C \times E \times I} \tag{3}$$

Where:

δ = Bellow End Displacement

F = Applied Shear Force

L = Unsupported Length

C = Bellow Stiffness Knockdown Factor

E = Young's Modulus

I = Moment of Inertia

7.3 Mars Drag Force

To reiterate, the conceptual design of the system has applications for both the Moon and Mars. Though the Moon does not have an atmosphere, Mars does and demands design considerations accordingly. The worst conditions on Mars create the most extreme circumstances in the scope of tunnel operation and were therefore used as design metrics. Mars has an atmosphere much thinner than that of Earth, containing nearly 95% carbon dioxide and winds up to 100 mph [66]. Abrasive dust exposure is one concern raised by these conditions and was addressed in section referring to electromagnetic dust rejection. Another concern was aerodynamic drag. To investigate the implications of external drag on the tunnel system, a drag force calculation was completed as seen below in equation four.

$$F_D = \frac{1}{2}\rho c_D A v^2 \tag{4}$$

$$F_D = 0.5(0.015\ kg/m^3)(0.54)(1.7569\ m^2)(44.7\ m/s)^2$$

$$F_D = 14.2\ N = 3.2\ lb_f$$

The 3.2lb$_f$ drag force acting on the tunnel, when compared with the forces and torques induced by conceptual system components and mass, was neglected as a concern within the scope of this project. The main contributor to this fact is the low atmospheric density on Mars relative to that of Earth.

8.0 Prototype Design

The prototype's purpose is to validate the conceptual actuation and control subsystems through a scaled down design. Additionally, the structure and connection methods are similar in behavior.

8.1 Prototype Specifications and Overall Design

The prototype is approximately 1/8 scale compared to the conceptual design when evaluated by cross-sectional area. Key prototype dimensions are provided in Table 6. The prototype was developed as an Earth-based functional demonstrator to validate the core actuation method, control architecture, user interface, pneumatic system, and simulated connection interface. It is not intended to fully replicate lunar vacuum, dust, gravity, or thermal conditions; instead, it provides a physical test article for demonstrating the primary functions required for system operation.

Table 6: Prototype Specifications

Outer Diameter	46”
Inner Diameter	30”
Condensed Length	31”
Extended Length	49”
Mock Hatch Height	77”
Mock Hatch Width	52”
Mock Hatch Length	36”



Figure 51. Prototype Assembly CAD

The prototype is divided into two primary systems: the tunnel system and the mock hatch system. These systems are further decomposed into structural, electrical, pneumatic, and software subsystems. The tunnel structure uses six large 3D-printed rings, with aluminum end plates serving as the simulated connection interfaces. Internally, two carbon fiber supports guide the floor assembly and allow it to move linearly as the tunnel changes length during operation.

The tunnel actuation system uses inflatable bellows to extend the structure, while winch assemblies maintain tension and provide controlled articulation. The pneumatic system includes 16 inflatable bellows, arranged as two rings of eight. Paired bellows sections are monitored using pressure sensors and protected with relief valves to reduce the risk of over-pressurization.

The electrical and control system is distributed across three electronics enclosures, with one enclosure mounted on each main ring assembly. These enclosures contain the controllers, motor drivers, MOSFET modules, relays, and power distribution components needed to operate the solenoids, motors, actuators, lights, and sensors within each section. The main control architecture uses a Raspberry Pi, two Arduino Megas, and an Arduino Nano to manage user commands, telemetry, pneumatic control, and actuation.

The prototype also includes five USB cameras that provide visual feedback to the user interface. These cameras support operator awareness, AprilTag detection, and alignment feedback during testing. The system is operated through a Flask-based HTML user interface and a Bluetooth controller, allowing the user to monitor telemetry, switch camera views, control pan-and-tilt cameras, and command the prototype

through its primary operating modes: standby, actuation, and extended use. The mock hatch system provides a simulated interface for testing alignment, latching behavior, and connection readiness.

8.2 Differences from Conceptual

Due to time and budget constraints, the prototype incorporates several simplifications compared to the conceptual design. One of the most significant changes is the reduction in the number of bellows per ring. While the conceptual design includes sixteen bellows per ring, the prototype uses only eight. This reduction is directly tied to a corresponding decrease in the number of valves and sensors required for individual bellow control. Additionally, given the prototype's outer diameter of 46 inches, integrating sixteen bellows within a single ring would present substantial geometric and packaging challenges.

Another key difference lies in the actuation system. In the conceptual design, the winch motors are housed within the connection interface cones. However, due to the reduced size of these cones in the subscale prototype, this configuration was not feasible. As a result, the winch motors were relocated to the interior of the outermost 3D-printed ring. From this position, they are mechanically linked to the middle ring using fishing line as a lightweight tension element.

Finally, the structural architecture differs between the conceptual and prototype models. The prototype incorporates additional rigid rings that serve multiple functions: housing pneumatic components and providing mounting points for valves, sensors, cameras, lighting, and electrical enclosures. In contrast, the conceptual design relies more heavily on inflatable softgoods for structural support.

A key area for future research is evaluating the spatial constraints and clearances around the bellows. This analysis would determine whether the conceptual design can realistically accommodate all required pneumatic and electrical components, or if additional structural elements, such as the rings used in the prototype, are necessary to ensure adequate space and system integration.

8.3 Actuation Subsystem

The prototype actuation subsystem consists of 16 TPU-coated nylon inflatable actuators and eight 3D-printed winch assemblies. Each inflatable actuator has an inflated diameter of approximately 5 in., a length of 12 in., and a material thickness of approximately 0.008 – 0.012 in. The actuators are used to provide axial extension force only, while the winch assemblies are used to control pitch and yaw, maintain tension in the tunnel structure, and retract the system back toward standby mode.

The winches are arranged as two sets of four, with one set located on each end hatch inner face. Each set includes four winches spaced 90° apart around the outside face of the connection interface. The winch cables run directly from the winch shaft to eyebolts mounted on the middle ring, allowing the cables to control the relative position of the tunnel during extension and retraction. The winch assemblies are 3D printed from PLA, and each assembly uses 180 lb fishing line as the cable material. This line was selected for the prototype because it provides high tensile strength in a compact form factor and is easy to route through the system.

During extension, the winches release cable as the inflatable actuators expand. The bellows provide the axial thrust needed to extend the tunnel, while the winches regulate motion and maintain tension to prevent uncontrolled movement. The bellows thrust load is assumed to be evenly distributed across the four winches on the active face. Each winch uses a spool radius of approximately 0.25 in (6.35 mm). to convert cable

tension into motor torque. The selected winch motor is rated at 6.86 Nm and 16 rpm before additional gearing. A 2:1 gear reduction is used, producing an estimated output of 13.72 N-m at 8 rpm.

The winch system is designed to provide approximately 5° to 10° of pitch and yaw correction during alignment. This allows the prototype to demonstrate controlled angular adjustment of the connection interface while the inflatable actuators provide axial extension. During retraction, the inflatable actuators are vented while the winches pull the tunnel back into its condensed standby configuration.

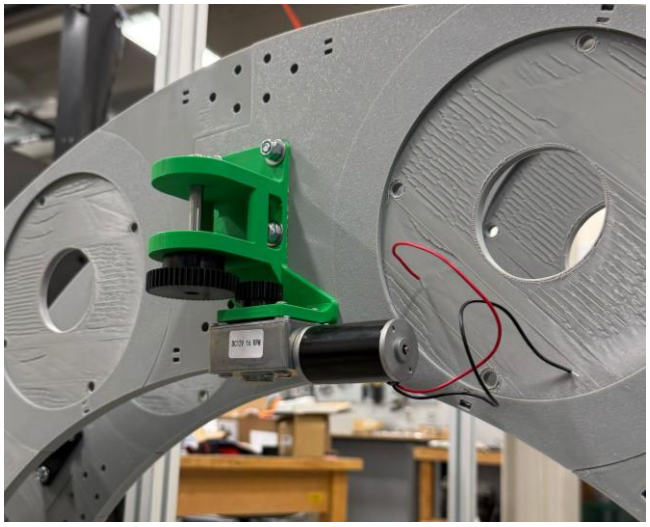

Figure 52. Prototype Winch Assembly

The primary validation metric for the actuation subsystem is whether the prototype can consistently extend, align, and visually seat against both mock hatch interfaces. Successful operation is determined through repeatable connection attempts, visual confirmation of seating, and the ability of the actuation system to support controlled motion during extension and retraction.

8.4 Structural Subsystem

The prototype structural subsystem consists of the 3D-printed structural ring assemblies, internal carbon fiber tube supports, and flooring system. The tunnel structure is organized into three primary ring assemblies: one assembly at each end of the tunnel and one assembly located near the center. Each ring assembly consists of two 3D-printed rings separated by a small internal gap. This gap provides mounting space for the electrical and pneumatic components located at each ring assembly.

The structural rings were manufactured from PLA filament and printed in smaller modular pieces due to printer build-volume limitations, ease of fabrication, and repairability. These pieces are press fit together to form the full ring geometry. The completed rings have an outer diameter of 46 in., an inner diameter of 30 in., and a thickness of approximately 0.5 in. The printed ring geometry includes a circular center section with recessed regions and bolt-hole cutouts for actuator mounting. Supporting side pieces slot into the center section and interlock to complete the circular ring structure. Standard 1/4-20 fasteners are used throughout the ring assemblies and attachment points.

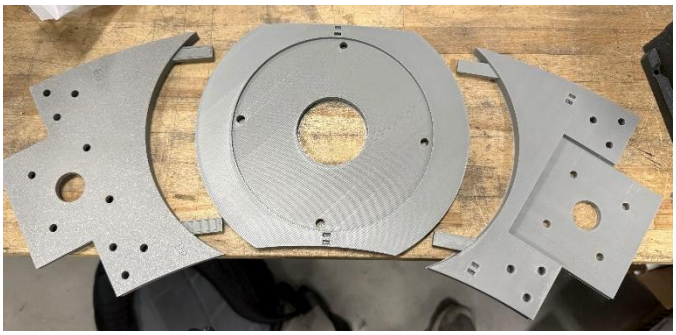

Figure 53: 3D Printed Sections

The three ring assemblies are connected using 3D-printed standoffs, creating the primary rigid sections of the prototype. The two gaps between the ring assemblies are bridged by the inflatable bellows and winch cables, allowing the tunnel to extend and retract during operation. The inflatable actuators are mounted to the rings using custom 3D-printed valve mounts, which provide both mechanical attachment and pneumatic routing.

Inside the tunnel, carbon fiber tubes provide additional support for the visual floor system. The tubes are nested into 3D-printed mounts and have an outer diameter of approximately 1.15 in. and a length of approximately 22 in. These tubes are used only to support the internal floor panels and are not intended to function as the primary structural guide for tunnel alignment. The internal floor panels are polypropylene injection-molded panels that simulate the walking surface used in the conceptual system. For the prototype, the floor is included for visual and functional representation only and is not designed to support crew loading. The prototype structural design was selected to support rapid fabrication, modular assembly, and integration with the pneumatic, electrical, and actuation subsystems. Success for the structural subsystem is based on its ability to be manufactured, assembled, and support the expected prototype loads during repeated actuation and connection testing.

8.5 Connection Interface

The connection interface of this tunnel will be located at the two ends of the tunnel and will be made of 5052 aluminum. It will also be referred to in this document as the bulkhead. It will be fixed to the 3D printed rings and will house a few major components. The first major component is the door. The door will be connected to the main body of the tunnel using hinges and will also contain an actuated latch and a window. The window will be made of polycarbonate. The window is secured in place by being sandwiched between two 3D-printed window frames. The actuated latch will be found on the interior of the tunnel. Once the tunnel is secure in place, the actuator will retract, allowing the doors to swing freely. To prevent the door from swinging inward, there will be a handle with a base that extends outward and contacts the main body of the bulkhead. Additionally, a latching bracket will provide a slot for the actuator to rest in the closed position. Another major part of the tunnel is the funnel cones. There will be four funnel cones that will be evenly spaced on the tunnel bulkhead. These cones will slot into the funnels on the mock hatch to allow for coarse alignment when the tunnel bulkhead approaches the mock hatch interface. Furthermore, there will be four alignment slots on the tunnel connection interface. The purpose of these slots is fine alignment. Once the tunnel gets close to positioning, there will be alignment blocks that slot into place to fully secure the tunnel. Both the alignment cones and the alignment slots will be 3d printed out of PLA to allow for rapid prototyping.

Redacted due to Export Control/CUI requirements.



Figure 54. Prototype Connection Interface CAD; Prototype Connection Interface Physical Assembly

8.6 Mock Hatches

The mock hatches serve the purpose of being the external connection interface that the tunnel guides itself towards.



Redacted due to Export Control/CUI requirements.

Figure 55: Prototype Mock Hatch Interface; Mock Hatch CAD

The mock hatches are comprised of two stands, which are roughly 5.75’ tall. The stands are made of 4040 aluminum extrusion. Connected to the stands are pieces of sheet aluminum (5052) with cutouts that allow the bulkhead doors to fully open. Also attached to these interfaces are guide channels. When the tunnel

bulkhead is flush with the mock hatch plate, there will be actuators that extend into the channels to complete the docking interaction. The tunnel will be fully secured in place when the actuators extend and hit a limit switch that will be attached to the guide block mechanism. To handle the coarse alignments, there will be four alignment cones which will slot into the funnels located on the mock hatch interface. These funnels are circular in shape and go from wide at the base to narrow at the tip. Also mounted to the stands will be four ultrasonic sensors; the purpose of the ultrasonic sensors is to detect when the tunnel is sufficiently close to engage the linear actuators and extend the alignment blocks. The signal from the ultrasonic sensors will be relayed to the onboard Arduino Mega, which will then engage the actuators.

The mock hatch will operate in two separate modes that are controlled by a switch that is mounted to the side of the electrical box. When the switch is engaged, it activates the ultrasonic sensors; when all 4 of the ultrasonic sensors sense that the connection interface is sufficiently close, the linear actuators start extending until the extending actuators trigger the limit switches. Once a limit switch is triggered the actuator that it is connected to stops actuating. When the switch on the side of the electrical box is set to off, the light turns on, and all of the linear actuators retract. Once they are fully retracted, the system remains in standby mode, cutting power to everything but the light that is mounted to the top of the mock hatch.

8.7 Pneumatic System

The prototype pneumatic system uses an external compressed-air supply, which may be provided by either a portable compressor or a stationary shop compressor. Airflow is regulated before entering the prototype using a manually adjusted pressure regulator located near the compressor. A long pneumatic hose then routes the regulated air to the system. During operation, the regulator is set to maintain the bellows pressure as close to the operating limit as possible without exceeding the safety threshold.

The prototype contains two rings of eight inflatable bellows, for a total of 16 inflatables. Each pair of bellows is pneumatically connected across the two rings and functions as a single controlled inflatable section. Because there is no disconnecting valve between the paired bellows, each pair shares the same pressure response during inflation and venting. A pressure sensor and relief valve are located near the middle of each paired section, allowing the system to monitor and protect each dual-bellows pneumatic volume.

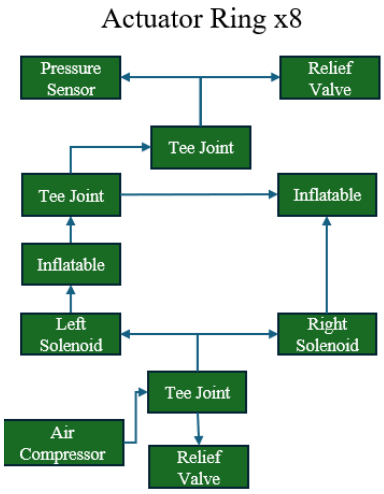

Figure 56. Prototype Pneumatics' Schematic

The system uses eight pressure sensors, with each sensor monitoring one paired bellows section. The sensors are rated up to 5 psi, so the control target during inflation is approximately 4.8 psi. This target keeps the bellows near the desired operating pressure while maintaining a small margin below the relief valve setting. Relief valves are set to 5 psi to prevent over pressurization and reduce the risk of unintentional bursting of the inflatable components.

Normally closed solenoid valves are used to control airflow into and out of the bellows. When the solenoids are de-energized, they remain closed and trap air inside the bellows, allowing the system to hold its current pneumatic state during a loss of power. Check valves are also implemented to enforce one-directional airflow throughout the pneumatic system and reduce unintended backflow. For the prototype, vented air is released directly to the atmosphere during deflation. In a lunar system, this vented gas would need to be recollected or managed to avoid unnecessary gas loss. Venting is currently controlled through software commands, and future versions could include a manual bleed or emergency dump valve for additional safety.

8.8 Controls System

The prototype electronics architecture is centered around a Raspberry Pi 5 with 8 GB of RAM, which serves as the primary computer for user control, telemetry display, video processing, and command distribution. The system is powered by a 12V lithium battery, which is stepped down to 5V using a buck converter to supply the Raspberry Pi. The Arduino controllers are powered through USB connections from the Raspberry Pi. All controller, sensor, motor driver, relay, MOSFET, and power supply grounds are tied together through a common ground bus to provide a shared electrical reference across the system.

The Raspberry Pi communicates with two Arduino Megas and one Arduino Nano through USB serial connections. During startup, the Raspberry Pi reads the USB addresses of the connected microcontrollers and assigns each device as Mega 1, Mega 2, or Nano. The two Arduino Megas divide the main actuation workload, with each Mega controlling one half of the solenoids, winch motors, and door actuators. Each Mega is responsible for eight solenoids, four winch motors, one door actuator, and four ultrasonic sensors. The Arduino Nano is responsible for reading the pressure sensors used for bellows monitoring and controlling the camera servos. This distributed architecture reduces the number of direct connections to the Raspberry Pi while allowing each ring assembly to control the motors, actuators, solenoids, and sensors located near that section of the prototype.

Each controller is stored underneath its respective ring assembly inside an electronics enclosure. These enclosures also contain the motor controllers, MOSFET modules, relays, and bus bars needed to distribute 12 V, 5 V, and ground throughout the local subsystem. This modular enclosure layout reduces wiring length, improves subsystem organization, and allows the electronics for each ring assembly to be managed independently.

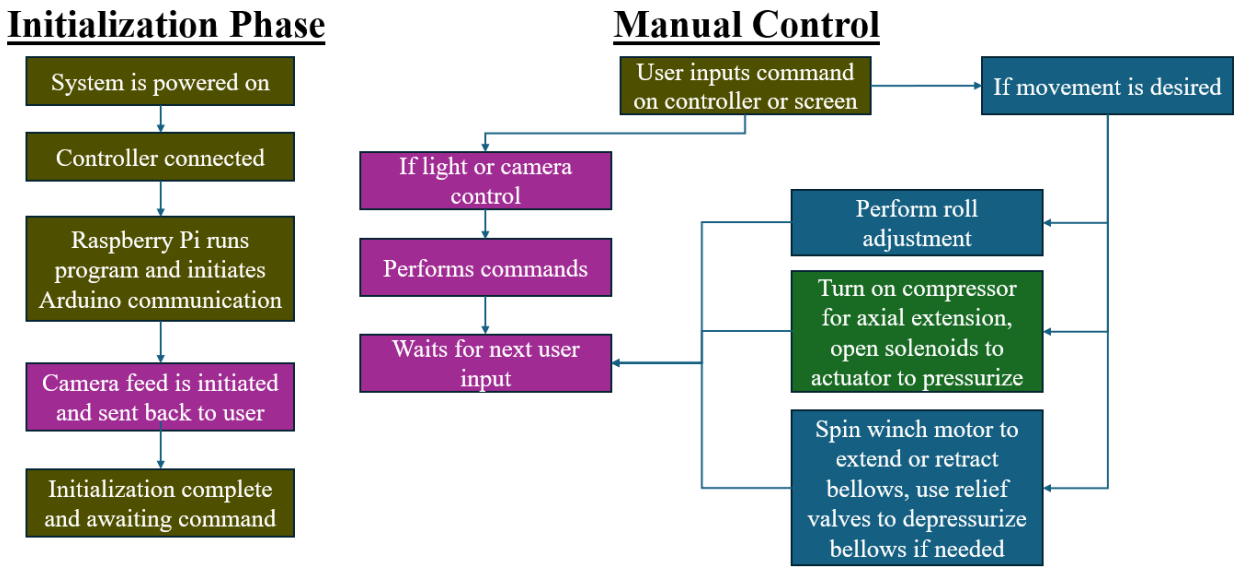

Figure 57. Manual Control Flow Chart

Operator control is performed using a Bluetooth controller connected to the Raspberry Pi. When a button is pressed, the Raspberry Pi interprets the input and determines the required action. If the command controls a device connected directly to the Raspberry Pi, such as the camera system or lighting controls, the Raspberry Pi activates the required GPIO pins or USB-connected devices. If the command controls a device connected to one of the Arduino controllers, the Raspberry Pi sends a string command over USB serial. The appropriate Arduino then interprets the command and activates the required GPIO pins, motor drivers, relays, or MOSFET modules to complete the action.

The camera system consists of five USB-A cameras connected to the Raspberry Pi through a multi-port USB hub. During startup, the Raspberry Pi reads the connected camera addresses and assigns them to user-facing camera numbers 1 through 5. Two camera feeds are displayed at a time, allowing the operator to switch between views while maintaining situational awareness during alignment and operation.

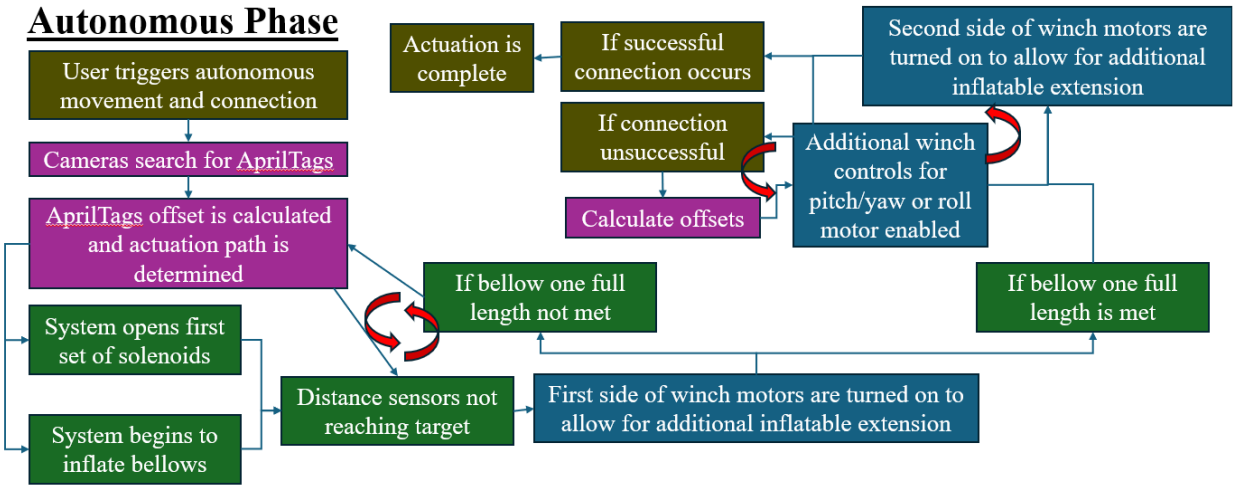

Figure 58. Autonomous Functionality Flow Chart

The mock hatch electronics are separated from the main prototype control system. Each mock hatch is powered by its own 12V battery and uses an Arduino Mega to control four linear actuators with limit switches for feedback control. Each hatch also includes four ultrasonic sensors to measure alignment distance and a 12V indicator light. A physical switch is used to change the mock hatch between connecting mode and standby mode. The mock hatch Arduinos communicate with the Raspberry Pi using Bluetooth modules, allowing hatch status information to be sent to the main system while also allowing the Raspberry Pi to transmit relevant commands back to the hatch controllers. Motor and actuator control is performed using BTS7960 motor driver modules, which provide bidirectional control for the prototype's DC actuation components.

8.9 Vision and Autonomy

The prototype vision system uses five USB-A webcams to support operator visibility, alignment, and future hazard avoidance functions. Four cameras are mounted externally, with two cameras located on each end of the tunnel. Each end includes one upper camera and one lower camera facing straight outward toward the mock hatch interface. A fifth camera is mounted inside the tunnel to monitor internal transfer operations and confirm that the transfer path remains clear during use.

Each camera streams at a resolution of 640 × 480 pixels using MJPG compression at 15 fps. The cameras have an estimated field of view of approximately 90 degrees, providing broad visual coverage of the interface area. Camera footage is processed through the Raspberry Pi, with a maximum of two camera feeds displayed at one time to reduce processing demand and maintain a usable operator interface. Camera switching is controlled manually by the operator, allowing the user to select the most useful camera views during testing. The compiled video stream and telemetry interface are transmitted over an Ethernet connection to a nearby monitor, allowing the operator to view system status and actively control the prototype.

The exterior cameras are paired with 12V lights pointed in the same viewing direction to improve visibility during alignment. The two upper exterior cameras and the interior camera include pan-and-tilt capability, allowing the operator to adjust the viewing direction and increase the observable area without requiring additional fixed cameras. Pan-and-tilt motion is controlled by the operator through the system controller. The exterior cameras are primarily used for mock hatch alignment, AprilTag detection, and operator awareness around the tunnel ends. The interior camera is used only to monitor the tunnel volume during transfer operations.

The alignment system uses AprilTags placed on the mock hatch interfaces. The prototype supports both the 36h11 and 25h9 AprilTag families, with the primary tags using ID 0 and a physical tag size of 100 mm. When detected, the AprilTags are highlighted directly on the camera feed, and the calculated six-degree-of-freedom offsets are shown in real time on the telemetry user interface. These offsets include the three translational offsets and three rotational offsets needed to support autonomous articulation. If AprilTag detection is lost during autonomous alignment, the system pauses actuation to prevent uncontrolled motion until the target is reacquired or the operator takes manual control. While the current camera layout provides the foundation for hazard detection and avoidance, full hazard avoidance capability is identified as a future implementation rather than a completed prototype function.

8.10 Guided User Interface

The prototype user interface is designed to provide the operator with real-time visual feedback, telemetry, and system status information during operation.

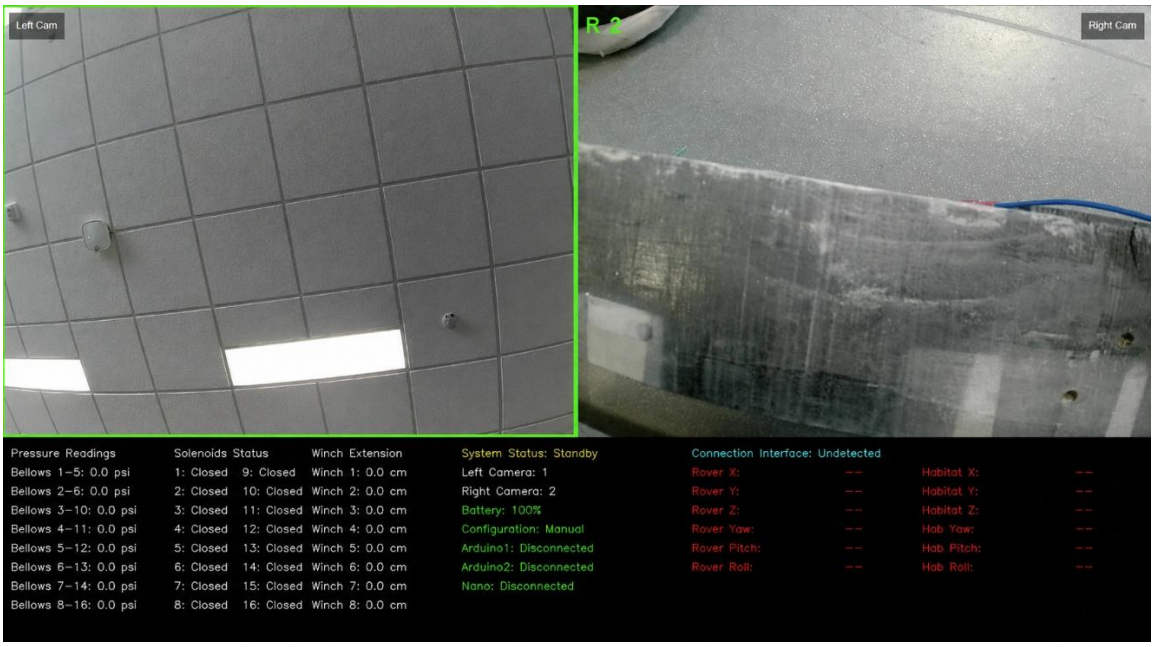

Figure 59: Guided User Interface

Figure 59: *Guided User Interface.* The interface is hosted by the Raspberry Pi using a Flask-based web application. The operator interface is displayed as an HTML webpage, with embedded styling and scripting used to organize the live camera feeds, telemetry values, and system status information. The interface is transmitted over an Ethernet connection to a nearby display, allowing the operator to monitor and control the system from a separate screen.

The screen layout consists of two live camera feeds positioned side by side at the top of the interface, with a telemetry and status banner located underneath. The left and right camera feeds can be cycled independently, allowing the operator to select any two of the five available camera views. The currently selected camera is highlighted on the interface, and each camera feed includes its assigned camera identification number. This allows the operator to identify which camera is active and determine whether pan-and-tilt control is available for that view.

The user interface also displays alignment information generated from AprilTag detection. When the mock hatch AprilTags are detected, the calculated offsets are displayed to the operator in real time. These values provide the translational and rotational alignment feedback needed to support autonomous articulation and manual monitoring during system operation.

Operational telemetry is displayed at approximately 15 Hz, corresponding to an update interval of about 0.067 seconds. This telemetry includes the pressure of each bellows, the estimated extension length of each winch, and the current commanded state of each solenoid. Winch extension feedback is estimated using ultrasonic sensor measurements, which provide an approximate indication of winch extension during

actuation. Solenoid states are displayed as open or closed based on the most recent software command, although future work could improve this by adding direct hardware feedback.

The interface also provides overall system status information for troubleshooting and operator awareness. Displayed values include the current system mode, streaming camera numbers, battery percentage, and communication status for the connected controllers, cameras, and Bluetooth controller. The system modes shown on the interface include standby, actuation, and extended use. Controller communication is checked by identifying the USB serial addresses assigned to the Arduino Mega, Arduino Nano, cameras, and other connected devices, then confirming feedback from each device. While the current interface does not include dedicated visual warning popups, future versions could implement warning indicators for conditions such as communication loss, AprilTag loss, high pressure, or emergency stop activation.

9.0 Inflatable Prototyping

9.1 TPU Coated Nylon Bellows

TPU Coated Nylon Bellows were manufactured for maximum axial force output while maintaining a reasonable margin of difference between each bellow to avoid squirming or unexpected moments as much as possible.



Figure 60: Pressurized Bellows - 5 PSI

9.1.1 TPU Coated Nylon Bellows – Considerations

The manufacturing process was the most important part of fabrication and was designed to make each bellow equal as possible, this was crucial as if each bellow differs vastly from one another, there is too much instability, something which will be underlined later in this section.

9.1.2 Laser Cutting

Laser Cutting using the 48 Epsilon Laser Cutter provided to the team by the architecture department at South Dakota State University improved the quality of each bellow significantly. Not only did this alternative to hand cutting save hours of work, but it also made each inner section of each bellow more consistent. This process is novel to SDSU as the laser cutter is typically only used for etching designs into wood or metal, so, an optimal cutting speed and power had to be selected as this material is thinner, and much more likely to burn. However, one benefit to laser cutting textile fabrics over wood or metal is that the speed can be increased significantly, thereby greatly reducing the time to cut.



Figure 61: AutoCAD Drawing

Figure 61: *AutoCAD Drawing*. This figure shows the laser cut section designed in AutoCAD, then uploaded into the laser cutter for cutting.

Some considerations were made for this design:

- Prepared 70D TPU-Coated Nylon. The Laser cutter has a usable area of only 50”x35” – To make sure the cutter can avoid clashing, the TPU coated nylon sheet should only span 45”x30” (not including additional margins which ensure proper framing).
- The color should be RGB Red (255,0,0) to ensure the most effective line reading by the machine.
- There should be NO overlaps in the drawing – Utilize OVERKILL command to eliminate any inconsistencies before uploading.
- At 1” heat seal, the design should be oversized to account for usable area lost during the hand sealing process.
- 0.83” is the proper fitting diameter for the team’s selected one-way nozzles.

Power	15
Speed	10
Frequency	50
Total Time	≈29 minutes
Bellows per cut	2

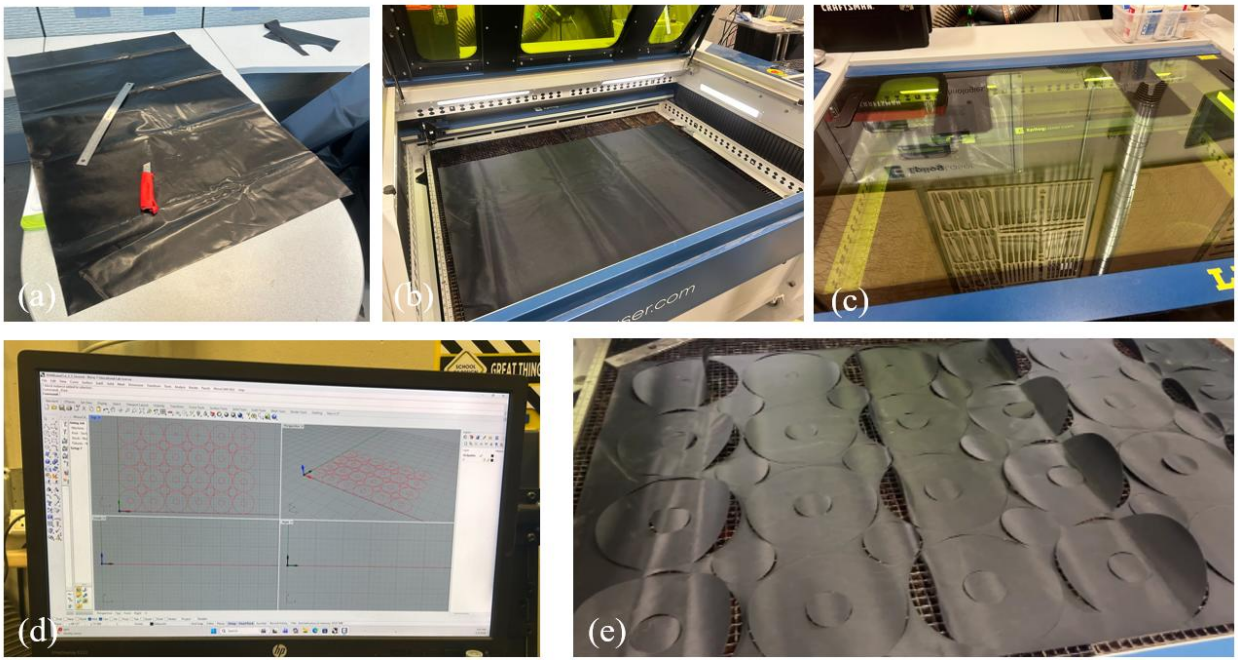

Figure 62: Steps to Laser Cut

Figure 62: *Steps to Laser Cut (a-e).*

a) A 45x30” Section of TPU Coated Nylon is prepared.
b) The section is placed flat in the laser cutter.
c) The section is secured and the settings are entered.
d) The DWG is opened and visualized.
e) The final cut out.

9.1.3 Hand Sealing

Hand Sealing of the TPU Coated Nylon inner rings was fabricated in a way which ensures maximum axial output and minimizes leaks.

The following figures detail each step of the heat sealing process in order.

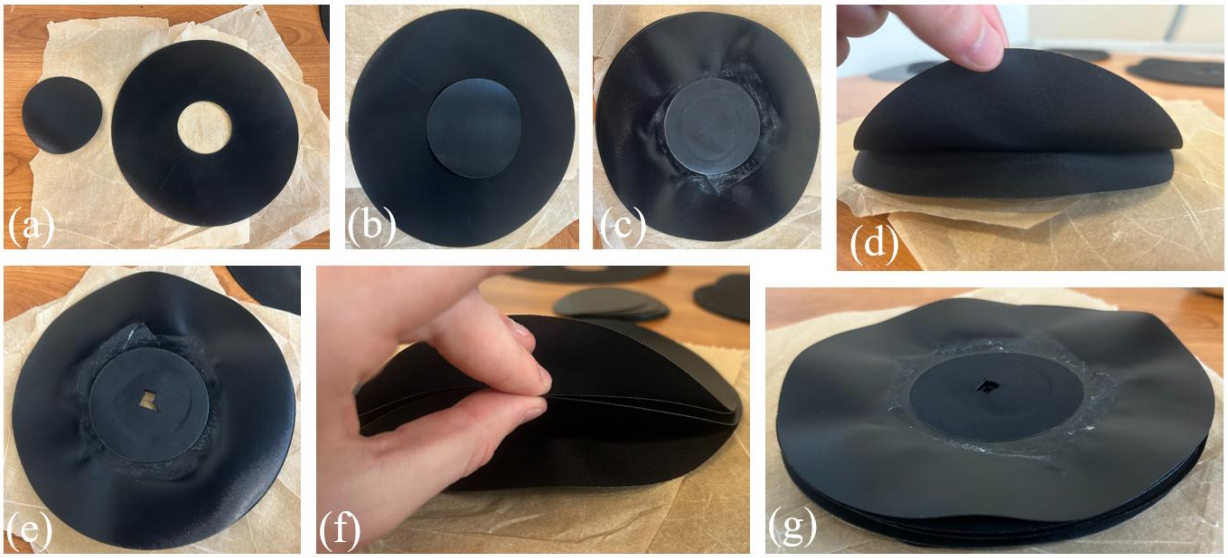

Figure 63: (a-g) Cut-to-bellow

Figure 63 (a): *Side-by-side cutout.* The inner ring side by side with the connection piece. TPU Coated Nylon must be sealed with TPU coated side facing TPU coated side (TPU-to-TPU), otherwise the seal is incapable of holding air, the rings were designed to account for this. The parchment paper is important to negate any binding of the material to anything other than the intended item, for example, the inner section as seen in the following. **Figure 63 (b):** *Overlapping sections.* This figure shows the layers in their intended configuration before sealing. These and all subsequent layers are heat sealed at 220°C (428°F) for ≈ 10 seconds, then pressure rolled to ensure no delamination of the seal. **Figure 63(c):** *Heat Sealed Overlapping Parts.* The heat profile seen surrounding the inner layer is excess seal. This heat profile is common as typical irons are rectangular or blocky, therefore do not fit the profile for a round seal; this does not affect the strength of the bellow. **Figure 63 (d):** *Side View – Heat Sealed Inner Sections.* This figure shows two of the sections seen in **Figure 63 (c)** connected, sealed under the same conditions as previously mentioned. **Figure 63 (e):** *Air-Hole Cutout.* After layers are sealed together, an inner airflow hole is cut before further sealing. The order for which this cut is completed in the process does not influence the final product. **Figure 63 (f):** *Side-View Second Seal.* This figure shows the final inner layering as well as how they were sealed. Each inner section was sealed along the edges 1” inwards.

9.2 TPU-Coated Nylon Testing

TPU Coated Nylon 70D is the ideal material for a prototype utilizing inflatable softgoods as manufacturing can be completed by hand with high strength. Still, to validate the design and manufacturing process, the team completed testing to validate the abilities of the material itself, as well as the design after manufacturing.

9.2.1 ASTM D1876-08 T-Peel Test [67]

To ensure that the manufacturing process for which the TPU Coated nylon is sealed aligns well with the values provided by the manufacturer, the team utilized ASTM D1876.

Figure or Table containing sensitive information, or possible unauthorized copyright information has been removed.

Figure 64: Test Panel & Test Specimen [67]

Figure 64: *Test Panel & Test Specimen*. The test specimen preparation is according to ASTM standard.

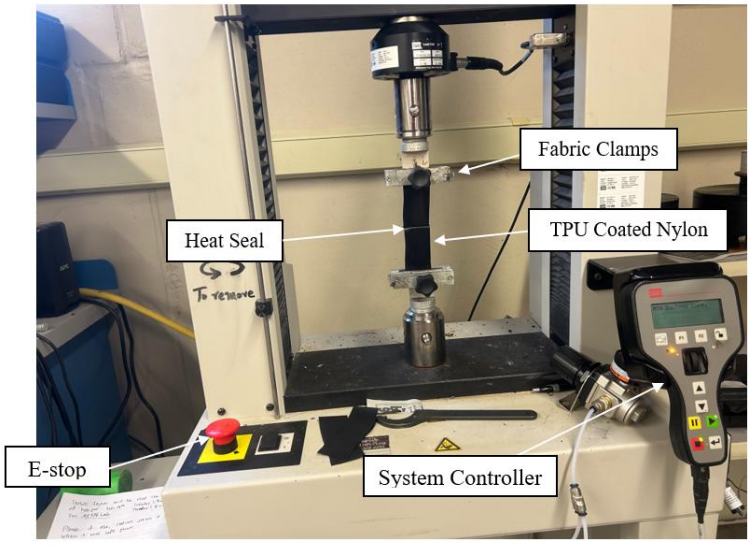

Figure 65: METLAB - Test Setup

Figure 65: *METLAB – Test Setup.* The test configuration using materials provided by South Dakota State University according to ASTM standards.

ASTM D1876-08 specifies the process of manufacturing must be noted in documentation. The only notable difference in the manufacturing process seen for this specific test was a sealing temperature of 392°F, all other parameters remain constant.

The test requires the following:

1. Two adhesive sections sealed together as recommended by the manufacturer:
2. Test specimen prepared as seen in **figure 64** where two adhesive sections (10" x 12") are overlapped flat and sealed at (10" x 9") leaving a small section unsealed for clamping (10"x3").
3. Cut into ten equal 1" width sections as seen in **figure 65**.
4. Allowed to cure under room-temperature conditions for a minimum of 7 days (if not otherwise specified by the manufacturer).
5. Fixed into a tensile tester using specialized fabric clamps as seen in **figure 65**.
6. Pulled apart as specified at a constant head speed of ten in/min.

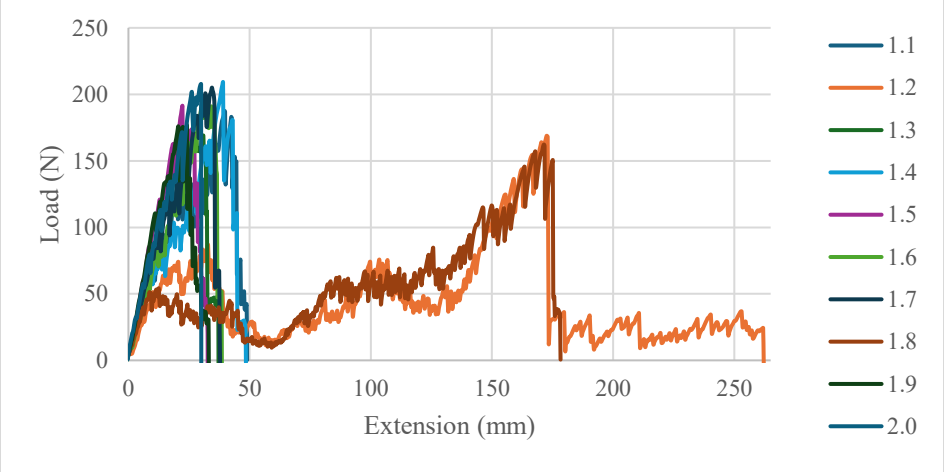

Figure 66: Load vs. Extension

Figure 66: *Load vs. Extension.* Graph detailing the results of the T-Peel test.

Table 7: Formatted Peel Test Results

Specimen	Peel Strength (N/mm)	Failure Mode	Max Load (N)	Extension Before Failure (mm)	Extension Before Fail (inch)
1.1	N/A	Substrate	187.6	49.0	1.9
1.2	2.31	Substrate	168.9	262.2	10.3
1.3	N/A	Substrate	170.6	37.2	1.5
1.4	N/A	Substrate	209.4	48.5	1.9
1.5	N/A	Substrate	191.5	32.7	1.3
1.6	N/A	Substrate	193.7	38.6	1.5
1.7	N/A	Substrate	205.1	37.8	1.5
1.8	2.44	Substrate	162.3	178.3	7.0
1.9	N/A	Substrate	177.0	33.2	1.3
2.0	N/A	Substrate	207.9	30.1	1.2

Table 7: *Formatted Peel Test Results.* The results tell that the manufacturing process the team has designed exceeded expectations as every specimen experienced a substrate failure. This indicates that the seam will

consistently outlive the material. Due to the overwhelming strength of the seam, the team cannot conclude with good confidence a peel strength, even still, results attained are promising. Manufacturer does not specify maximum load; however, results are consistent with a resulting coefficient of variation at 9.13%.

9.2.2 Bellow Burst Test

To measure a safety factor against simulations, and to validate findings from earlier experiments, the team completed a burst test where a test specimen was fabricated in the same fashion as working bellows, then connected to fixtures, then pressurized until failure.

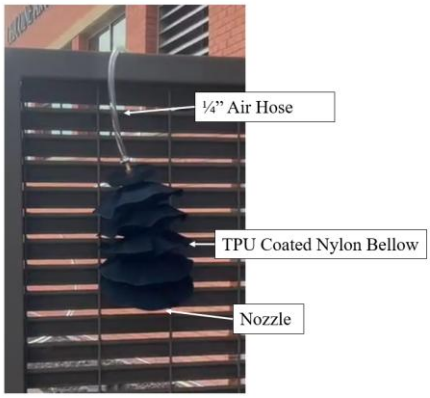

Figure 67: Burst Test Setup

Figure 67: *Burst Test Setup*. The fabric bellow was fixed to an air hose and pressurized. This bellow was not pressure cycled to ensure consistency.

The team noted the following:

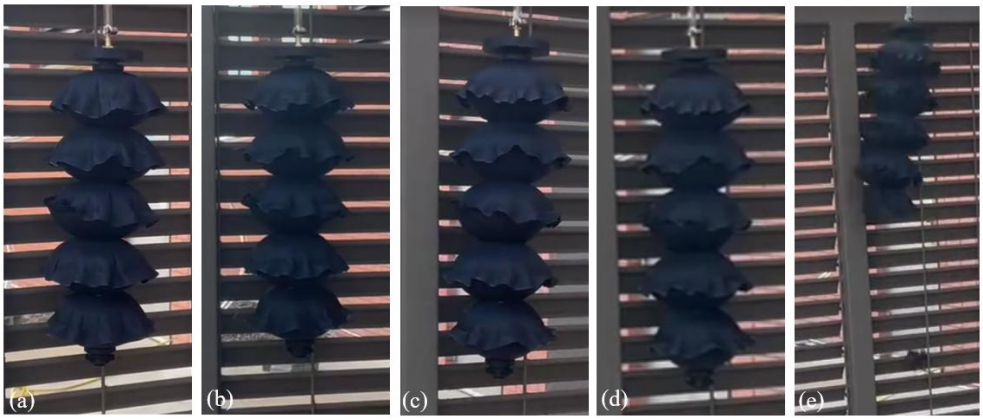

Figure 68: Bellow Burst Test Progression

Figure 68: *Bellow Burst Test Progression*. This figure shows the test as it progresses and pressure increases. **Figure 68 (a)** 5 psi, this is the working pressure of each bellow. **Figure 68 (b)** 10 psi, at this pressure there is a clear displacement of the nozzle, and a clear bulge of the material, but nothing extraordinary otherwise. **Figure 68 (c)** 13 psi, the material secured by the nozzle has a leak which is audible, the test continues. **Figure 68 (d)** 20 psi, the nozzle stops leaking air i.e., the sound disappears. **Figure 68 (e)** 20 psi, the bellow bursts suddenly and the test is concluded.



Figure 69: Failure Point

Figure 69: *Failure Point*. The bellow failed where experimentation and simulation predicted, all seams remain intact and the main point of failure is the material itself.

9.2.3 Force Testing

Force testing in the MTS Insight - universal tensile tester was completed to visualize force output of a single bellow. This test came with complications which displayed expected, and unexpected bellow behavior.

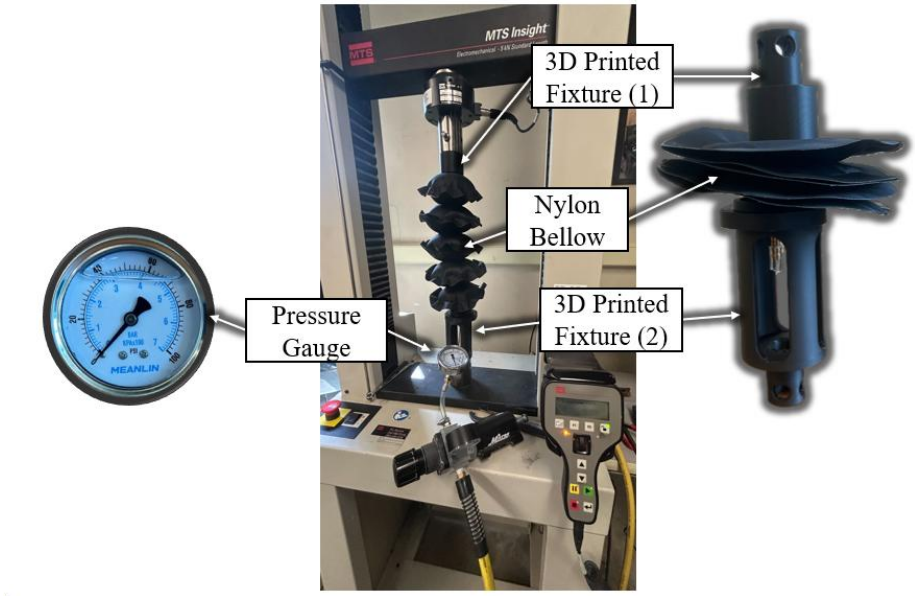

Figure 70: Force Test Setup

Figure 70: *Force Test Setup*. This figure shows the setup for the force test with a high-pressure pressure-gauge and custom fabricated 3D printed fixtures which provide stability to the bellow during the test. The bellow is fully extended through pressurization, and baseline pressure is at 2.5 psi.

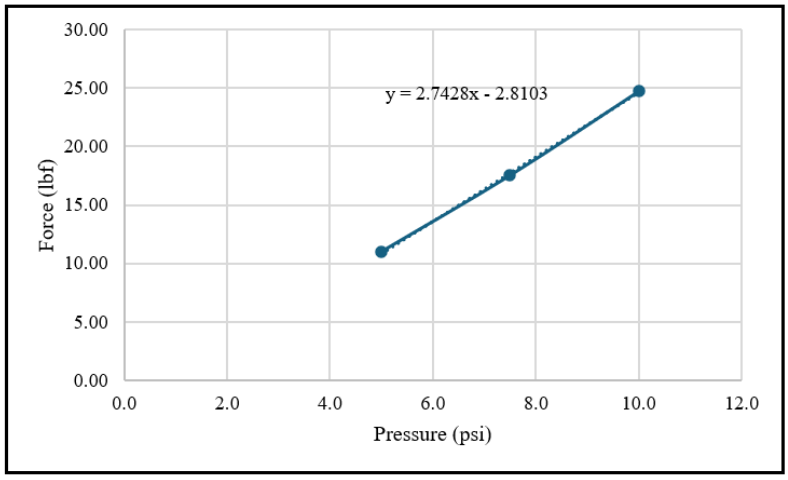

Figure 71: Force vs. Pressure Graph (imperial)

Figure 71: *Force vs. Pressure Graph (imperial)*. This figure shows the graphed results of the force-pressure test. Using the plot, the team can find an equation which can be used to estimate the force output at any given moment, for any given number of bellows:

$$F = N \times [(2.7428 \times P) - 2.8103]$$

Where:

F = Force output (lb_f)

N = Number of bellows

P = Pressure ($\frac{lb_f}{in^2}$)

Note: The equation for force related to pressure in metric is found in the same fashion.

$$F = N \times [(0.0018 \times P) - 12.5]$$

Where:

F = Force output (N)

N = Number of bellows

P = Pressure (Pascals)

The results of this test were hardly conclusive. The test varied pressure from 0-10 psi in increments of 2.5 psi with outside intervention needed to fully constrain the system for this test. See the following:



Figure 72: Pressurized Test Specimen - Squirm

Figure 72: *Pressurized Test Specimen – Squirm*. This figure shows the test specimen pressurized to 10 psi. At roughly 5 psi of pressure, a noticeable amount of column instability, or "squirm," occurs. This squirm seen in the bellows makes force output incredibly difficult to gauge and derives from the manufacturing process. The bellows are manufactured (see **sections 9.1.2-9.1.3**) with a large outer diameter (7 inches), and a small inner (2 inches), meaning the effective area is less than ideal to output force. It is worth noting that even if the bellow is redesigned (which would improve force output and stability), a large reason for instability comes from variation between each bellow. It is nearly impossible to manufacture bellows which are identical to one another without significant infrastructure. This is one drawback for this design, even more so since the team is heat-sealing by hand.

9.3 TPU printed Bellow Design and Testing

3D printed TPU bellows are being investigated for their control over geometry and low manufacturing setup time. However, they are not the primary mode of soft actuation being investigated due to their high print time, number of failure points (layers), and differences from the concept of operations (compared to the TPU-coated fabric bellows).

These bellows are manufactured out of TPU 85A, which offers a good balance of rigidity and flexibility. The outer diameter of the inflatable region is 6", with a total height of the bellows being 8.9". The effective height however, is lower, due to the conical shape of the top required to print both without sharp overhangs and without the need for supports. The effective height of the bellows once the top is compressed is 6.45 inches. The peak-to-peak wall thickness of the bellows is 2.5mm. As shown in **figure 73**, there are gaps within the print to accommodate for the nut side of a bulkhead fitting to be inserted with a print pause. After the print is finished this will be threaded with the bolt end of the bulkhead fitting and then into a ¼" bulkhead fitting where the pneumatic line can be attached.

Print Settings:

- Layer Height: 0.3 mm
- Sparse Infill Density: 100%
- Seam Position: Nearest
- Wall Generator: Arachne
- Print Speed: 24 mm/s

- Print Speed for Top Conical Region: 12 mm/s

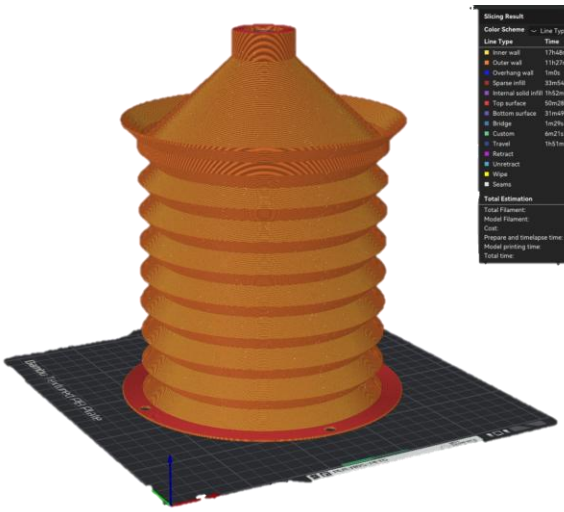

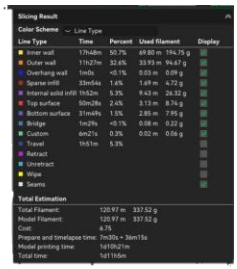

Redacted due to Export Control/CUI requirements.

Redacted due to Export Control/CUI requirements.



Figure 73. Top Left: TPU Bellow Slicer, Top Right: CAD Cross Section, Bottom Left: CAD Isometric, Bottom Right: Printed Prototype

10.0 Prototype Results

10.1 Actuation Success

Actuation success was evaluated through two primary tests: pneumatic actuation of the inflatable bellows and full system extension using integrated controls.

10.1.1 Pneumatic Actuation Test

The pneumatic actuation test is a preliminary test conducted by the team with the sole purpose of visualizing extension due to pressurization of the fabric bellows alone.

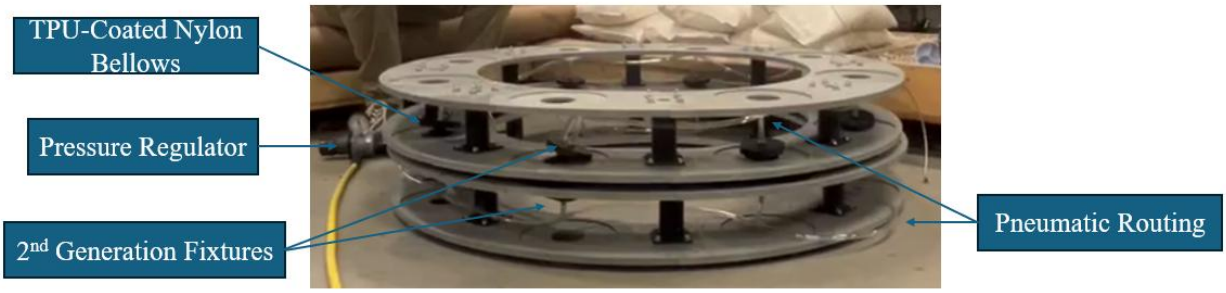

Figure 74: Pneumatic Actuation Test Setup

Figure 74: *Pneumatic Actuation Test Setup*. Two sections of the tunnel were connected via fabric bellows paired with custom 3D printed fixtures. Pneumatic routing was routed to ensure airflow to each vessel.

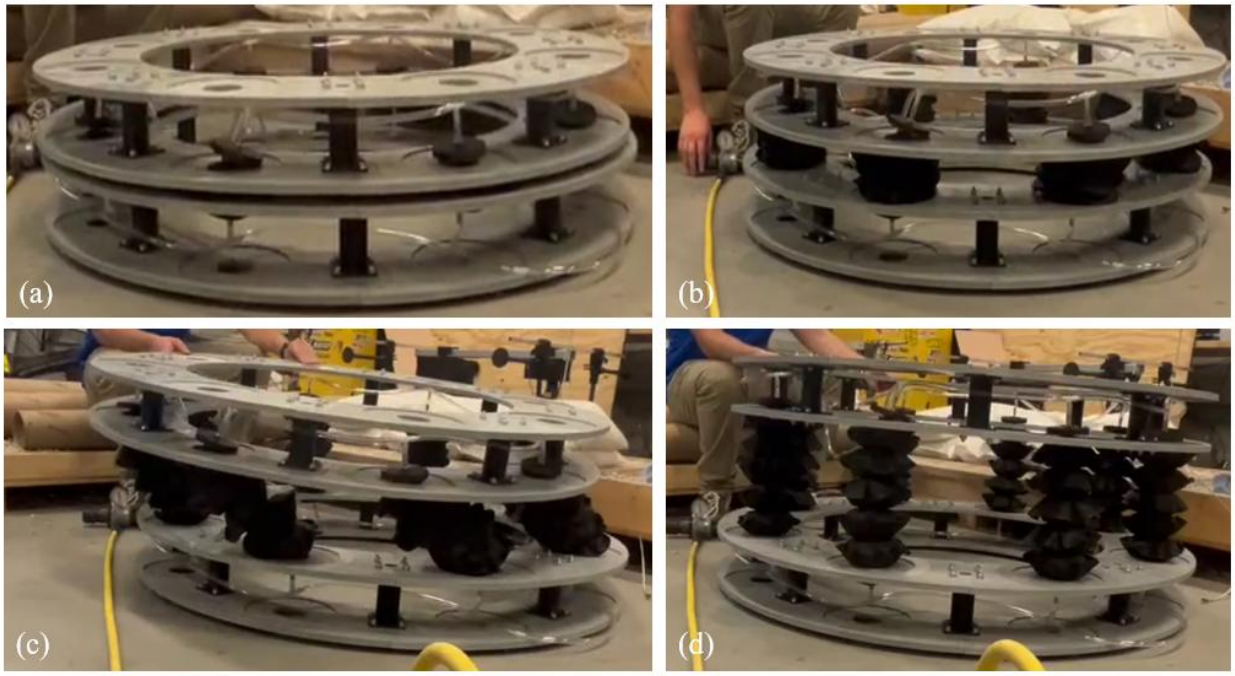

Figure 75: Pneumatic Actuated Test Progression

Figure 75: *Pneumatic Actuated Test Progression*. Airflow is introduced slowly. See **figure 75 (a)** to see the baseline, as pressure is slowly introduced, instability is seen immediately. This instability is worsened

as pressure is further increased **(figure 75 (c))** and to fully actuate, outside interference is needed to constrain the system (**figure 75 (d)**). This instability is highlighted in **section 9.2.3**.

10.1.2 Controls-Implemented Actuation

After implementation of controls, the team evaluated the overall capabilities of the system.

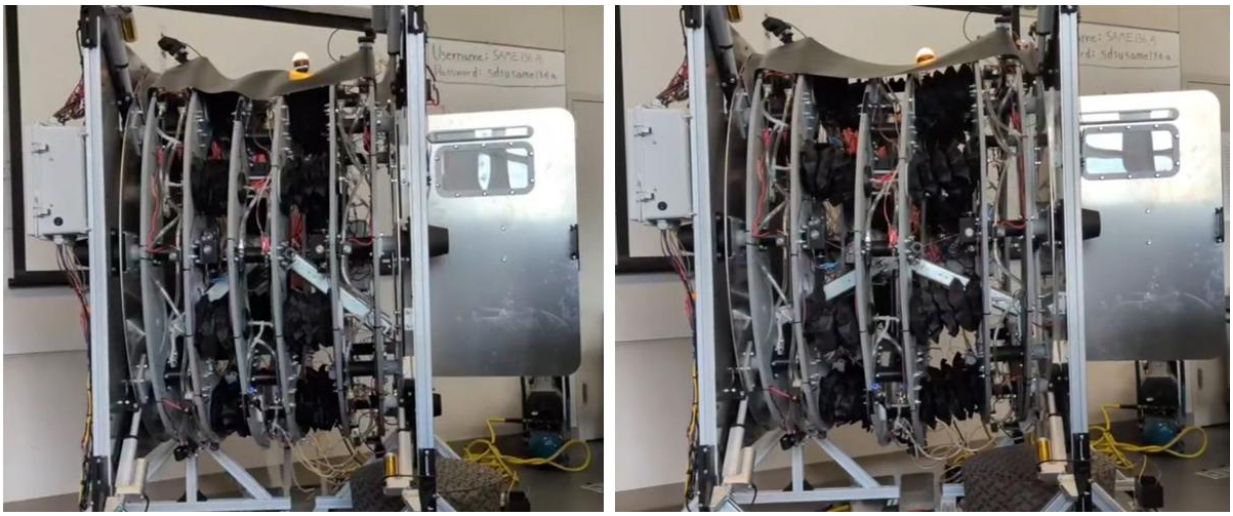

Figure 76: Full Controls Integrated System Extension

Figure 76: *Full Controls Integrated System Extension*. The system's maximum extension was limited by the allowable load of the selected cables. As seen above, the system successfully extends as intended, though a noticeable sag occurs in the middle section post-extension. The driving pressure ranges from 0-3 psi, which is lower than the predicted 5 psi working pressure of the bellows; however, operating at this lower working pressure increased the observed sag. To mitigate this, pressure is introduced incrementally until approximately 1 psi, at which point the winch motors activate to maintain constant tension in adherence to standard CDPR principles.

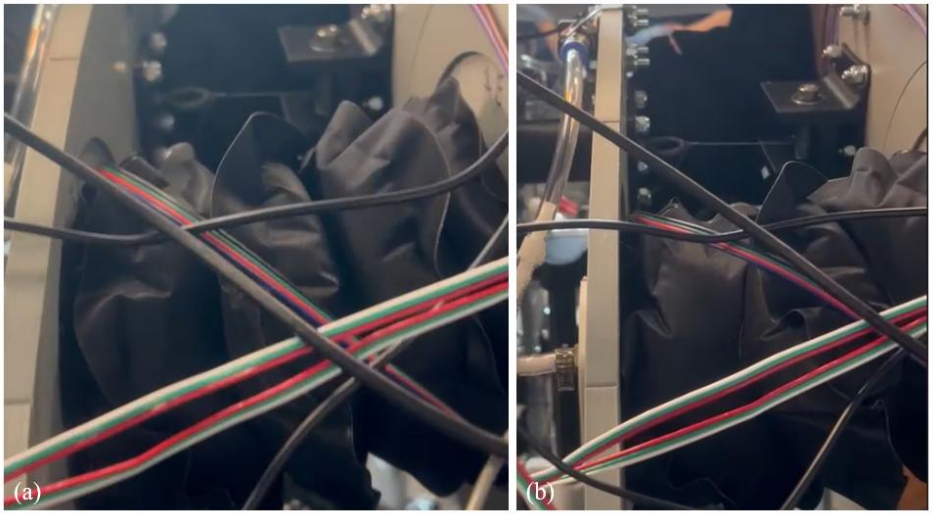

Figure 77: (a) extended, (b) further extended winch and fabric bellow combination.

Figure 77: *(a) extended, (b) further extended winch and fabric bellow combination.* As internal pressure increases, the cable extends according to the control logic. However, rapid inflation can induce cable fracture. While a fractured cable is less catastrophic than a structural failure of the PLA components, it introduces severe strain on the fabric and internal wiring as these components must now compensate for loss of tension, potentially leading to more severe part failure. To prevent this, the team manually regulates pressure while monitoring system progression, resulting in a controlled, deliberate extension.

Furthermore, as referenced in **section 9.2.2**, inflatable squirm appears as pressure is incremented. However, the squirm observed after full control integration is negligible, and the bellows actuate within acceptable parameters.

10.2 Mock Hatch Results

The prototype mock hatch successfully validated the conceptual latching mechanism and demonstrated that the hatch could provide a rigid connection to the main tunnel system on each side.

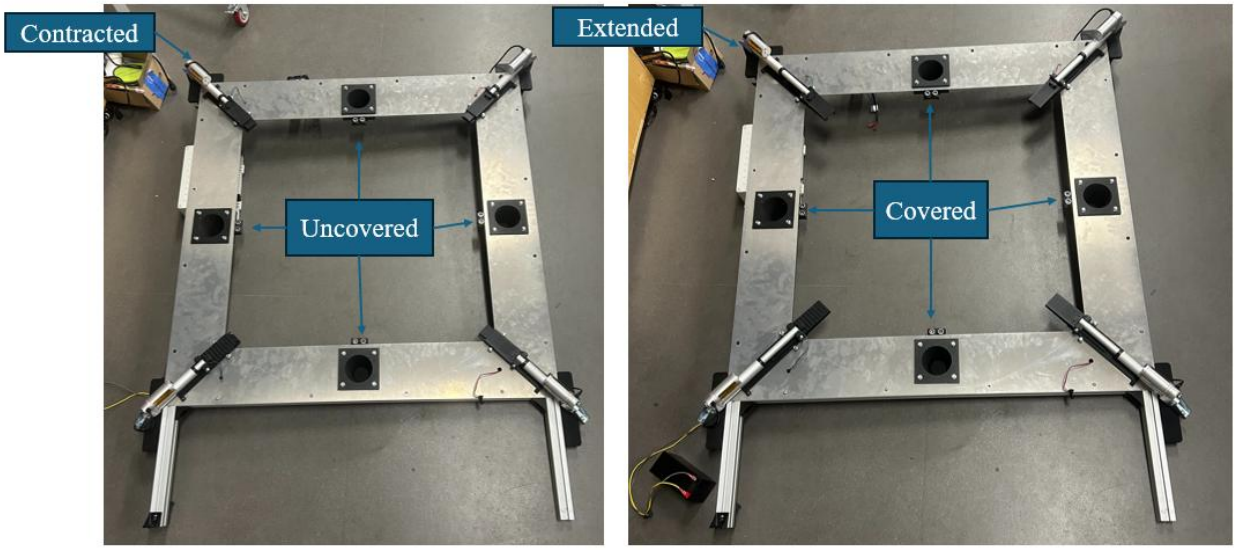

Figure 78: Mock Hatch - Contracted/Extended

Figure 78: *Mock Hatch – Contracted/Extended.* The mock hatch was designed as a simplified proof-of-concept rather than a full-scale final interface, allowing the team to focus on latch engagement, sensor-triggered actuation, and mechanical capture behavior. Both tunnel ends were tested under the same conditions. When the connection interface face was positioned within a few inches of all four ultrasonic sensors, the four linear actuators engaged simultaneously and drove the wedges into the corresponding holders. The actuation sequence stopped once the limit switches were triggered, preventing overtravel after full connection. After engagement, the latches held the interface firmly and provided a stable mechanical connection to the prototype system.

The test also showed that the geometry of the wedge holders had a significant effect on alignment performance. One tunnel end used holders with a guiding chamfer, while the other used holders without the chamfer. The chamfered side performed much better because the lead-in geometry reduced snagging and increased the allowable misalignment before the wedges contacted the holder walls. The non-chamfered side required more precise positioning and, when misaligned, caused the wedge to contact the wall of the

holder instead of sliding into place. This introduced a moment load into the rear actuator mount and resulted in a small crack during testing. The system tolerated axial offset along the tunnel extension direction better than lateral misalignment, but successful engagement still required ideal positioning, with lateral misalignment limited to approximately 0.08 in. The system was evaluated roughly ten times, but additional trials would be needed to fully evaluate repeatability.

Overall, the mock hatch demonstrated that a simple hardware and control approach could support the proposed latching concept. The use of four distance sensors provided a basic confirmation that the interface was within range before actuation, although future designs may benefit from relocating sensors closer to each latch or replacing the ultrasonic sensors with laser distance sensors for improved accuracy. The testing also showed that mechanical capture zones are necessary before final latching, especially if the system is expected to tolerate imperfect alignment. Future iterations should include chamfered or otherwise tapered lead-in features on all wedge holders, slightly larger wedges, and longer cones or improved guide geometry to better support autonomous or semi-autonomous connection. While the mock hatch did not fully demonstrate repeated disconnection and reconnection under unsupported tunnel sag conditions, it provided strong early evidence that the latching concept is feasible and should be developed further.

11.0 Future Work/Community Outreach

11.1 Future Work

Future work should focus on improving the maturity of the bellows, scalability, controls, and alternate applications of the BLIMP system. Additional testing should be performed on the inflatable bellows to better understand their mechanical performance, pressure response, fatigue life, and long-term durability. Future studies should also investigate Vectran-based bellows or softgoods counterparts to determine whether they provide improved strength, mass efficiency, abrasion resistance, and pressure retention compared to the current prototype materials.

Environmental testing should also be expanded. Individual bellows could be tested inside a vacuum chamber or temperature-controlled freezer to better simulate lunar-relevant pressure and thermal conditions. These tests would help evaluate material behavior, leak risk, stiffness changes, and actuation performance under more representative surface conditions.

Further work should also investigate whether 3D-printed TPU bellows can operate in a reversible airflow system. In this approach, vacuum pressure would be used to collapse the bellows into a condensed configuration, while positive pressure would be used to inflate the bellows and extend the tunnel. This testing would help determine whether additively manufactured TPU bellows are suitable for repeatable inflation and deflation cycles, or whether higher performance softgoods materials are required for future versions.

Scalability should be studied in greater detail for both length and diameter. Future prototypes should include additional structural rings and bellows sections to evaluate how the system performs as more tunnel segments are added. This would allow the team to assess increased articulation capability, structural stability, mass growth, and control complexity for longer tunnel configurations.

Future software development should include simulation-based testing using tools such as Isaac Sim. A simulation environment could be used to train and validate autonomous alignment algorithms, test AprilTag recognition, evaluate control logic, and reduce risk before physical testing. This would also allow the software to be tested across a wider range of alignment errors, lighting conditions, camera positions, and interface geometries than would be practical with the physical prototype alone.

Additional future work could also investigate off-surface applications of the system. While the current design is focused on lunar and Martian surface infrastructure, similar technology could potentially be adapted for orbital applications, such as connecting one moving spacecraft or satellite to another. This would require further research into microgravity dynamics, relative motion control, docking loads, and softgoods behavior in an orbital environment.

11.2 Community Outreach

Our community outreach initiative supported the InSimEd Space Design Competition, a weekend event designed to engage high school students from Iowa, Minnesota, Nebraska, and South Dakota who are interested in the future of human space exploration. Members of the X-Hab team served as mentors throughout the competition, helping students develop conceptual designs for a sustainable lunar civilization focused on long-term mining operations. Student teams designed systems for lunar resource extraction and

processing, including water ice and rare metals, while also developing supporting infrastructure such as crew habitats, power systems, agricultural spaces, recreational areas, and laboratories.

To provide continuous support, X-Hab members mentored students in rotating shifts throughout the event. In-person guidance was provided during the first day before the competition transitioned to a virtual format due to weather conditions. Remote mentorship then continued through final presentations on the second day.

Following the student presentations, the X-Hab team delivered a technical presentation highlighting the project focused on developing a lightweight actuation system for a pressurized lunar and Martian tunnel. The presentation introduced the project objectives, mission requirements, and conceptual solution utilizing inflatable soft actuators to reduce system mass compared to traditional mechanical actuation methods. System-level renders were presented to illustrate deployment and docking operations, and the team discussed ongoing work comparing TPU-coated nylon inflatable actuators and additively manufactured TPU bellows. Manufacturing methods and video demonstrations were also presented to show the performance and effectiveness of each approach. Through this outreach effort, the X-Hab team promoted STEM engagement while sharing the technical goals and innovations of the project with future engineers.

The X-Hab team also participated in the Engineering Expo hosted by the Jerome J. Lohr College of Engineering. The event showcased senior design projects from all engineering disciplines, in addition to computer science projects and exhibits from various engineering student organizations. Open to the public, the expo provided the team with an opportunity to present the project to local community members, visiting high school students on educational field trips, and a panel of engineers from industry.

During the event, industry professionals evaluated and ranked the projects, with the X-Hab team earning second place overall. The team showcased progress on the mock hatch, tunnel, and lightweight actuation mechanism prototype through physical demonstrations, technical posters, rack cards, and video renders illustrating the Concept of Operations (ConOps). These outreach efforts allowed the team to communicate both the technical specifications and broader mission objectives of the conceptual design and prototype to a diverse audience.

12.0 Conclusion

In conclusion, the BLIMP project demonstrated the feasibility of using lightweight inflatable actuation, winch-controlled tensioning, and simplified mechanical latching to support a scalable pressurized transfer pathway for future lunar and Martian surface infrastructure. Through research, trade studies, conceptual design, structural analysis, inflatable fabrication, controls integration, and prototype testing, the team developed a functional proof-of-concept that addressed the major project goals of reducing system mass, supporting active alignment, and limiting the need for EVA-based crew and cargo transfer. Testing showed that the inflatable bellows could produce useful extension, the winch system could improve controlled motion, and the mock hatch could provide a rigid connection using a simple sensor-driven latching sequence. However, the prototype also revealed important areas for improvement, including bellow stability, unsupported tunnel sag, repeatable autonomous alignment, sensor placement, and more forgiving connection interface geometry. Overall, the project successfully advanced the BLIMP concept from an initial design challenge into a working prototype and identified a clear path for future development through improved softgoods materials, expanded environmental testing, refined autonomy, and larger-scale system demonstrations.

13.0 References

[1] K. K. De Groh, B. A. Banks, C. E. Mccarthy, R. N. Rucker, L. M. Roberts, and L. A. Berger, "MISSE PEACE Polymers Atomic Oxygen Erosion Results," 2006, Available: http://www.sti.nasa.gov

[2] "System Engineering Handbook: Appendix - NASA." Available: https://www.nasa.gov/reference/system-engineering-handbook-appendix/

[3] "Outgassing Database User Guide | Goddard Engineering and Technology Directorate." Available: https://etd.gsfc.nasa.gov/capabilities/outgassing-database/user-guide/

[4] J. Ku, "Introduction to Heat Pipes GSFC· 2015".

[5] S. Qian, B. Zi, W. W. Shang, and Q. S. Xu, "A review on cable-driven parallel robots," *Chinese Journal of Mechanical Engineering (English Edition)*, vol. 31, no. 4, pp. 66-, Aug. 2018, doi: 10.1186/S10033-018-0267-9/FIGURES/19.

[6] "Carbon Fiber Sleeve Tempers Battery Thermal Runaway | T2 Portal." Available: https://technology.nasa.gov/patent/MSC-TOPS-119

[7] "Machining And Fabrication – NASA." Available: https://www.nasa.gov/centers-and-facilities/white-sands/machining-and-fabrication/

[8] "6 DoF Cockpit Simulator - NASA." Available: https://www.nasa.gov/image-article/6-dof-cockpit-simulator/

[9] A. Ridley, "ECLSS Evolution Overview," 2023. Available: https://ntrs.nasa.gov/api/citations/20230009144/downloads/Lunch%20and%20Learn%202023.pdf

[10] S. Plucinsky, "NASA's Dust Shield Successfully Repels Lunar Regolith on Moon," NASA.

[11] "Extravehicular Activities - NASA." Available: https://www.nasa.gov/johnson/exhibits/extravehicular-activities/

[12] C. Rubin, "DESIGN THROUGH MANUFACTURING: THE SOLID MODEL-FINITE ELEMENT ANALYSIS INTERFACE," 2000.

[13] "Superseding NASA-STD-5001A STRUCTURAL DESIGN AND TEST FACTORS OF SAFETY FOR SPACEFLIGHT HARDWARE," 2014, Available: https://standards.nasa.gov.

[14] "Lidar Profiling Satellite Observations for Air Quality Applications | NASA Earthdata." Available: https://www.earthdata.nasa.gov/learn/trainings/lidar-profiling-satellite-observations-air-quality-applications

[15] H. F. Riley, "Micrometeoroids and Orbital Debris (MMOD)," NASA.

[16] "Materials Test Systems." Available: https://www.mts.com/en/products/materials

[17] J. McFatter, K. Keiser, T. Rupp, and T. Boeing Company, "NASA Docking System Block 1: NASA's New Direct Electric Docking System Supporting ISS and Future Human Space Exploration Figure 1. NASA Docking System Block 1".

[18] "6.0 Structures, Materials, and Mechanisms - NASA." Available: https://www.nasa.gov/smallsat-institute/sst-soa/structures-materials-and-mechanisms/

[19] D. W. Wisander' and R. L. Johns, "Aiid Film Lubricant Composition for Use at High Sliding Velocities in Liquid Nitrogen /NAA FILE COPY".

[20] R. H. Bush, T. Chyczewski, K. Duraisamy, B. Eisfeld, C. L. Rumsey, and B. R. Smith, "Recommendations for Future Efforts in RANS Modeling and Simulation".

[21] "RGB Products." Available: https://weather.ndc.nasa.gov/sport/goesrpg/rgb.html

[22] "State-of-the-Art of Small Spacecraft Technology - NASA." Available: https://www.nasa.gov/smallsat-institute/sst-soa/

[23] "ESTANE® ALR TPU (Thermoplastic Polyurethane) - Lubrizol." Available: https://www.lubrizol.com/solutions/products/estane/estane-alr

[24] "Technology Readiness Levels - NASA." Available: https://www.nasa.gov/directorates/somd/space-communications-navigation-program/technology-readiness-levels/

[25] "NASA Technology Roadmaps - TA 6: Human Health, Life Support, and Habitation Systems," 2015. Available: https://www.nasa.gov/offices/oct/home/taxonomy

[26] J. R. Gaier, "The Effects of Lunar Dust on EVA Systems During the Apollo Missions," 2005. Available: http://www.sti.nasa.gov

[27] D. Litteken, P. Brown, M. Goit, and C. Ohland, "Inflatable Softgoods Design of an Articulating Crew Transfer Tunnel," 2025. Available: https://ntrs.nasa.gov/api/citations/20240016215/downloads/AIAA_Softgoods_Design_Articulating_Tunnel.pdf

[28] "Moon to Mars eXploration Systems and Habitation (M2M X-Hab) Academic Innovation Challenge - FY26 Solicitation," Mar. 2025.

[29] "Fig. 2 Drawing of Coil Spring Structure on Top of Stewart Platform II. FEEDBACK CONTROL OF STEWART PLATFORM".

[30] Z. Zhang *et al.*, “State-of-the-art on theories and applications of cable-driven parallel robots,” *Frontiers of Mechanical Engineering 2022 17:3*, vol. 17, no. 3, pp. 37-, Sep. 2022, doi: 10.1007/S11465-022-0693-3.
[31] D. Rus and M. T. Tolley, “Design, fabrication and control of soft robots,” *Nature 2015 521:7553*, vol. 521, no. 7553, pp. 467–475, May 2015, doi: 10.1038/nature14543.
[32] “Air-Supported TEMPER Tents Maximizes Readiness | Article | The United States Army.” Available: https://www.army.mil/article/223675/air_supported_temper_tents_maximizes_readiness
[33] “(PDF) Air-Inflated Fabric Structures.” Available: https://www.researchgate.net/publication/235213999_Air-Inflated_Fabric_Structures
[34] G. Valle, D. Litteken, and T. Jones, “Review of Habitable Softgoods Inflatable Design, Analysis, Testing, and Potential Space Applications,” Jan. 2019. Available: https://ntrs.nasa.gov/api/citations/20190000847/downloads/20190000847.pdf
[35] J. Sisson, “Dreams of Space - Books and Ephemera.”
[36] D. A. Litteken and T. C. Jones, “DEVELOPMENT OF AN INFLATABLE AIRLOCK FOR DEEP SPACE EXPLORATION,” 2018.
[37] H. De La Fuente, J. L. Raboin2, G. R. Spexarth\, and G. D. Valle, “AIAA 2000-1822 TRANSHAB: NASA’s LARGE-SCALE INFLATABLE SPACECRAFT.”
[38] NASA, “Bigelow Expandable Activity Module (BEAM),” NASA.
[39] W. Steigerwald, “NASA’s LRO Finds Lunar Pits Harbor Comfortable Temperatures,” NASA.
[40] K. B. Hille, “The Fact and Fiction of Martian Dust Storms,” NASA.
[41] D. Logreira, “Mars Facts,” NASA. Available: https://science.nasa.gov/mars/facts/
[42] J. Rask, V. Wenonah, B. J. Navarro, and A. Krause, “The Radiation Challenge.”
[43] B. Ridgeway, “NASA to Test Solution for Radiation-Tolerant Computing in Space,” NASA.
[44] A. M. Abd El-Hameed, “Radiation effects on composite materials used in space systems: a review,” *NRIAG Journal of Astronomy and Geophysics*, vol. 11, no. 1, pp. 313–324, Dec. 2022, doi: 10.1080/20909977.2022.2079902.
[45] “Blue Moon Mark 1.” Available: https://www.blueorigin.com/blue-moon/mark-1
[46] “Super Nova Lunar Lander.” Available: https://www.intuitivemachines.com/build/super-nova-lunar-lander
[47] “Giant Leap in Microgravity Research: Sierra Space’s Successful Habitat Test.” Available: https://futuramic.com/giant-leap-in-microgravity-research-sierra-spaces-successful-habitat-test/
[48] eTek Outdoor Textiles, “eTek Outdoor Textiles Products Catalog,” 2025. Available: etekoutdoortextiles.com
[49] “LIQUID CRYSTAL POLYMER FIBER TECHNOLOGY Enhance • Transform • Discover.”
[50] G. N. Szatkowski *et al.*, “SansEC Wireless Strain Sensor for Softgoods Habitats and Inflatable Space Structures”, Available: http://www.sti.nasa.gov
[51] fpm, “SOLIMIDE ® AC-530”, Available: www.boydcorp.com
[52] “Teflon PTFE (Polytetrafluoroethylene),” Plastics International. Available: https://www.plasticsintl.com/media/hotni4w0/ptfe-data-sheet.pdf
[53] “Solimide AC-530,” Boyd Trusted Innovation. Available: https://info.boydcorp.com/hubfs/Engineered-Materials/Insulation-Shielding/Boyd-SOLIMIDE-AC-530-Datasheet.pdf
[54] “Composition of POLYETHYLENE TEREPHTHALATE (MYLAR).” Available: https://pml.nist.gov/cgi-bin/Star/compos.pl?matno=222
[55] R. C. Linton, A. F. Whitaker, and M. M. F. Nasa, “SPACE ENVIRONMENT DURABILITY OF BETA CLOTH IN LDEF THERMAL BLANKETS.”
[56] R. B. Fette and M. F. Sovinski, “Vectran Fiber Time-Dependent Behavior and Additional Static Loading Properties,” 2004, Available: http://www.sti.nasa.gov/STI-homepage.html
[57] R. Destefanis, F. K. Schaefer, M. Lambert, M. Faraud, and E. Schneider, “Enhanced Space Debris Shields for Manned Spacecraft,” *Int. J. Impact Eng.*, vol. 29, pp. 215–226, 2003.
[58] T. Sabir, “Fibers used for high-performance apparel,” *High-Performance Apparel: Materials, Development, and Applications*, pp. 7–32, Jan. 2017, doi: 10.1016/B978-0-08-100904-8.00002-X.
[59] “NASA Technical Memorandum /N-oq.”
[60] Dunmore, “Dunmore Beta® Cloth Sell Sheet.” Available: https://www.dunmore.com/pdf/ss/dun-beta-cloth-sell-sheet.pdf
[61] D. W. Wisander and R. L. Johns, “Aiid Film Lubricant Composition for Use at High Sliding Velocities in Liquid Nitrogen /NAA FILE COPY,” 1960.
[62] D. Selman, “Contribution to the geometric, kinematics and dynamic modeling of bionic continuum robots.” Available: https://www.researchgate.net/publication/362583160_Contribution_to_the_geometric_kinematics_and_dynamic_modeling_of_bionic_continuum_robots

[63] “Exploration Systems Development Mission Directorate Moon-to-Mars Architecture Definition Document (ESDMD-001),” Apr. 2023. Available: http://www.sti.nasa.gov

[64] “Exploration Systems Development Mission Directorate Moon-to-Mars Architecture Definition Document (ESDMD-001) ,” Apr. 2023. Available: https://ntrs.nasa.gov/api/citations/20230002706/downloads/M2MADD_ESDMD-001%28TP-20230002706%29.pdf

[65] Seattle Fabrics, “Heat Sealable Fabric _ Coated Oxford Fabric _ Seattle Fabrics,” 2026, Available: https://www.seattlefabrics.com/56-58-200-D-Heat-Sealable-Coated-Oxford-2950-linear-yard_p_44.html

[66] N. Bochis, “How Strong Are The Winds On Mars?,” BGR.

[67] “Test Method for Peel Resistance of Adhesives (T-Peel Test),” May 01, 2023, *ASTM International, West Conshohocken, PA*. doi: 10.1520/D1876-08R23.